RESOURCE ALLOCATION METHODS FOR NEXT-GENERATION NETWORKS

by

İlke Altın

B.S., Electrical and Electronics Engineering, Middle East Technical University, 2008

M.S., Electrical Engineering, Delft University of Technology, 2010

Submitted to the Institute for Graduate Studies in
Science and Engineering in partial fulfillment of
the requirements for the degree of
Doctor of Philosophy

Graduate Program in Electrical and Electronics Engineering

Boğaziçi University

2023

ACKNOWLEDGEMENTS

First, I would like to express my gratitude to my advisor Prof. Mehmet Akar for accepting me as his student and his continuous support during my Ph.D. study. I am thankful to him for letting me do research independently, and guiding me when I needed a helping hand.

Additionally, I would like to thank my thesis committee: Prof. Mutlu Koca, and Assoc. Prof. Onur Cihan for their valuable comments on the research that we have conducted, and important suggestions to widen this research. I am grateful to Prof. Hakan Deliç and Prof. Hakan Ali Çırpan for serving on my jury.

I would like to thank my dear friends Ceren, Burak, and Yiğit in our tiny study group for all the fun that we had.

I am thankful to my parents for their endless love and support, I would not be able to achieve anything without them. They have been my inspiration in life.

Finally, I would like to thank my wife for being so supportive during my Ph.D. study. Her patience and understanding has been indispensable for me.

ABSTRACT

RESOURCE ALLOCATION METHODS FOR NEXT-GENERATION NETWORKS

In 5G and beyond systems, the number of connections and data traffic is expected to grow significantly. To support the ever-increasing requirements, new solutions such as Mobile Edge Computing (MEC), Non-Orthogonal Multiple Access (NOMA), and Heterogeneous Networks (HetNets) are studied extensively. This thesis focuses on the resource allocation methods for uplink Hybrid NOMA for MEC offloading, downlink Hybrid NOMA, and downlink HetNets. First, a joint resource allocation that minimizes the total energy consumption of users for uplink Hybrid NOMA MEC Offloading is proposed. By solving the joint optimization problem, we propose a novel optimal Hybrid NOMA scheme referred to as Switched Hybrid NOMA for power and time allocation. Subsequently, we propose an algorithm to solve the sub-channel allocation (SCA) problem. We demonstrate that the proposed methods outperform the results in the literature analytically and by simulations. Then, we switch to the downlink communication, and study a resource allocation scheme that minimizes the total weighted energy consumption in the network. We propose a novel optimal Hybrid NOMA scheme for two users and then extend this idea to multiple users. Via simulations, we demonstrate that the Hybrid NOMA method outperforms Orthogonal Multiple Access (OMA) and NOMA methods. Afterward, we investigate novel distributed sub-channel and power allocation algorithms for HetNets. We introduce an SCA algorithm that minimizes the effective interference experienced by users in the network. Then, a distributed algorithm for power allocation is proposed, and a joint resource allocation method is constructed by combining the proposed algorithms, which outperforms the existing methods in the literature.

ÖZET

YENİ NESİL AĞLARDA KAYNAK ATAMA YÖNTEMLERİ

5G ve ötesi iletişim sistemlerinde, bağlı kullanıcı sayısının ve veri trafiğinin önemli oranda artması beklenmektedir. Sürekli artan gereksinimleri karşılamak için sınır bilişim (MEC), dikgen olmayan çoklu erişim (NOMA) ve heterojen ağ (HetNet) gibi yöntemler detaylı olarak çalışılmaktadır. Bu çalışmada, bahsi geçen yöntemlerle ilgili üç farklı kaynak atama problemi incelenmiştir. İlk olarak, yukarı yönlü bağlantı için sınır bilişim ve hibrit NOMA yöntemi için enerji verimliliğini arttıran bir kaynak atama algoritması önerilmiştir. Optimizasyon problemi çözülerek, yeni bir çoklu erişim yöntemi bulunmuştur. Sonrasında, frekans kaynağı ataması problemini çözmek için bir algoritma önerilmiştir. Önerilen yöntemlerin literatürde bulunan yöntemlerden daha verimli olduğu kuramsal analiz ve benzetim çalışmaları ile gösterilmiştir. Sonrasında, aşağı yönlü bağlantı için hibrit NOMA yöntemi için tüm ağdaki enerji verimliliği incelenmiştir. Öncelikle iki kullanıcı için hibrit NOMA yöntemi önerilmiş, sonrasında daha fazla kullanıcıya uygulanabilecek şekilde geliştirilmiştir. Benzetim çalışmalarıyla, önerilen hibrit NOMA yönteminin dikgen çoklu erişim (OMA) ve NOMA yöntemlerinden daha verimli çalıştığı gösterilmiştir. Son olarak, heterojen ağlar için dağıtık kaynak ataması problemi incelenmiştir. Öncelikle, etkin girişim miktarını azaltan dağıtık bir frekans kaynağı ataması algoritması önerilmiştir. Daha sonra, güç ataması için de bir dağıtık algoritma geliştirilip, kaynak atamasını dağıtık ve bütünleşik olarak gerçekleştiren bir algoritma önerilmiştir. Önerilen yöntemin literatürdeki yöntemlerden daha yüksek veri trafiğini desteklediği benzetim çalışmaları ile gösterilmiştir.

TABLE OF CONTENTS

LIST OF FIGURES

LIST OF TABLES

LIST OF SYMBOLS

a	Exponential value of MP-XPC algorithm
B	Sub-channel bandwidth
$\mathbf{B_d}$	Diagonal power update function constant matrix
c_{ij}^k	Channel gain from cell j to cell i on sub-channel k
D_l	Longer delay constraint in a NOMA pair
D_s	Shorter delay constraint in a NOMA pair
D_u	Maximum allowed delay of user u
D_μ	Mean of delay constraints
D_σ	Standard deviation of delay constraints
$e_i(t)$	Normalized Interference-Noise exponent in cell i
$\mathbf{E_d}$	Diagonal normalized interference-noise exponent matrix
f_c	Carrier frequency
F	MEC server computational capacity
G	Base station antenna gain
h_{ij}^k	Normalized gain from cell j to cell i on sub-channel k
$h_{u,k}$	Channel gain of user u on sub-channel k
$\mathbf{H^k}$	Normalized gain matrix
$\mathbf{L}$	Laplacian matrix of the graph
L_u	Latency constraint of user u
L_u^{ul}	Uplink latency of user u
L_u^{ms}	MEC Server latency of user u
L_u^{dl}	Downlink latency of user u
n_i^k	Normalized thermal noise power
$\mathbf{n^k}$	Normalized thermal noise power matrix
N_0	Noise floor
N_μ	Mean of data transfer requirements
N_σ	Standard deviation of data transfer requirements
N_u	Data transfer requirement of user u

$O(.)$	Complexity in Big-O notation
p_i^k	Transmit power of base station i on sub-channel k
$\mathbf{p^k}$	Transmit power vector
P	Total power consumption
P^b	Transmit rate dependent power of the base station
P_C	Constant circuit power consumption
P_C^b	Constant circuit power consumption in the base station
P_C^u	Constant circuit power consumption in the user
$P_{i,k}$	Transmit power of user i on sub-channel k
$P_{j,k}^1$	Transmit power of user j on sub-channel k in T_1
$P_{j,k}^2$	Transmit power of user j on sub-channel k in T_2
P_M^{TM}	Macrocell maximum transmit power
P_M^{TRS}	Macrocell CS-RS transmit power
P_N	Noise power
P_P^{TM}	Picocell maximum transmit power
P_P^{TRS}	Picocell CS-RS transmit power
P^u	Transmit rate dependent power of user u
$P_{x,i}$	Transmit power allocated to user x in period i
$P_{y,i}$	Transmit power allocated to user y in period i
r	Data transfer requirement ratio for UL H-NOMA
R	Cell radius
R_m	Mean network throughput
R_M	Macrocell radius
R_P	Picocell radius
R_N	Data transfer requirement ratio for DL H-NOMA
s	NOMA user selection parameter
T_1	The first transmission period of H-NOMA
T_2	The second transmission period of H-NOMA
T_j	Transmission period of user j
w_i^k	Sub-channel k interference-noise power in cell i
$W(.)$	Lambert function

x_i^k	SINX target on sub-channel k in cell i
z_i^k	Sub-channel k normalized interference-noise power in cell i
α	Power amplifier efficiency
β	Power update function constant
γ	SINR target
γ_i^k	SINR on sub-channel k in cell i
γ_L	Path loss exponent
γ_M	Macrocell SINR
$\mathbf{\Gamma^k}$	SINR matrix
ζ	SINP target
ζ_i^k	SINP on sub-channel k in cell i
λ_1	Largest eigenvalue
ν_i^k	Effective interference on sub-channel k
$\rho(.)$	Spectral radius of matrix
ρ_m	Mean spectral radius
σ_S	Standard deviation of shadowing
ϕ_i^{kl}	Pairing status of sub-channel k and user l for cell i
$\mathbf{\Phi_i}$	Two-dimensional assignment matrix for cell i
$\psi_{i,j,k}$	Pairing status of user i to user j on sub-channel k
$\mathbf{\Psi}$	Three-dimensional pairing matrix for users and sub-channels
ω	Battery charge/discharge energy efficiency

LIST OF ACRONYMS/ABBREVIATIONS

2DAP	Two-Dimensional Assignment Problem
2ES	Two-Sided Exchange Stable
3DAP	Three-Dimensional Assignment Problem
5G	Fifth Generation
AJFI	Average Jain's Fairness Index
AMC	Adaptive Modulation and Coding
B-TES	Bootstrapped Total-Reward Exchange Stable
CBPA	Consensus Based Power Allocation
CBPA-M	Consensus Based Power Allocation Modified
CoMP	Coordinated Multi-Point
CSI	Channel State Information
D2D	Device-to-Device
DTPC	Dynamic Target Power Control
eMBB	Enhanced Mobile Broadband
EXS	Exhaustive Search
ES	Exchange Stable
FBC	Finite Blocklength Codes
FM	Foschini-Miljanic
GT	Gabow-Tarjan
HARQ	Hybrid Automatic Repeat Request
HetNets	Heterogeneous Networks
H-NOMA	Hybrid Non-Orthogonal Multiple Access
ICI	Inter-cell Interference
IRS	Intelligent Reflecting Surface
JFI	Jain's Fairness Index
JFPUA	Joint Frequency and Power Update Algorithm
JRA	Joint Resource Allocation
KKT	Karush-Kuhn-Tucker

LBAP	Linear Bottleneck Assignment Problem
LQP	Link Quality Protection
MEC	Mobile Edge Computing
MEIM	Maximum Effective Interference Minimization
mMTC	Massive Machine Type Communication
MP-XPC	Message-Passing-based Exponential Power Control
MP-XPCE	Message-Passing-based Exponential Power Control Extended
NOMA	Non-Orthogonal Multiple Access
OFDMA	Orthogonal Frequency Division Multiple Access
OMA	Orthogonal Multiple Access
OPC	Opportunistic Power Control
QoS	Quality of Service
RAND	Random Sub-Channel Allocation
SCA	Sub-Channel Allocation
SH-NOMA	Switched Hybrid Non-Orthogonal Multiple Access
SIC	Successive Interference Cancellation
SINP	Signal and Interference-Noise Product
SINR	Signal and Interference-Noise Ratio
SINX	Signal to Interference-Noise Exponential Ratio
TaN	Treat as Noise
TDD	Time Division Duplex
TDMA	Time Division Multiple Access
TES	Total-Reward Exchange Stable
TH	Two-Round Hungarian
TJFI	Total Jain's Fairness Index
URLLC	Ultra Reliable Low Latency Communication

1. INTRODUCTION

The next-generation telecommunication networks aim to connect a vast amount of subscribers that have different service requirements. These service requirements mapped to three sets in the 5G standard are listed below [1]:

- **Enhanced Mobile Broadband (eMBB):** The services grouped under eMBB require very high data rates (20 Gbps peak data rate per user). These services can be listed as hologram calls, 4K video transfer, fixed wireless access, etc.
- **Massive Machine Type Communication (mMTC):** The services grouped under mMTC require low data rates for a very high number of users (1 million devices/km^2). These services are usually different applications of IoT, such as smart cities, smart grids, health monitoring devices, etc.
- **Ultra Reliable Low Latency Communication (URLLC):** The services grouped under URLLC require very low latency (below 1 ms) with very high transmission reliability. URLLC services apply to various fields, such as mission-critical communications, autonomous vehicles, smart factories, etc.

In addition to these challenging requirements, the data traffic is expected to grow more than double by 2024, which mandates the research to enhance the effectiveness of communication networks [2]. The scientific and technical community proposes different solutions, and in this work, we analyze the following methods: Mobile Edge Computing (MEC), Non-Orthogonal Multiple Access (NOMA), and Heterogeneous Networks (HetNets).

MEC is a concept that moves the computational resources from the central network to the edge of the network, which is closer to the users [3]. By utilizing MEC, the traffic in the central network can be reduced, and the communication latency can be reduced. To ensure that the edge devices are utilized efficiently, the users for each edge device shall be coordinated regarding user grouping and resource allocation.

NOMA is the separation of users assigned to the same communication resource in the power domain or code domain [4]. This work focuses on the power domain NOMA, which can be utilized for uplink and downlink communications. User grouping, resource allocation, and power allocation are the most critical factors for the effectiveness of NOMA.

In HetNets, small cells are distributed in the same geographical area within a macro cell to increase the network density and reduce the load on the macro cells. In this work, we consider dense networks for 5G with small cells as introduced in [5].

1.1. Related Literature

Different NOMA techniques, in power-domain and code-domain are studied thoroughly in the literature [6] for 5G and beyond communication systems. In this work, power-domain NOMA is considered and it is referred to as NOMA. Utilizing NOMA enables the users to share the same frequency and time resources by a separation in the power domain; thereby, increasing the spectral efficiency of the whole system [4]. It has been shown that when NOMA is applied, the spectral efficiency can be enhanced by 30% compared to the Orthogonal Frequency Division Multiple Access (OFDMA) [7]. The effectiveness of NOMA-based systems depends on the power and sub-channel allocation; thus, the resource allocation problem is one of the major research areas in NOMA [8].

NOMA resource allocation problem for downlink systems with a throughput maximization focus is studied in [9]. The authors have separately dealt with the power and sub-channel allocation problems. In [10], the downlink NOMA resource allocation problem is studied for a secure wireless power transfer-based communication system focusing on energy efficiency. Downlink NOMA idea is extended to hybrid long-packet and short-packet communications in [11]. The resource allocation problem for an enhanced downlink NOMA system with partial hybrid automatic repeat request (HARQ) is studied in [12]. In [13], downlink NOMA sub-channel allocation for Coor-

dinated Multi-Point (CoMP) systems is solved with the Two-Sided Exchange Stable (2ES) algorithm. In [14], the resource allocation problem for Intelligent Reflecting Surface (IRS) aided downlink NOMA networks is investigated. The authors proposed an alternating optimization algorithm that deals with power allocation, IRS reflection matrix, and sub-channel allocation sequentially. The uplink NOMA resource allocation to enhance spectral efficiency is studied in [15], where the power optimization is handled by the water-filling algorithm, and the sub-channel allocation is determined by Dinkelbach's algorithm. The authors proposed an interference reduction scheme for Device-to-Device (D2D) users based on NOMA in [16]. A branch-and-bound algorithm does the power control, and the 2ES algorithm determines the sub-channel allocation. In [17], the authors have given the optimal power allocation and a 2ES algorithm-based sub-channel allocation for an uplink NOMA MEC offloading scenario with imperfect channel state information (CSI).

Hybrid NOMA (H-NOMA) techniques that combine NOMA with Time Division Multiple Access (TDMA) are proposed to further enhance the energy efficiency of NOMA systems [18]. In [19], the minimization of the transaction time difference between H-NOMA users is studied. A H-NOMA scheme with all users sharing the same frequency resources is analyzed in [20]. In [21, 22], the authors utilize the H-NOMA idea to the URLLC scenario. For URLLC scenarios, Finite Blocklength Codes (FBC) are used; therefore, the Shannon capacity formula is no longer accurate, and the FBC capacity formula is used instead. In these articles, the authors work on the non-convex transmission energy minimization problem with the FBC rate formula and propose different solutions by convex approximation methods. A downlink hybrid TDMA-NOMA-based method with infinite blocklength codes for a wireless power transfer-based communication system is given in [23]. The authors have provided a solution that utilizes fixed transmission phases for energy harvesting and data transmission for two users. In [24], the resource allocation problem of a hybrid TDMA-NOMA-based network is analyzed with a spectral efficiency objective. The hybrid TDMA-NOMA-based network scenario is further improved with the addition of IRS and wireless power transfer in [25]. In [26], uplink H-NOMA power allocation problem is analyzed for the

ideal circuit power consumption scenario, whereas the downlink H-NOMA scenario is indicated as a future research topic.

Another concept that is expected to be widely used in 5G is MEC. By the application of MEC, the computational capabilities of the network are shifted to the edge, and the latency of applications is decreased by localization [3]. There are many different applications of MEC; and in this work, we focus on MEC data offloading. MEC data offloading tasks can be grouped into two [27]: binary offloading which considers the transfer of data that cannot be partitioned, and partial offloading which considers the transfer of data that can be partitioned. In [28], the energy efficiency and latency trade-off for a partial MEC offloading scenario is analyzed. In [29], the energy efficiency aspect of the partial offloading is studied. The authors propose centralized and distributed solutions to the resource allocation and data offloading decision problem.

NOMA can be utilized to enhance MEC offloading in different aspects, such as delay minimization, computational energy reduction, transmission energy minimization, etc. In [30], the system energy efficiency is analyzed for a NOMA MEC offloading scenario with partial offloading. In [31], a NOMA scheme for MEC offloading that selects between complete offloading, partial offloading, and complete local processing depending on the channel conditions and the quality of service (QoS) requirements is presented. Partial task offloading, and optimal utilization of NOMA for MEC offloading scenario is studied in [32]. Energy efficiency is enhanced by controlling the NOMA transmission duration via partial offloading. In [33], an energy efficient solution to the NOMA aided MEC offloading scenario with user cooperation is given. The problem that is analyzed considers partial offloading and users with the same latency constraints. In [34], a NOMA based MEC offloading scenario with multiple users is analyzed with an energy efficiency objective. The scenario assumes partial offloading and different latency constraints for users. In [35], the authors have inspected the resource allocation problem in a NOMA based edge computing scenario. The authors have dealt with sub-channel allocation and computational resource allocation problems separately.

H-NOMA scheme is applied to MEC offloading scenarios to reduce energy consumption in [36]. The H-NOMA scheme is proposed to enhance the energy efficiency of NOMA for two users with different latency constraints. In [37], the optimal task allocation and power allocation problems are solved for the MEC offloading scenario. In [38], the power, time, and sub-channel allocation problem for multiple H-NOMA users is solved. The shortcomings of H-NOMA without user selection and its comparison to optimal OMA is introduced in [39]. A joint resource allocation scheme for uplink H-NOMA for MEC offloading with non-ideal transmission circuits is proposed in [40].

A delay minimization focused NOMA MEC offloading scenario for two users with different latency constraints is studied in [41]. In [42], a delay minimization NOMA MEC offloading problem with partial data offloading is considered. An optimal solution for the two-user case, and a sub-optimal solution for the multi-user case is proposed by the authors. In [43], energy efficiency and minimization of the completion time for the NOMA MEC offloading scenario is jointly studied. In [44], Orthogonal Multiple Access (OMA), NOMA, and H-NOMA methods are analyzed with a focus on delay minimization for MEC offloading. In [45], an iterative NOMA scheme for MEC offloading with a focus on latency minimization is given. In order to minimize the overall latency of the users in the network, partial offloading and NOMA is employed. In [46], a two user NOMA MEC scenario with user cooperation is analyzed for partial data offloading. In [47], a NOMA MEC offloading scenario with partial data offloading is investigated. The authors propose a locally optimal solution to the resource allocation and offloading decision problem for latency minimization.

Another key technology to cope with this high network density is heterogeneous networks (HetNets) [5]. HetNets comprise base stations of different tiers with coinciding coverage areas: macrocells, microcells, picocells, and femtocells in the order of decreasing power levels. In HetNets, small cell base stations such as microcells, picocells, and femtocells reside in the macrocell coverage area, transmitting on the same frequency resources. Thus, in the downlink, there is inter-cell interference (ICI) from

the macrocell base station to the small cell users and from the small cell base station to the macrocell users. ICI is one of the significant issues to be tackled to unlock the potential of HetNets [48]. Interference-aware power and sub-channel allocation algorithms can solve the ICI problem. Additionally, in large-scale HetNets, centralized resource allocation schemes are inappropriate due to the computational load and backhaul limitations. Therefore, distributed power and sub-channel allocation algorithms that can handle ICI are of great importance to HetNets.

The Foschini-Miljanic (FM) algorithm [49] is one of the first distributed power control algorithms in the literature. In the FM algorithm, the users aim to reach predetermined Signal to Interference-Noise Ratio (SINR) targets iteratively by using only local information. This algorithm has been widely studied due to its elegance and low complexity. However, the algorithm has two main drawbacks: a pre-determined feasible SINR target is required for each user, and the attained network throughput is low.

In [50], the opportunistic power control (OPC) algorithm is presented as an improvement to the network throughput problem of the FM algorithm. In the OPC algorithm, the agents have Signal and Interference-Noise Product (SINP) targets, which is a metric that favors the users with better channel conditions. It has been shown that the OPC algorithm outperforms FM regarding network throughput. However, while the network throughput is improved, the throughput is significantly degraded for the users with worse channel conditions. Additionally, dependence on the calculation of feasible targets becomes even more complex with SINP, which is not as physically meaningful as SINR. The dynamic target-SIR power control (DTPC) algorithm is proposed in [51]. The algorithm combines the OPC algorithm and the FM algorithm with threshold-based switching. The algorithm is fairer than the DTPC, but calculating SINR and SINP targets remains an open issue. A DTPC-inspired algorithm is applied to a full-duplex energy harvesting network in [52]. In [53], an improved version of the DTPC algorithm is given, which reduces the network's total energy consumption while satisfying the users' target SINR values.

A feedback-based power control algorithm is proposed for HetNets in [54]. It has been shown that the small cell base stations reach a common SINR value that depends on the spectral radius of the normalized interference matrix. In [55], authors have given a consensus-based downlink power allocation (CBPA) algorithm for heterogeneous networks, where the femtocell transmit powers are determined depending on the SINR values of the neighbor cells in a distributed fashion. In [56], a modified version of the CBPA algorithm (CBPA-M) is proposed, where the macrocell base station SINR target is considered. The CBPA and CBPA-M algorithms are shown to be fair between users based on Jain's fairness index (JFI) [57]. In [58], another consensus-based algorithm is proposed for scenarios where the base stations have imperfect connections. In [59], the downlink heterogeneous network scenario with each base station serving multiple users is analyzed, and a joint frequency and power update algorithm (JFPUA) is proposed. A gossip-based consensus algorithm with modified weights for asymmetrical networks is presented in [60].

In [61], the authors have proposed a power allocation algorithm, which utilizes statistical channel state information for users with pre-defined SINR targets. In [62], the authors have analyzed the power control problem to maximize the energy efficiency in the network while satisfying the SINR targets. A distributed algorithm based on game theory is proposed to solve the problem. This idea is extended to include delay minimization by selecting a cost function that depends on the weighted summation of the energy efficiency and delay in [63]. In [64, 65], a game-theoretical power control algorithm with access control is proposed for users with pre-defined SINR targets. In [66], the authors have analyzed the power allocation problem in full-duplex femtocell networks. A game-theoretical algorithm is proposed to minimize the outage probability. In [67], the power allocation problem for an underlaying D2D network is studied. The authors have proposed a game-theoretical algorithm that maximizes the D2D traffic while satisfying the interference power limitation of the base station. In [68], a power control algorithm that maximizes the total SINR of the femtocells while satisfying the SINR limits of the macrocell users is proposed.

In [69], joint sub-channel allocation and power control problem is analyzed where the sub-channel allocation is done by the Hungarian algorithm and the power allocation is done by the FM algorithm. In [70], the authors worked on the throughput maximization problem by jointly controlling the sub-channel and power allocation. In [71], the joint resource allocation problem with a throughput maximization is enhanced by adding the quality of service (QoS) parameters. In [72], the QoS parameters and the weighted fairness of the network are considered while maximizing the system's energy efficiency via joint resource allocation. In [73], joint resource allocation for Orthogonal Frequency Domain Multiple Access (OFDMA) networks is tackled with the help of the DTPC idea in [51]. The effective interference and SINR target values are utilized to determine the sub-channel allocation, and a DTPC-like algorithm is used for power assignment.

1.2. The Motivation of the Thesis

In this work, we analyze three different resource allocation problems and propose solutions that improve the available solutions in the literature.

1.2.1. Uplink Hybrid NOMA

We propose a novel resource allocation method for uplink H-NOMA MEC Offloading to solve the following drawbacks in the solutions from the literature:

- The methods in [21, 22] are designed for FBC scenarios, and cannot be applied to the problem at hand, which is focused on infinite blocklength regime and the Shannon rate formula.
- The main objective in [41–45] is latency minimization; thus, the solutions considered therein cannot be applied to our scenario.
- The methods in [9,10,30–33,35,46] are based on NOMA, and they are sub-optimal for the analyzed scenario where users have different latency requirements.
- H-NOMA method, which is utilized in [19, 20, 36–38], is only valid for a special

case of the two user MEC offloading scenario in which the user data offloading requirements are equal. Furthermore, H-NOMA is a sub-optimal resource allocation method when the constant circuit power consumption of the transmitter is considered, and for certain channel conditions.

- The proposed algorithms in [23–25] require pre-allocated time slots and do not consider the user latency requirements, whereas the problem that is analyzed in this chapter is for users with heterogeneous latency requirements.
- The sub-channel allocation methods that are utilized in [9, 35, 38] are less energy efficient than the sub-channel allocation algorithm that we propose.

1.2.2. Downlink Hybrid NOMA

We introduce a novel downlink resource allocation method that utilizes H-NOMA for users with heterogeneous latency and data transfer requirements to overcome the following shortcomings of the available literature:

- The methods in [9, 10, 13, 15, 17] are based on NOMA, and we show that NOMA-based methods are sub-optimal when users have different latency requirements.
- The uplink H-NOMA method studied in [16, 20, 26, 36–38, 40, 41], is only valid for the uplink scenario since the interference channel gains are different in downlink NOMA and uplink NOMA [74].
- The methods in [11, 21, 22] are only accurate for FBC scenarios and cannot be applied to the problem at hand, which is focused on the infinite blocklength regime.
- The proposed algorithms in [23–25] require pre-allocated time slots and do not consider the user latency requirements, whereas the problem that is analyzed in this chapter is for users with heterogeneous latency requirements.
- The sub-channel allocation methods proposed in [9,12,13,35,38,40] are less energy efficient than the sub-channel allocation algorithm that we introduce.

1.2.3. Downlink Heterogeneous Networks

We come up with a distributed downlink resource allocation method for HetNets to correct the listed deficiencies in the literature:

- The power control methods in [49–53, 61–68, 73] require the pre-defined SINR targets for the users to be feasible, which is not always the case. The methods in [50–53, 73] require the calculation of SINP targets for OPC and thresholds for the DTPC algorithm, which involves network specific calibration.
- Although SINR targets are usually available depending on the service the user is getting, the SINR targets may not always be feasible, especially for small cell users with severe interference. Soft SINR targets can be used to mitigate the feasibility issue for certain services. For example, for video streaming, which accounts for 70% of the entire mobile data traffic [2], adaptive bit-rate targets can be used without severe disruption to the service. The network can utilize adaptive modulation and coding (AMC) schemes to support different bit rates according to the SINR of the received signal [75].
- The target-free power allocation methods in [54, 56, 58–60] converge to an equal SINR target value in all the cells disregarding the channel conditions. Although these methods are fair, the average throughput of the network is low compared to other methods. Additionally, the resource allocation method proposed in [59] reduces the average throughput further while guaranteeing absolute fairness between sub-channels.
- The resource allocation methods in [69–73] depend on the power assignment, which depends on the power allocation algorithms given in these articles. Since the power allocation methods in the articles are target-dependent, these methods cannot be applied to the problem at hand.

1.3. The Contributions of the Thesis

The major contributions of the thesis are summarized as follows:

- We propose a novel multiplexing scheme called Switched Hybrid NOMA (SH-NOMA) for MEC Offloading users with distinct latency constraints and data transfer requirements, which is the optimal solution of the power and time allocation problem. We analytically prove that the proposed SH-NOMA multiplexing scheme consumes less energy than H-NOMA. Furthermore, we show by simulations that SH-NOMA outperforms H-NOMA, NOMA, and OMA.
- We show that finding the optimal resource allocation is an NP-complete problem, and we propose the Total-Reward Exchange Stable (TES) algorithm. We prove by induction that the TES algorithm outperforms the 2ES algorithm which is widely used in the literature. We also manifest this improvement in the performance via simulations. Moreover, we demonstrate by simulations that the TES algorithm performs very close to the optimal solution acquired via exhaustive search (EXS).
- We propose a novel downlink H-NOMA multiplexing scheme for users with different latency constraints and data transfer requirements. The power and time allocation of the H-NOMA scheme is the optimal solution considering the transmit power consumption of the base station and the circuit power consumption of the users. We present the simulation results, which manifest the efficiency of H-NOMA compared to OMA and NOMA.
- We introduce the Bootstrapped Total-Reward Exchange Stable (B-TES) algorithm to solve the sub-channel allocation (SCA) problem. We compare its performance to the existing methods in the literature and the optimal solution that can be determined by exhaustive search (EXS) by simulations. We show that the B-TES algorithm outperforms the 2ES and TES algorithms from the literature. Furthermore, we show that the B-TES algorithm performs very close to the optimal solution.
- We propose a distributed downlink sub-channel allocation algorithm independent of the power allocation, which we refer to as the maximum effective interference minimization (MEIM) algorithm. We show that the MEIM algorithm reduces the maximum interference in the HetNet analytically.
- We introduce a novel distributed downlink power control algorithm based on message passing, which we call the message-passing-based exponential power control

(MP-XPC) algorithm. The algorithm increases the throughput of the HetNets compared to similar consensus-based algorithms and does not require complete channel state information, pre-defined targets, or network-dependent thresholds. We also extend the MP-XPC algorithm for scenarios where a feasible macrocell SINR target is available and refer to it as MP-XPCE.

- We combine the proposed methods to form a joint downlink resource allocation method for HetNets with multiple sub-channels per base station. We show that the proposed joint resource allocation method outperforms the existing methods in the literature. We also demonstrate the convergence of the joint resource allocation method by simulations.

1.4. The Organization of the Thesis

In Chapter 2, the uplink H-NOMA MEC Offloading resource allocation problem is analyzed. For the power and time allocation problem, the SH-NOMA algorithm is proposed. Then, sub-channel allocation problem is analyzed for the multi-user scenario, and the TES algorithm is introduced. Finally, the superiority of the proposed algorithms against the literature is shown. In Chapter 3, the downlink H-NOMA resource allocation problem is investigated. The downlink H-NOMA algorithm is proposed for the power and time allocation problem. Afterward, the multi-user scenario is studied, and the B-TES algorithm is introduced. Lastly, the proposed algorithms are compared to the existing algorithms in the literature. In Chapter 4, the distributed downlink resource allocation problem for HetNets is investigated. The sub-channel allocation problem is solved by the proposed MEIM algorithm, and the power allocation problem is solved by the MP-XPC and the MP-XPCE algorithms. Then, a joint resource allocation method is designed by combining the proposed sub-channel and power allocation methods. We show that the proposed joint resource allocation method outperforms the existing methods in the literature. We also demonstrate the convergence of the joint resource allocation method by simulations. In Chapter 5, concluding remarks and outcomes of the thesis are given.

2. RESOURCE ALLOCATION FOR UPLINK HYBRID NOMA

In this chapter, we analyze the resource allocation problem for uplink H-NOMA MEC offloading. We first describe the considered system model and introduce the multiplexing methods. Then, the main resource allocation problem is formulated, and separated into two sub-problems. The optimal power and time allocation in a single sub-channel for different scenarios are derived by solving the first sub-problem. Afterward, the TES algorithm is proposed to determine the sub-channel allocation as a solution to the second sub-problem. We show the performance improvement of the proposed methods analytically and by simulations.

2.1. System Model

We examine a MEC offloading scenario with $2K$ users with different latency constraints L_u and data transfer requirements N_u, where u is the user index. Each user offloads its computationally intensive tasks to the MEC server, and the MEC server computes the tasks and sends the result packets to the user. The result packets are assumed to be significantly smaller than the offloaded packets, which is similar to the studies in the literature [28, 29]. The users transmit their data to the base station connected to the MEC server via OFDMA through K sub-channels. In addition to the OFDMA, each sub-channel can be shared by multiple users via NOMA. We assume the base station has perfect uplink CSI and a perfect Successive Interference Cancellation (SIC) receiver for NOMA decoding. Moreover, we assume two NOMA users per sub-channel to reduce the complexity of the SIC receiver as in many studies in the literature [19, 36, 38, 41, 46]. The two-user scheme also limits the performance degradation in real-world applications due to hardware impairments [76].

Throughout the chapter, we assume that another controller makes the offloading decision, and the data transfer requirement N_u of user u refers to the amount of data to

be offloaded by user u. Additionally, we assume an uplink-dominated model for latency and power consumption similar to [29]. The total latency imposed by the offloading process consists of the uplink transmission time L_u^{ul}, the computation time in the MEC server L_u^{ms}, and the downlink transmission time L_u^{dl}. The downlink transmission time is negligible compared to the uplink transmission time due to the smaller packet size in the downlink. The computation time in the MEC server can be calculated as follows

$$L_u^{ms} = \frac{N_u}{F}, \tag{2.1}$$

where F corresponds to the capacity of the MEC server. Since this work is focused on reducing the energy consumption of the transmission to the MEC server, the latency constraint for the uplink transmission of the user u, which we denote as D_u can be calculated in the central controller as

$$D_u \leq L_u^{ul} = L_u - L_u^{ms}, \tag{2.2}$$

where the capacity of the MEC server, and the offloading data amount of the users are known.

The total power consumption of the offloading comprises the uplink transmission power, and the downlink reception power. Because of the smaller packet size in the downlink, the downlink reception power is neglected. In this work, the total uplink transmission power consumption P is modeled as in [77]

$$P = \frac{P^u}{\alpha} + P_C, \tag{2.3}$$

where P^u is the transmission rate-dependent power of the user, α is the efficiency of the power amplifier that satisfies $1 > \alpha > 0$, and P_C is the constant circuit power.

An example network model with four groups and two NOMA users per group, each sharing the same sub-channel, is given in Figure 2.1. In the network model, the channel gains of the users are denoted as $h_{u,k}$, where k is the sub-channel index allocated to the user u. We assume an independent Rayleigh channel with a path loss parameter γ_L and a log-normal shadowing standard deviation σ_S for all sub-channels. Each sub-channel is allocated to two users, user i and user j. Throughout this paper, we assume that the delay constraint of user i is stricter than that of user j, i.e.,

$D_i \leq D_j$. Furthermore, the users are ordered according to their latency constraints: $D_1 \leq D_2 \leq ...D_u... \leq D_{2K}$. The data transfer requirements of users i and j are denoted as N_i and N_j, respectively. Additionally, we assume a parameter $r = \frac{N_j}{N_i}$ that represents the ratio of the data requirements of users that are assigned to the same sub-channel. Additional parameters can be summarized as follows; the noise power P_N, which corresponds to the common noise floor of N_0, and the sub-channel bandwidth is B.

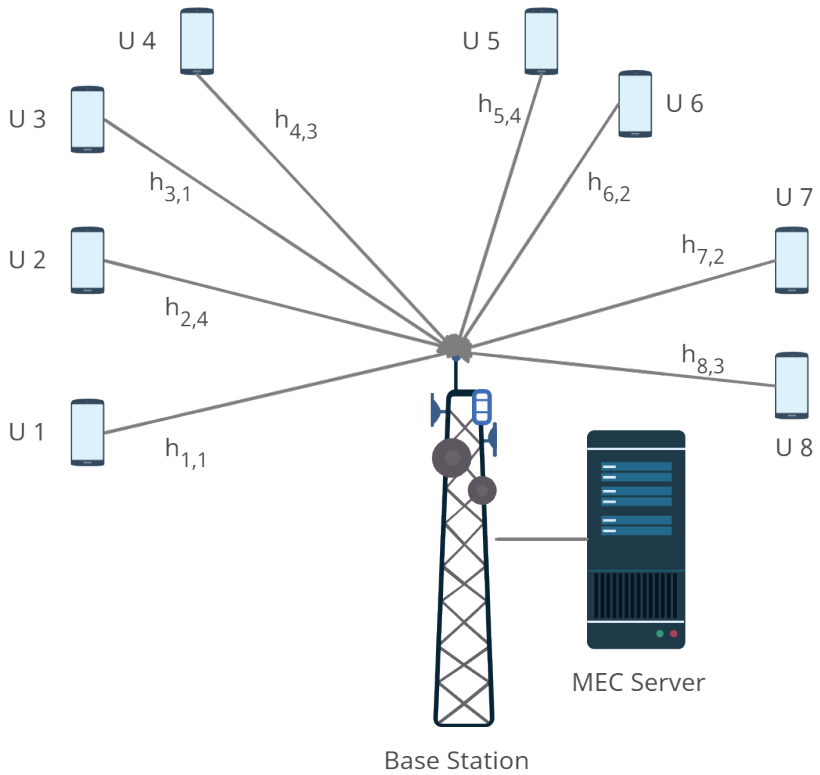

Figure 2.1. An example network diagram for uplink H-NOMA.

The underlying multiplexing scheme is OFDMA in the system model under consideration, so there is no interference between sub-channels. Therefore, the sub-channels can be analyzed independently. The channel capacity of the users utilizing the same sub-channel depends on the selected multiplexing method on top of OFDMA. This work analyzes four different multiplexing methods: OMA, NOMA, H-NOMA, and the proposed SH-NOMA for two scenarios. In Scenario A, user i, which has the stricter latency constraint, has a lower channel gain than or equal to user j, i.e., $|h_{i,k}|^2 \leq |h_{j,k}|^2$.

In Scenario B, the channel gain of user i is higher than the channel gain of user j, i.e., $|h_{i,k}|^2 > |h_{j,k}|^2$.

For the basic OMA scheme with two users, TDMA is applied on top of the existing OFDMA scheme, and the users in the pair are separated in time. For the basic NOMA scheme, both users transmit during the shorter latency constraint D_i. In NOMA, the users are decoded by a SIC receiver in a specific order. The user decoded first is affected by the interference of the second user. The other user is decoded after subtracting the first user's signal; thus, it is not affected by the first user. In this work, we call the user decoded first as the affected user and the user decoded second as the unaffected user.

H-NOMA scheme with two users, which combines OMA and NOMA schemes, can be explained as follows [36,38]: User i, which has the stricter latency requirement, is always selected to be the unaffected NOMA user. In the first transmission period, $t = [0, D_i]$, both users transmit. User i transmits as the unaffected user, and user j transmits as the affected user to offload the first part of its data. In the second transmission period, $t = [D_i, D_i + T_j]$, user j transmits in OMA to offload the rest of its data; where T_j is the sole transmission time of user j, and $T_j \leq D_j - D_i$.

In the SH-NOMA scheme proposed in this paper, the user with better channel conditions is selected to be the affected user, increasing energy efficiency. This selection follows from the general result given in [78], where the optimal SIC decoding order for uplink NOMA is the descending order of the channel gains of the users. SH-NOMA behaves differently in the two different scenarios that we consider. In Scenario A, user i has worse channel conditions, and we have the same transmission scheme as in H-NOMA. In Scenario B, user i has better channel conditions and is selected as the affected user. In the first transmission period, $t = [0, D_i]$, both users transmit. User j transmits as the unaffected user to offload the first part of its data, and user i transmits as the affected user to offload its data. In the second transmission period, $t = [D_i, D_i + T_j]$, user j transmits in OMA to offload the rest of its data.

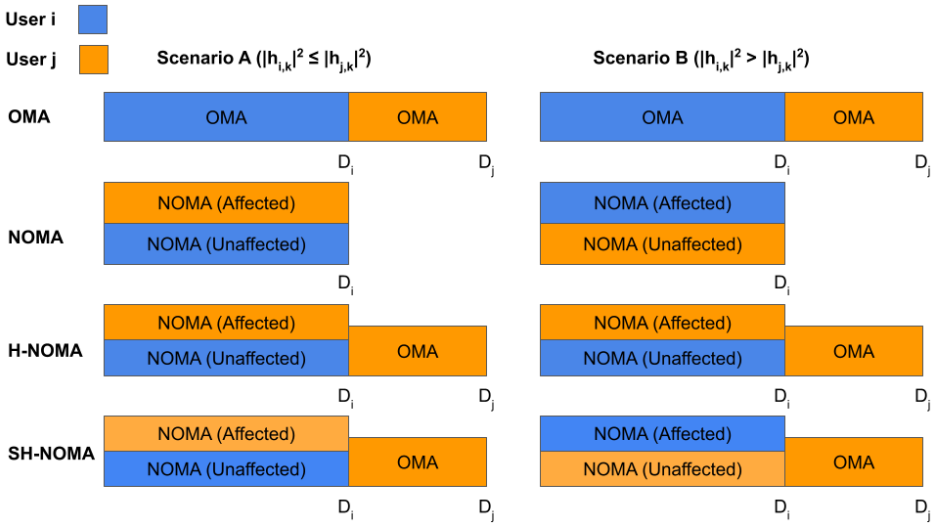

Figure 2.2. Comparison of OMA, NOMA, H-NOMA, and SH-NOMA methods.

The comparison of OMA, NOMA, H-NOMA, and SH-NOMA for different scenarios is given in Figure 2.2. As seen from the figure, the time slot assignment depends on the latency constraints for the OMA scheme. The whole transmission is done during $t = [0, D_i]$, and the user with the lower channel gain is selected as the unaffected NOMA user when the NOMA scheme is utilized. For the H-NOMA scheme, the user with the shorter latency constraint is always selected as the unaffected user. For the SH-NOMA scheme, the user that experiences worse channel conditions is selected as the unaffected user. User i and user j transmit together during the first transmission period, and only user j transmits afterward for both H-NOMA and SH-NOMA schemes.

2.2. Problem Formulation

In this chapter, we study the resource allocation problem for multiple users in a Hybrid NOMA MEC Offloading scenario focusing on energy consumption. In OFDMA, there is no interference between sub-channels, and each sub-channel can be analyzed independently. The total energy consumption for K sub-channels, and $2K$ users can be shown as

$$\sum_{i=1}^{2K-1} \sum_{j=i+1}^{2K} \sum_{k=1}^{K} \psi_{i,j,k} \left[\left(\frac{P_{i,k} + P_{j,k}^{1}}{\alpha} + 2P_C \right) D_i + \left(\frac{P_{j,k}^{2}}{\alpha} + P_C \right) T_j \right], \tag{2.4}$$

where $P_{i,k}$ is the transmit power of the user i, which is the user with the stricter latency requirement, $P^1_{j,k}$ is the transmit power of the user j in the first transmission period, and $P^2_{j,k}$ is the transmit power of the user j in the second transmission period, and $\psi_{i,j,k}$ is the entry of the binary three-dimensional resource allocation matrix Ψ that describes the pairing relation of user i to user j on sub-channel k. If the corresponding index is set to one, then the indicated sub-channel is assigned to these two users. Otherwise, the indicated sub-channel is not assigned to these users, or the users do not form a pair. In the calculation, the sub-channel index is iterated from 1 to K, which is the number of available sub-channels. The index for user i, which is the user with the stricter delay constraint, is iterated from 1 to $2K-1$ since each user can be the first user of a pair except for the user with the highest delay constraint. The index for user j is iterated from i to $2K$ since user j must have a looser latency constraint than user i. The amplifier efficiency coefficient α is a constant, and the total energy consumption can be scaled with it to simplify the equation as

$$\sum_{i=1}^{2K-1}\sum_{j=i+1}^{2K}\sum_{k=1}^{K}\psi_{i,j,k}\left[\left(P_{i,k}+P^1_{j,k}+2\alpha P_C\right)D_i+\left(P^2_{j,k}+\alpha P_C\right)T_j\right]. \tag{2.5}$$

Utilizing the resource allocation matrix, and the total energy consumption formula; the energy consumption minimization focused Hybrid NOMA MEC Offloading resource allocation problem can be formulated as

$$\min_{\Psi,P_{u,k},T_j} \quad f_0=\sum_{i=1}^{2K-1}\sum_{j=i+1}^{2K}\sum_{k=1}^{K}\psi_{i,j,k}\left[\left(P_{i,k}+P^1_{j,k}\right)D_i+\left(P^2_{j,k}+\alpha P_C\right)T_j\right] \tag{2.6a}$$

$$\text{s.t.} \quad \psi_{i,j,k}\in\{0,1\} \quad \forall i,j,k, \quad \sum_i\sum_j\psi_{i,j,k}=2, \quad \forall k, \tag{2.6b}$$

$$\sum_j\sum_k\psi_{i,j,k}=1, \quad \forall i, \quad \sum_i\sum_k\psi_{i,j,k}=1, \quad \forall j, \tag{2.6c}$$

$$N_i-BD_i\log_2\left(1+\frac{P_{i,k}|h_{i,k}|^2}{P_N+(1-s)P^1_{j,k}|h_{j,k}|^2}\right)\le 0, \tag{2.6d}$$

$$rN_i-BD_i\log_2\left(1+\frac{P^1_{j,k}|h_{j,k}|^2}{P_N+sP_{i,k}|h_{i,k}|^2}\right) - BT_j\log_2\left(1+\frac{P^2_{j,k}|h_{j,k}|^2}{P_N}\right)\le 0, \tag{2.6e}$$

$$-P_{i,k}\le 0, \quad -P^1_{j,k}\le 0, \quad -P^2_{j,k}\le 0, \tag{2.6f}$$

$$-T_j\le 0, \quad T_j-(D_j-D_i)\le 0, \tag{2.6g}$$

where $f_0(\Psi, P_{i,k}, P^1_{j,k}, P^2_{j,k}, T_j)$ is the objective function with constant term $2\alpha P_C D_i$ removed, and $s \in \{0, 1\}$ is the affected/unaffected user selection parameter. If $|h_{i,k}|^2 \leq |h_{j,k}|^2$ for the users i, and j on the allocated sub-channel k, then user i is selected as the unaffected user, and s is set to one. Otherwise, user j is selected as the unaffected user, and s is set to zero. Constraints (2.6b)-(2.6c) guarantee that each sub-channel is allocated to two users, and each user is assigned to a single sub-channel. Constraints (2.6d)-(2.6e) ensure that the required data transmission is satisfied with the determined resource allocation. Constraints (2.6f)-(2.6g) are the feasibility constraints for power and time allocation. We call the vector of constraint functions related to the power and time variables $\boldsymbol{f_{c0}}$.

The formulated resource allocation problem, which aims to optimize power, time, and sub-channel allocation, is a mixed integer problem due to the constraints in (2.6b)-(2.6c). In this work, we separate the power and time allocation and the sub-channel allocation problems optimally by optimizing over the power and time variables first and the sub-channel variables afterward as described in [79]. First, we define the function $\tilde{f}_0$, which is the minimized version of f_0 with respect to power and time variables, which is shown by

$$\tilde{f}_0(\Psi) = inf\{f_0(\Psi, P_{i,k}, P^1_{j,k}, P^2_{j,k}, T_j) | \boldsymbol{f_{c0}} \leq 0\}. \tag{2.7}$$

The power and time optimization problem to solve for $\tilde{f}_0$ can be defined as

$$\min_{P_{i,k}, P^1_{j,k}, P^2_{j,k}, T_j} \quad \sum_{i=1}^{2K-1} \sum_{j=i+1}^{2K} \sum_{k=1}^{K} \psi_{i,j,k} \left[\left(P_{i,k} + P^1_{j,k}\right) D_i + \left(P^2_{j,k} + \alpha P_C\right) T_j \right] \tag{2.8a}$$

$$\text{s.t.} \quad N_i - BD_i \log_2(1 + \tfrac{P_{i,k}|h_{i,k}|^2}{P_N + (1-s)P^1_{j,k}|h_{j,k}|^2}) \leq 0, \tag{2.8b}$$

$$rN_i - BD_i \log_2(1 + \tfrac{P^1_{j,k}|h_{j,k}|^2}{P_N + sP_{i,k}|h_{i,k}|^2}) - BT_j \log_2(1 + \tfrac{P^2_{j,k}|h_{j,k}|^2}{P_N}) \leq 0, \tag{2.8c}$$

$$-P_{i,k} \leq 0, \quad -P^1_{j,k} \leq 0, \quad -P^2_{j,k} \leq 0, \tag{2.8d}$$

$$-T_j \leq 0, \quad T_j - (D_j - D_i) \leq 0, \tag{2.8e}$$

where $\psi_{i,j,k}$ is an unknown constant for the partial optimization problem $\tilde{f}_0$. The cost function is the sum of the energy consumption of $K(2K-1)$ different matchings over

K sub-channels with different weights $\psi_{i,j,k}$. Due to OFDMA, sub-channels do not cause any interference with each other, and the optimal solution for each sub-channel can be found separately. Thus, the equation above can be separated into $K^2(2K-1)$ problems for every different matching on every sub-channel. An equivalent problem to (2.6) can be defined by using $\tilde{f}_0$ in (2.7) as

$$\min_{\Psi} \quad \tilde{f}_0(\Psi) \tag{2.9a}$$

$$\text{s.t.} \quad \psi_{i,j,k} \in \{0,1\} \quad \forall i,j,k, \quad \sum_i \sum_j \psi_{i,j,k} = 2, \quad \forall k, \tag{2.9b}$$

$$\sum_j \sum_k \psi_{i,j,k} = 1, \quad \forall i, \quad \sum_i \sum_k \psi_{i,j,k} = 1, \quad \forall j. \tag{2.9c}$$

In the next two sections, the power and time allocation problem given in (2.8), and the sub-channel allocation problem given in (2.9) will be analyzed, respectively.

2.3. Power and Time Allocation

As stated in Section 2.2, the solution to the total minimization problem in (2.8) can be determined by solving the minimization problem for each sub-channel. The optimization problem for a single sub-channel is given by

$$\min_{P_{i,k},P^1_{j,k},P^2_{j,k},T_j} \quad P_{i,k}D_i + P^1_{j,k}D_i + P^2_{j,k}T_j + \alpha P_C T_j \tag{2.10a}$$

$$\text{s.t.} \quad N_i - BD_i \log_2(1 + \tfrac{P_{i,k}|h_{i,k}|^2}{P_N + (1-s)P^1_{j,k}|h_{j,k}|^2}) \leq 0, \tag{2.10b}$$

$$rN_i - BD_i \log_2(1 + \tfrac{P^1_{j,k}|h_{j,k}|^2}{P_N + sP_{i,k}|h_{i,k}|^2}) - BT_j \log_2(1 + \tfrac{P^2_{j,k}|h_{j,k}|^2}{P_N}) \leq 0, \tag{2.10c}$$

$$-P_{i,k} \leq 0, \quad -P^1_{j,k} \leq 0, \quad -P^2_{j,k} \leq 0, \tag{2.10d}$$

$$-T_j \leq 0, \quad T_j - (D_j - D_i) \leq 0. \tag{2.10e}$$

which needs to be solved for all K sub-channels in the network.

To determine the optimal time and power allocation to the users, we analyze two aforementioned scenarios. In Scenario A, the channel gain of user j is higher than or equal to the channel gain of user i ($|h_{i,k}|^2 \leq |h_{j,k}|^2$) and in Scenario B, the channel gain of user i is higher than the channel gain of user j ($|h_{i,k}|^2 > |h_{j,k}|^2$).

2.3.1. Scenario A

In Scenario A, user j has the higher channel gain; therefore, it is selected as the affected user, and the s parameter is set to one. The optimization problem can be reduced since the data constraint for user i is satisfied as equality in the minimum energy consumption scenario. Utilizing this fact, we can derive $P_{i,k} = \frac{P_N}{|h_{i,k}|^2}(2^{\frac{N_i}{BD_i}} - 1)$. The reduced form of the optimization problem is given by

$$\min_{P_{j,k},T_j} \quad f_1(P^1_{j,k}, P^2_{j,k}, T_j) = P^1_{j,k}D_i + P^2_{j,k}T_j + \alpha P_C T_j \tag{2.11a}$$

$$\text{s.t.} \quad rN_i - BD_i \log_2(1 + \frac{P^1_{j,k}|h_{j,k}|^2}{2^{\frac{N_i}{BD_i}} P_N}) - BT_j \log_2(1 + \frac{P^2_{j,k}|h_{j,k}|^2}{P_N}) \leq 0, \tag{2.11b}$$

$$-P^1_{j,k} \leq 0, \quad -P^2_{j,k} \leq 0, \tag{2.11c}$$

$$-T_j \leq 0, \quad T_j - (D_j - D_i) \leq 0, \tag{2.11d}$$

where we call the vector of constraint functions related to the power variables $\boldsymbol{f_{c1}}$. The solution to the problem with $P^1_{j,k} > 0$ is given by Theorem 2.1.

Theorem 2.1. *Optimal power and time allocation in Scenario A can be given as*

$$\begin{aligned}
P_{i,k} &= \frac{P_N}{|h_{i,k}|^2}(2^{\frac{N_i}{BD_i}} - 1), \\
P^1_{j,k} &= \frac{P_N}{|h_{j,k}|^2}(2^{\frac{(r+1)N_i}{B(T_j+D_i)}} - 2^{\frac{N_i}{BD_i}}), \\
P^2_{j,k} &= \frac{P_N}{|h_{j,k}|^2}(2^{\frac{(r+1)N_i}{B(T_j+D_i)}} - 1), \\
T_j &= \begin{cases} D_j - D_i, & \text{if } c_1 \geq 0 \\ \frac{x_a}{1+W(\nu)} - D_i, & \text{else if } \frac{x_a}{1+W(\nu)} > D_i \\ 0, & \text{otherwise} \end{cases}
\end{aligned} \tag{2.12}$$

where W is the Lambert function, $\nu = \frac{\alpha P_C |h_{j,k}|^2 - P_N}{P_N e}$, $c_1 = e^{\frac{x_a}{D_j}} \frac{x_a}{D_j} - e^{\frac{x_a}{D_j}} + 1 - \frac{\alpha P_C |h_{j,k}|^2}{P_N}$, and $x_a = \frac{(r+1)N_i \ln 2}{B}$.

Proof. The optimal power and time allocation can be determined by solving the reduced optimization problem in (2.11). This problem is not convex due to the multiplication of

the optimization variables in the objective function. However, the equivalent sequential optimization problem that consists of two convex problems can be constructed by defining two partial optimization problems for power and time variables. The minimized version of f_1 with respect to power variables is given by

$$\tilde{f}_1(T_j) = inf\{f_1(P^1_{j,k}, P^2_{j,k}, T_j) | \boldsymbol{f_{c1}} \leq 0\}. \tag{2.13}$$

The optimization problem to solve $\tilde{f}_1(T_j)$ can be given as

$$\min_{P^1_{j,k}, P^2_{j,k}} \quad f_1 = D_i P^1_{j,k} + T_j P^2_{j,k} + T_j \alpha P_C \tag{2.14a}$$

$$\text{s.t.} \quad rN_i - BD_i \log_2(1 + \frac{P^1_{j,k}|h_{j,k}|^2}{2^{\frac{N_i}{BD_i}} P_N}) - BT_j \log_2(1 + \frac{P^2_{j,k}|h_{j,k}|^2}{P_N}) \leq 0, \tag{2.14b}$$

$$-P^1_{j,k} \leq 0, \quad -P^2_{j,k} \leq 0. \tag{2.14c}$$

The Lagrangian of this problem is

$$L(P^1_{j,k}, P^2_{j,k}, \boldsymbol{\mu}) = D_i P^1_{j,k} + T_j P^2_{j,k} + T_j \alpha P_C + \boldsymbol{\mu}^T \boldsymbol{g_1}, \tag{2.15a}$$

$$\boldsymbol{g_1} = [g_{11}\ g_{12}\ g_{13}]^T, \tag{2.15b}$$

$$g_{11} = -\frac{BD_i}{\ln 2} \ln(\frac{2^{\frac{N_i}{BD_i}} P_N + P^1_{j,k}|h_{j,k}|^2}{2^{\frac{N_i}{BD_i}} P_N}) - \frac{BT_j}{\ln 2} \ln(\frac{P_N + P^2_{j,k}|h_{j,k}|^2}{P_N}) + rN_i, \tag{2.15c}$$

$$g_{12} = -P^1_{j,k}, \quad g_{13} = -P^2_{j,k}. \tag{2.15d}$$

where $\boldsymbol{\mu} = [\mu_1\ \mu_2\ \mu_3]^T$ is the vector of Karush-Kuhn-Tucker (KKT) multipliers, and g_{1i} are the constraint functions. The optimization problem in (2.14) is convex if the Hessian of $g_{11}(P^1_{j,k}, P^2_{j,k})$ in (2.15c) is positive semi-definite since the rest of the equations are linear. The Hessian is given by

$$H(g_{11}) = \begin{bmatrix} \frac{BD_i}{\left(2^{\frac{N_i}{BD_i}} \frac{P_N}{|h_{j,k}|^2} + P^1_{j,k}\right)^2 \ln 2} & 0 \\ 0 & \frac{BT_j}{\left(\frac{P_N}{|h_{j,k}|^2} + P^2_{j,k}\right)^2 \ln 2} \end{bmatrix}, \tag{2.16}$$

which is positive semi-definite since the diagonal terms are larger than or equal to zero for every feasible value of the optimization parameters and the constants. Therefore, this problem can be solved by convex optimization techniques, and KKT conditions

are satisfied at the global minimum. The KKT conditions of this problem are

$$\frac{\partial L}{\partial P_{j,k}^1} = D_i - D_i\mu_1 \frac{B|h_{j,k}|^2}{\ln 2\big(2^{\frac{N_i}{BD_i}} P_N + P_{j,k}^1|h_{j,k}|^2\big)} - \mu_2 = 0, \tag{2.17a}$$

$$\frac{\partial L}{\partial P_{j,k}^2} = T_j - T_j\mu_1 \frac{B|h_{j,k}|^2}{\ln 2\big(P_N + P_{j,k}^2|h_{j,k}|^2\big)} - \mu_3 = 0, \tag{2.17b}$$

$$\boldsymbol{g_1^T \mu} = 0. \tag{2.17c}$$

Constraint g_{11} shall be satisfied as equality to avoid extra transmission power or transmission time than the required amount. In this solution, we consider $P_{j,k}^1 > 0$; thus, constraint g_{12} is satisfied as inequality. The constraint g_{13} shall not be satisfied as equality because it is more energy efficient for user j to transmit in the time interval T_j due to the lower interference than D_i. Therefore, μ_2 and μ_3 are equal to zero. We derive two expressions for μ_1, from (2.17a) and (2.17b) as

$$\mu_1 = \frac{\ln 2\big(2^{\frac{N_i}{BD_i}} P_N + P_{j,k}^1|h_{j,k}|^2\big)}{B|h_{j,k}|^2}, \quad \mu_1 = \frac{\ln 2\big(P_N + P_{j,k}^2|h_{j,k}|^2\big)}{B|h_{j,k}|^2}, \tag{2.18}$$

where μ_1 is greater than zero, as required by KKT conditions. Utilizing the expressions of μ_1 in (2.18), we can find a relation between $P_{j,k}^1$, and $P_{j,k}^2$ as follows

$$P_{j,k}^1 + \big(2^{\frac{N_i}{BD_i}} - 1\big)\frac{P_N}{|h_{j,k}|^2} = P_{j,k}^2, \tag{2.19}$$

which can be combined with (2.15c) to determine $P_{j,k}^1$, and $P_{j,k}^2$ as

$$\begin{aligned} P_{j,k}^1 &= \frac{P_N}{|h_{j,k}|^2}(2^{\frac{(r+1)N_i}{B(T_j+D_i)}} - 2^{\frac{N_i}{BD_i}}), \\ P_{j,k}^2 &= \frac{P_N}{|h_{j,k}|^2}(2^{\frac{(r+1)N_i}{B(T_j+D_i)}} - 1). \end{aligned} \tag{2.20}$$

The second partial optimization problem that depends on the time variable can be given as

$$\min_{T_j} \quad \tilde{f}_1 = D_i\frac{P_N}{|h_{j,k}|^2}(2^{\frac{(r+1)N_i}{B(T_j+D_i)}} - 2^{\frac{N_i}{BD_i}}) + T_j\frac{P_N}{|h_{j,k}|^2}(2^{\frac{(r+1)N_i}{B(T_j+D_i)}} - 1) + T_j\alpha P_C, \tag{2.21a}$$

$$\text{s.t.} \quad -T_j \le 0, \quad T_j - D_j + D_i \le 0. \tag{2.21b}$$

The objective function can be simplified by converting power of 2 terms to power of e

terms and getting rid of the constant term $D_i 2^{\frac{N_i}{BD_i}}$. The simplified $\tilde{f}_1(T_j)$ is given by

$$\tilde{f}_1 = D_i \frac{P_N}{|h_{j,k}|^2}(e^{\frac{(r+1)N_i \ln 2}{B(T_j+D_i)}}) + T_j \frac{P_N}{|h_{j,k}|^2}(e^{\frac{(r+1)N_i \ln 2}{B(T_j+D_i)}} - 1) + T_j \alpha P_C. \tag{2.22a}$$

Since the constraint functions are linear, the optimization problem in (2.21) is convex if the second derivative of $\tilde{f}_1$ with respect to T_j is greater than zero. The second derivative of $\tilde{f}_1$ is given by

$$\frac{d^2 \tilde{f}_1}{dT_j^2} = e^{\frac{\frac{(r+1)N_i \ln 2}{B}}{T_j+D_i}} \frac{\left(\frac{(r+1)N_i \ln 2}{B}\right)^2}{(T_j+D_i)^3}, \tag{2.23}$$

which is always positive for the valid values of the parameters, therefore, the optimization problem is convex. The Lagrangian for the problem is given by

$$L(T_j) = \tilde{f}_1(T_j) + \mu_1(T_j - D_j + D_i) - \mu_2 T_j, \tag{2.24}$$

where μ_2 is always set to zero since the constraint $T_j \geq 0$ shall be satisfied as inequality. The derivative of the Lagrangian can be expressed as

$$\begin{aligned} \frac{dL}{dT_j} &= e^{\frac{x_a}{T_j+D_i}} - e^{\frac{x_a}{T_j+D_i}} \frac{x_a}{T_j+D_i} - 1 + \frac{\alpha P_C |h_{j,k}|^2}{P_N} + \mu_1, \\ x_a &= \frac{(r+1)N_i \ln 2}{B}. \end{aligned} \tag{2.25}$$

The constraint $T_j \leq D_j - D_i$ can be satisfied as equality or inequality. The KKT multiplier μ_1 shall be greater than or equal to zero when the constraint is satisfied as equality. The condition for this is given by

$$c_1 = e^{\frac{x_a}{D_j}} \frac{x_a}{D_j} - e^{\frac{x_a}{D_j}} + 1 - \frac{\alpha P_C |h_{j,k}|^2}{P_N} \geq 0. \tag{2.26}$$

If the constraint is satisfied as inequality, then the solution could be determined with the help of the Lambert W function as follows

$$\begin{aligned} e^{\frac{x_a}{T_j+D_i}} \frac{x_a}{T_j+D_i} - e^{\frac{x_a}{T_j+D_i}} &= \frac{\alpha P_C |h_{j,k}|^2}{P_N} - 1, \\ e^{\frac{x_a}{T_j+D_i}-1} \left(\frac{x_a}{T_j+D_i} - 1\right) &= \frac{\alpha P_C |h_{j,k}|^2 - P_N}{P_N e}, \\ \frac{x_a}{T_j+D_i} - 1 &= W\left(\frac{\alpha P_C |h_{j,k}|^2 - P_N}{P_N e}\right), \\ T_j &= \frac{x_a}{1 + W\left(\frac{\alpha P_C |h_{j,k}|^2 - P_N}{P_N e}\right)} - D_i, \\ T_j &= \frac{x_a}{1 + W(\nu)} - D_i, \end{aligned} \tag{2.27}$$

where $\nu = \frac{\alpha P_C |h_{j,k}|^2 - P_N}{P_N e}$. □

Remark 2.2. *Theorem 2.1 extends the results given in [36–38]. Theorem 2.1 has no restriction on the data offloading requirement of the users, whereas the results in [36–38] are only applicable for users with the same data offloading requirement. Additionally, Theorem 2.1 considers the constant circuit power in the energy consumption calculations.*

Corollary 2.3. *The power and time allocation for OMA in Scenario A is given by*

$$\begin{aligned} P_{i,k} &= \frac{P_N}{|h_{i,k}|^2}(2^{\frac{N_i}{BD_i}} - 1), \\ P_{j,k}^2 &= \frac{P_N}{|h_{j,k}|^2}(2^{\frac{rN_i}{B(D_j - D_i)}} - 1), \\ T_j &= (D_j - D_i). \end{aligned} \tag{2.28}$$

Proof. The time allocation is done according to the latency constraints, and the power allocation follows from the rate equations. □

The solution to the problem in (2.11) reduces to the OMA solution, when applying NOMA is not feasible. The feasibility condition is described in Corollary 2.4.

Corollary 2.4. *The feasibility of NOMA for user j in Scenario A is given by*

$$(P_{j,k}^1 > 0)\,\&\,(E_{NOMA} < E_{OMA}). \tag{2.29}$$

Proof. The solution given in Theorem 2.1 is only applicable if $P_{j,k}^1 > 0$. Moreover, NOMA shall only be activated if it is more efficient than OMA. □

2.3.2. Scenario B

In Scenario B, user i has the higher channel gain, therefore, it is selected as the affected user and s parameter is set to zero. The simplified optimization problem for this scenario is given by

$$\min_{P_{i,k},P_{j,k},T_j} \quad f_2(P_{i,k}, P_{j,k}^1, P_{j,k}^2, T_j) = D_i P_{i,k} + D_i P_{j,k}^1 + T_j P_{j,k}^2 + \alpha P_C T_j \tag{2.30a}$$

$$\text{s.t.} \quad N_i - BD_i \log_2(1 + \tfrac{P_{i,k}|h_{i,k}|^2}{P_N + P_{j,k}^1 |h_{j,k}|^2}) \leq 0, \tag{2.30b}$$

$$rN_i - BD_i \log_2(1 + \tfrac{P^1_{j,k}|h_{j,k}|^2}{P_N}) \tag{2.30c}$$

$$- BT_j \log_2(1 + \tfrac{P^2_{j,k}|h_{j,k}|^2}{P_N}) \leq 0, \tag{2.30d}$$

$$P^1_{j,k} \geq 0, \quad P^2_{j,k} \geq 0, \quad P_{i,k} \geq 0, \tag{2.30e}$$

$$T_j \geq 0, \quad T_j \leq (D_j - D_i), \tag{2.30f}$$

where we call the vector of constraint functions related to the power variables $\boldsymbol{f_{c2}}$. The solution to the problem with $P^1_{j,k} > 0$ is given by Theorem 2.5.

Theorem 2.5. *Optimal power and time allocation in Scenario B is shown by*

$$\begin{aligned}
P_{i,k} &= \frac{P_N 2^{\frac{rN_i}{B(T_j+D_i)}}(2^{\frac{N_i}{BD_i}} - 1)(|h_{i,k}|^2)^{-\frac{D_i}{T_j+D_i}}}{(|h_{j,k}|^2(2^{\frac{N_i}{BD_i}} - 1) + |h_{i,k}|^2)^{(1-\frac{D_i}{T_j+D_i})}}, \\
P^1_{j,k} &= \frac{P_{i,k}|h_{i,k}|^2}{(2^{\frac{N_i}{BD_i}} - 1)|h_{j,k}|^2} - \frac{P_N}{|h_{j,k}|^2}, \\
P^2_{j,k} &= P_{i,k} + \frac{P_{i,k}|h_{i,k}|^2}{(2^{\frac{N_i}{BD_i}} - 1)|h_{j,k}|^2} - \frac{P_N}{|h_{j,k}|^2}, \\
T_j &= \begin{cases} D_j - D_i, & \text{if } c_2 \geq 0 \\ \frac{x_c}{1+W(\nu)} - D_i, & \text{else if } \frac{x_c}{1+W(\nu)} > D_i \\ 0, & \text{otherwise} \end{cases}
\end{aligned} \tag{2.31}$$

where $c_2 = e^{\frac{x_c}{D_j}}\frac{x_c}{D_j} - e^{\frac{x_c}{D_j}} + 1 - \frac{\alpha P_C|h_{j,k}|^2}{P_N}$, $x_c = \ln(c_i + 1)D_i + x_b$, *and* $x_b = \frac{rN_i \ln 2}{B}$.

Proof. The optimal power and time allocation can be determined by solving the optimization problem in (2.30). This problem is not convex due to the multiplication of the optimization variables in the objective function. However, the equivalent sequential optimization problem that consists of two convex problems can be constructed by defining two partial optimization problems for power and time variables similar to Scenario A. The minimized version of f_2 with respect to power variables is given by

$$\tilde{f}_2(T_j) = inf\{f_2(P_{i,k}, P^1_{j,k}, P^2_{j,k}, T_j) | \boldsymbol{f_{c2}} \leq 0\}. \tag{2.32}$$

The optimization problem to solve $\tilde{f}_2(T_j)$ can be given as

$$\min_{P_{i,k}, P^1_{j,k}, P^2_{j,k}} \quad f_2 = D_i P_{i,k} + D_i P^1_{j,k} + T_j P^2_{j,k} + T_j \alpha P_C \tag{2.33a}$$

$$\text{s.t.} \quad N_i - BD_i \log_2(1 + \tfrac{P_{i,k}|h_{i,k}|^2}{P_N + P^1_{j,k}|h_{j,k}|^2}) \leq 0, \tag{2.33b}$$

$$rN_i - BD_i \log_2(1 + \tfrac{P^1_{j,k}|h_{j,k}|^2}{P_N})$$
$$- BT_j \log_2(1 + \tfrac{P^2_{j,k}|h_{j,k}|^2}{P_N}) \leq 0, \tag{2.33c}$$
$$- P_{i,k} \leq 0, \quad -P^1_{j,k} \leq 0, \quad -P^2_{j,k} \leq 0. \tag{2.33d}$$

The Lagrangian of this problem is

$$L(P_{i,k}, P^1_{j,k}, P^2_{j,k}, \boldsymbol{\mu}) = D_i P_{i,k} + D_i P^1_{j,k} + T_j P^2_{j,k} + \boldsymbol{\mu}^T \boldsymbol{g}, \tag{2.34a}$$
$$\boldsymbol{g_2} = [g_{21}\ g_{22}\ g_{23}\ g_{24}\ g_{25}]^T, \tag{2.34b}$$
$$g_{21} = -\tfrac{BD_i}{\ln 2} \ln(1 + \tfrac{P_{i,k}|h_{i,k}|^2}{P_N + P^1_{j,k}|h_{j,k}|^2}) + N_i, \tag{2.34c}$$
$$g_{22} = -\tfrac{BD_i}{\ln 2} \ln(1 + \tfrac{P^1_{j,k}|h_{j,k}|^2}{P_N}) - \tfrac{BT_j}{\ln 2} \ln(1 + \tfrac{P^2_{j,k}|h_{j,k}|^2}{P_N}) + rN_i, \tag{2.34d}$$
$$g_{23} = -P^1_{j,k}, \quad g_{24} = -P^2_{j,k}, \quad g_{25} = -P_{i,k,}, \tag{2.34e}$$

where $\boldsymbol{\mu} = [\mu_1\ \mu_2\ \mu_3\ \mu_4\ \mu_5]^T$ is the vector of KKT multipliers, and g_{2i} are the constraint functions. The optimization problem in (2.33) is convex if the Hessian of $g_{22}(P_{i,k}, P^1_{j,k}, P^2_{j,k})$ in (2.34d) is positive semi-definite since (2.34c) can be written in linear form as $(2^{\frac{N_i}{BD_i}} - 1)(P_N + P^1_{j,k}|h_{j,k}|^2) - P_{i,k}|h_{i,k}|^2 \leq 0$, and the rest of the equations are linear. The Hessian is given by

$$H(g_{22}) = \begin{bmatrix} 0 & 0 & 0 \\ 0 & \frac{BD_i}{\left(\frac{P_N}{|h_{j,k}|^2} + P^1_{j,k}\right)^2 \ln 2} & 0 \\ 0 & 0 & \frac{BT_j}{\left(\frac{P_N}{|h_{j,k}|^2} + P^2_{j,k}\right)^2 \ln 2} \end{bmatrix} \tag{2.35}$$

which is positive semi-definite since the diagonal terms are larger than or equal to zero for every feasible value of the optimization parameters and the constants. Therefore, this problem can be solved by convex optimization techniques, and KKT conditions are equivalent to the global minimum. The KKT conditions of this problem are:

$$\frac{\partial L}{\partial P_{i,k}} = D_i - \frac{D_i \frac{B}{\ln 2}|h_{i,k}|^2}{P_N + P^1_{j,k}|h_{j,k}|^2 + P_{i,k}|h_{i,k}|^2}\mu_1 - \mu_5 = 0, \tag{2.36a}$$
$$\frac{\partial L}{\partial P^1_{j,k}} = D_i - \frac{D_i \frac{B}{\ln 2}|h_{j,k}|^2}{P_N + P^1_{j,k}|h_{j,k}|^2} \left(\mu_2 - \frac{P_{i,k}\mu_1|h_{i,k}|^2}{(P_N + P^1_{j,k}|h_{j,k}|^2 + P_{i,k}|h_{i,k}|^2)}\right)$$
$$- \mu_3 = 0, \tag{2.36b}$$
$$\frac{\partial L}{\partial P^2_{j,k}} = T_j - \frac{T_j \frac{B}{\ln 2}|h_{j,k}|^2}{P_N + P^2_{j,k}|h_{j,k}|^2}\mu_2 - \mu_4 = 0, \tag{2.36c}$$
$$\boldsymbol{g^T \mu} = 0. \tag{2.36d}$$

Constraints g_1 and g_2 shall be satisfied as equalities to avoid extra transmission power or transmission time than the required amount. In this solution, we consider $P^1_{j,k} > 0$; thus, constraint g_3 is satisfied as inequality. The constraint g_4 shall be satisfied as inequality because the more user j transmits in the time interval T_j, the less energy is consumed by user i in the time interval D_i. The constraint g_5 cannot be satisfied as equality since the Shannon Rate would be zero for zero transmission power. Therefore, μ_3, μ_4, and μ_5 are equal to zero. We determine μ_1, and μ_2 from (2.36a) and (2.36c) as

$$\mu_1 = \frac{\ln 2(P_N + P^1_{j,k}|h_{j,k}|^2 + P_{i,k}|h_{i,k}|^2)}{B|h_{i,k}|^2}, \quad \mu_2 = \frac{\ln 2(P_N + P^2_{j,k}|h_{j,k}|^2)}{B|h_{j,k}|^2}, \tag{2.37}$$

where μ_1 and μ_2 are greater than zero, as KKT conditions require. Utilizing the values of μ_1 and μ_2 in (2.37) and (2.36b); we can express the relation of the powers as

$$P^2_{j,k} = P^1_{j,k} + P_{i,k}. \tag{2.38}$$

Utilizing (2.34c) and (2.38), we can determine $P^1_{j,k}$, $P^2_{j,k}$ in terms of $P_{i,k}$ as

$$\begin{aligned} P^1_{j,k} &= \frac{P_{i,k}|h_{i,k}|^2}{(2^{\frac{N_i}{BD_i}} - 1)|h_{j,k}|^2} - \frac{P_N}{|h_{j,k}|^2}, \\ P^2_{j,k} &= P_{i,k} + \frac{P_{i,k}|h_{i,k}|^2}{(2^{\frac{N_i}{BD_i}} - 1)|h_{j,k}|^2} - \frac{P_N}{|h_{j,k}|^2}. \end{aligned} \tag{2.39}$$

Finally, substituting the values of $P^1_{j,k}$, and $P^2_{j,k}$ into (2.34c), we show that

$$P_{i,k} = \frac{P_N 2^{\frac{rN_i}{B(D_i+T_j)}}(2^{\frac{N_i}{BD_i}} - 1)(|h_{i,k}|^2)^{\frac{-D_i}{D_i+T_j}}}{(|h_{j,k}|^2(2^{\frac{N_i}{BD_i}} - 1) + |h_{i,k}|^2)^{\frac{T_j}{D_i+T_j}}}. \tag{2.40}$$

Akin to Scenario A, the optimal power values can be substituted into the second partial optimization problem that depends on the time variable, and the reduced form of the resulting problem is given by

$$\begin{aligned} \min_{T_j} \quad & \tilde{f}_2 = \frac{P_N(D_i + T_j)}{|h_{j,k}|^2} 2^{\frac{rN_i}{B(D_i+T_j)}} \left((2^{\frac{N_i}{BD_i}} - 1)\frac{|h_{j,k}|^2}{|h_{i,k}|^2} + 1\right)^{\frac{D_i}{D_i+T_j}} \\ & - \frac{P_N T_j}{|h_{j,k}|^2} + T_j \alpha P_C \qquad (2.41a) \\ \text{s.t.} \quad & -T_j \leq 0, \quad T_j - D_j + D_i \leq 0. \qquad (2.41b) \end{aligned}$$

which is convex if the second derivative of $\tilde{f}_2$ with respect to T_j is greater than zero

since the constraint functions are linear. The second derivative of $\tilde{f}_2$ is

$$\begin{aligned}
\frac{d^2\tilde{f}_1}{dT_j^2} &= \frac{c_i^{\frac{D_i}{T_j+D_i}}\left(x_b + D_i\ln\left(c_i\right)\right)^2 \mathrm{e}^{\frac{x_b}{T_j+D_i}}}{|h_{j,k}|^2\left(T_j+D_i\right)^3},\\
c_i &= \frac{2^{\frac{N_i}{BD_i}}|h_{j,k}|^2 + |h_{i,k}|^2}{|h_{i,k}|^2},\\
x_b &= \frac{\ln\left(2\right)N_i r}{B},
\end{aligned} \tag{2.42}$$

which is always non-negative for the feasible parameters. Therefore, the time optimization problem is a convex problem. The Lagrangian for the problem is given by

$$L(T_j) = \tilde{f}_2(T_j) + \mu_1(T_j - D_j + D_i) - \mu_2 T_j, \tag{2.43}$$

where μ_2 is always set to zero since the constraint $T_j \geq 0$ shall be satisfied as inequality. The derivative of the Lagrangian can be expressed as

$$\begin{aligned}
\frac{dL}{dT_j} &= e^{\frac{x_c}{T_j+D_i}} - e^{\frac{x_c}{T_j+D_i}}\frac{x_c}{T_j+D_i} - 1 + \frac{\alpha P_C|h_{j,k}|^2}{P_N} + \mu_1,\\
x_c &= \ln(c_i+1)D_i + x_b.
\end{aligned} \tag{2.44}$$

The constraint $T_j \leq D_j - D_i$ can be satisfied as equality or inequality. The KKT multiplier μ_1 shall be greater than or equal to zero when the constraint is satisfied as equality. The condition for this is given by

$$c_2 = e^{\frac{x_c}{D_j}}\frac{x_c}{D_j} - e^{\frac{x_c}{D_j}} + 1 - \frac{\alpha P_C|h_{j,k}|^2}{P_N} \geq 0. \tag{2.45}$$

If the constraint is satisfied as inequality, then the solution could be determined with the help of the Lambert W function as follows

$$\begin{aligned}
e^{\frac{x_c}{T_j+D_i}}\frac{x_c}{T_j+D_i} - e^{\frac{x_c}{T_j+D_i}} &= \frac{\alpha P_C|h_{j,k}|^2}{P_N} - 1,\\
e^{\frac{x_c}{T_j+D_i}-1}\left(\frac{x_c}{T_j+D_i} - 1\right) &= \frac{\alpha P_C|h_{j,k}|^2 - P_N}{P_N e},\\
\frac{x_c}{T_j+D_i} - 1 &= W\left(\frac{\alpha P_C|h_{j,k}|^2 - P_N}{P_N e}\right),\\
T_j &= \frac{x_c}{1+W\left(\nu\right)} - D_i.
\end{aligned} \tag{2.46}$$

□

Remark 2.6. *Theorem 2.5 is one of the major theoretical contributions of this chapter, and it gives the solution with a different affected user selection compared to H-NOMA in [36–38]. The SH-NOMA scheme is always more energy efficient than H-NOMA when user i has the larger channel gain due to this switching. The difference in the energy consumption is shown in Section 2.5 analytically and in Section 2.6 by simulations. Additionally, Theorem 2.5 considers the constant circuit power in the energy consumption calculations.*

The solution to the problem in (2.30) with OMA is the same as in Corollary 2.3. The solution to the problem in (2.30) reduces to the OMA solution when applying NOMA is not feasible. The feasibility condition is the same as Corollary 2.4.

2.4. Sub-channel Allocation

The equivalent SCA problem to the problem in (2.9) can be presented by

$$\min_{\Psi,P_{i,k},P^1_{j,k},P^2_{j,k},T_j} \quad \tilde{f}_0(\Psi) = \sum_{i=1}^{2K-1}\sum_{j=i+1}^{2K}\sum_{k=1}^{K}\psi_{i,j,k}[(P^s_{i,k}+P^{1,s}_{j,k})D_i + P^{2,s}_{j,k}T^s_j] \tag{2.47a}$$

$$\text{s.t.} \quad \psi_{i,j,k}\in\{0,1\} \quad \forall i,j,k, \quad \sum_i\sum_j \psi_{i,j,k}=2, \quad \forall k, \tag{2.47b}$$

$$\sum_j\sum_k \psi_{i,j,k}=1, \quad \forall i, \quad \sum_i\sum_k \psi_{i,j,k}=1, \quad \forall j, \tag{2.47c}$$

where $P^s_{i,k}$, $P^{1,s}_{j,k}$, $P^{2,s}_{j,k}$, and T^s_j are the optimal solutions derived from the partial optimization problem $\tilde{f}_0(\Psi)$ for every possible matching on every sub-channel. Although this problem has a lower complexity compared to (2.6), it is a three-dimensional assignment problem (3DAP), which is shown to be NP-complete [80]. The global-optimal solution can be found by the EXS algorithm, which is highly complex. We propose the TES algorithm with lower complexity for the analyzed problem. Moreover, we study the 2ES algorithm [81], which is a widely used game theoretic algorithm for NOMA SCA problems [9, 35, 38].

2.4.1. Description of the TES Algorithm

The TES algorithm is a game theoretic algorithm for the matching problem based on the compensational stability notion in [82]. The TES algorithm starts with a random initial assignment in which all agents are paired and assigned to sub-channels. Then, each agent searches through the agents for a swapping opportunity. The swap is allowed if the total reward in the system is increased after the swap. This condition corresponds to the reduction of the total energy consumption of the system for our scenario. The total reward calculation is based on a cost matrix M_E with dimensions $(2K \times 2K \times K)$ which contains the energy consumption values for every possible permutation of user pairings and sub-channel allocations. The algorithm halts when the maximum number of iterations is reached, or no swap is allowed at an iteration. The steps of the TES algorithm are given in Figure 2.3. Next, we analyze the convergence and the stability of the TES algorithm.

Theorem 2.7. *The TES algorithm converges to a total-reward exchange stable solution.*

Proof. First, we prove that the solution of the algorithm is total-reward exchange stable. Since users look for all the swapping opportunities at each iteration, if the algorithm halts at a specific matching, there cannot be a swap that would decrease the total energy consumption. Thus, the final matching is total-reward exchange stable. Then, the convergence can be proven as follows. Before the algorithm halts, at least one swap occurs at each iteration. The users can perform a swap operation if and only if the total energy consumption of the system decreases after the swap. Since the initial total energy consumption and the number of users are bounded, the algorithm shall always converge to a solution in a finite number of iterations. □

Remark 2.8. *Theorem 2.7 states that the TES algorithm converges to a stable solution, which has not been given in the literature. Therefore, the TES algorithm can be applied to resource allocation problems where the 2ES algorithm is utilized [9, 35, 38].*

Input: Energy consumption matrix for every possible user and sub-channel permutation (M_E).

Output: Stable pairing matrix M_P.

Randomly initialize the pairing matrix (M_P), set $idx = 0$ and $swaps = 1$.
while $(idx < max)\&(swaps > 0)$ **do**
  Increment idx and set $swaps = 0$.
  for $(idx_s < 2K)$ **do**
    for $(idx_e < 2K)$ **do**
      Initialize $M_P^s = M_P$, and then swap the users idx_u and idx_e.
      Calculate the original energy consumption E_T by summing all elements of $M_P \odot M_E$.
      Calculate the swapped energy consumption E_T^s by summing all elements of $M_P^s \odot M_E$.
      if $E_T^s < E_T$ **then**
        Approve the swap, increment $swaps$, and set $M_P = M_P^s$.
      end if
    end for
  end for
end while
return M_P

Figure 2.3. TES algorithm.

The number of iterations for the exchange-stable algorithms such as TES or 2ES to converge cannot be determined analytically [9, 81, 82]. However, in Section 2.6, we show that the maximum number of iterations can be limited with almost no effect on the resulting energy consumption. Furthermore, we demonstrate by simulations that the TES algorithm performs close to the optimal solution.

2.4.2. Complexity Analysis

The EXS algorithm compares all possible permutations for $2K$ users assigned to K sub-channels, disregarding the ordering within the pairs. The number of different pairs in such a setting is $\frac{(2K)!}{2^K}$, which can be approximated using Stirling's approximation for factorials as K^{2K} [83]. In Big-O notation, the complexity is equivalent to $O(N^N)$.

For both of the exchange stable (ES) algorithms, the following steps are executed. First, a three-dimensional cost matrix needs to be constructed, which needs $2K^3$ operations. Then, $2K(2K-2)$ comparisons shall be made at each iteration, where the number of iterations is denoted as C. Since C cannot be determined for ES algorithms [9,81,82], the complexity can be determined by bounding the number of allowed iterations. The total number of computations for ES algorithms is $2K^3+C\,2K\,(2K-2)$, which is in the order of $O(N^3)$ for $C \leq K$. To avoid increasing the complexity, we limit the number of iterations to K, which does not cause any performance degradation, as shown in Section 2.6.

2.5. Analytical Results

In this section, we analytically compare the proposed methods to the existing methods in the literature. First, we compare the optimal SH-NOMA multiplexing to the H-NOMA multiplexing in the literature. Then, we move on to the SCA problem and show that the TES algorithm outperforms the 2ES algorithm by induction.

2.5.1. Analytical Comparison of SH-NOMA to H-NOMA

We have stated in Section 2.3 that the H-NOMA solution in [36–38] is a special case of the SH-NOMA solution in Scenario A with equal offloading data requirements and no constant circuit power consumption. Since the H-NOMA method is only applicable for equal data offloading cases, we limit our comparison to $r = 1$. Additionally,

T_j is optimally determined for SH-NOMA concerning the constant circuit power P_C. In contrast, it is set to $D_j - D_i$ for H-NOMA since constant circuit power is neglected while deriving the H-NOMA resource allocation [36–38]. Therefore, in this section, we assume $P_C = 0$ to show that SH-NOMA outperforms H-NOMA even when the circuit power is not considered. The power allocation scheme for H-NOMA is the same for both scenarios, and it is equal to the solution in (2.12) with $r = 1$. Thus, in Scenario A, H-NOMA and SH-NOMA are identical for $r = 1$ and $P_C = 0$. On the other hand, in Scenario B, H-NOMA and SH-NOMA methods have different power allocations given by (2.12) and (2.31) with $r = 1$ and $P_C = 0$, respectively.

Corollary 2.9. *SH-NOMA is more energy efficient than H-NOMA [36–38].*

Proof. In Scenario A, the energy consumption of both methods are the same. In Scenario B, the time allocations are the same, but the power allocations are different. The energy consumption for a pair is given by $E = D_i P_{i,k} + D_i P^1_{j,k} + T_j P^2_{j,k}$. The energy consumption difference between SH-NOMA, and H-NOMA is defined as $\Delta E = E_{SH} - E_H$, which can be calculated by substituting the power and time allocations from (2.12) and (2.31) as

$$\begin{aligned} \Delta E &= 2^{\frac{N_i}{BD_j}}[(2^{\frac{N_i}{BD_i}} - 1)\frac{|h_{j,k}|^2}{|h_{i,k}|^2} + 1]^{\frac{D_i}{D_j}} - 2^{\frac{2N_i}{BD_j}} - \frac{D_i}{D_j}(\frac{|h_{j,k}|^2}{|h_{i,k}|^2} - 1)(2^{\frac{N_i}{BD_i}} - 1), \\ \Delta E &\leq \Delta E_U = -\frac{D_i}{D_j}(\frac{|h_{j,k}|^2}{|h_{i,k}|^2} - 1)(2^{\frac{N_i}{BD_i}} - 1) \leq 0. \end{aligned} \tag{2.48}$$

where the inequality $[(2^{\frac{N_i}{BD_i}} - 1)\frac{|h_{j,k}|^2}{|h_{i,k}|^2} + 1]^{\frac{D_i}{D_j}} < 2^{\frac{N_i}{BD_j}}$ is utilized. □

2.5.2. Analytical Comparison of TES to 2ES

TES and 2ES algorithms behave the same except for how the swap-allowing decision is made. The TES algorithm considers the total change in the total energy consumption to allow a swap, whereas the 2ES algorithm considers the change in the energy consumption in each pair. To express this difference mathematically, we define $\Delta E_B = \Delta E_{P1} + \Delta E_{P2}$, where ΔE_B is the change in the total energy consumption of both pairs after the swap; and ΔE_{P1}, and ΔE_{P2} are the change in the energy

consumption of pair 1, and pair 2, respectively. The swap condition for TES algorithm is $\Delta E_B > 0$, whereas the swap condition for 2ES algorithm is $(\Delta E_{P1} \geq 0)\&(\Delta E_{P2} \geq 0)\&(\Delta E_B > 0)$. We show that TES always outperforms 2ES in Theorem 2.10.

Theorem 2.10. *The TES algorithm performs better or equal to the 2ES algorithm [9, 35, 38] regarding energy efficiency.*

Proof. From the swapping conditions of the TES and 2ES algorithms, it can be seen that the set of swaps allowed by the TES algorithm is a superset of the set of swaps allowed by the 2ES algorithm. Therefore, we can state that the TES algorithm would have more than or equal number of swaps than the 2ES algorithm for any given scenario. Since the energy consumption of the system decreases at each swap operation, the TES algorithm performs better than or the same as the 2ES algorithm regarding energy efficiency. □

2.6. Simulation Results

In this section, first, we compare SH-NOMA with OMA, NOMA, and H-NOMA multiplexing methods from the literature by simulations. Then, we combine these methods with the EXS algorithm to assess their performance. After showing the superiority of SH-NOMA to other methods, we continue with the SCA algorithms. We give the maximum number of iterations required for the TES algorithm to converge by Monte Carlo simulations. Then, we compare the proposed TES algorithm to the optimal EXS algorithm, and the widely used 2ES algorithm from the literature [9, 35, 38].

The simulation parameters are given in Table 2.1, where R is the cell radius, N_0 is the noise floor, and f_c is the carrier frequency. G is the receiver antenna gain, γ_L is the path loss exponent, and σ_S is the standard deviation of shadowing. B is the bandwidth of a single sub-channel, N_μ is the mean value of the data transmission requirements per user, D_μ is the mean value of the latency constraints per user, D_σ is the standard deviation of the latency constraints per user. α is the power amplifier efficiency, and P_C is the constant circuit power.

Table 2.1. Simulation parameters.

Symbol	Parameter	Value
R	Cell radius	$2000\,m$
N_0	Receiver noise floor	$-116\,dBm$
f_c	Carrier frequency	$800\,MHz$
G	Receive antenna gain	$18\,dB$
γ_L	Path loss exponent	3
σ_S	Shadowing loss standard deviation	$6\,dB$
B	Bandwidth of a single sub-channel	$180\,kHz$
N_μ	Mean value of the data transfer requirement	$500000\,bits$
D_μ	Mean value of the latency constraint	$2.25\,s$
D_σ	Standard deviation of the latency constraint	$\frac{1.5}{\sqrt{12}}\,s$
α	Power amplifier efficiency of the mobile device	0.35
P_C	Constant power consumption of the transmitter	$50\,mW$

2.6.1. Analysis of SH-NOMA for a single pair

The effects of the latency constraints on the performance can be analyzed to assess SH-NOMA in a single-pair scenario. For the analysis, the latency constraint of user j, which has the less strict latency constraint, is set to 3 seconds. The latency constraint of the other user is determined by the parameter $\frac{D_i}{D_j}$ ratio. Additionally, the channel gains of the users are set to constants to focus only on the effects of the latency constraints. In Scenario A, where $|h_i|^2 \leq |h_j|^2$, the channel gains are set as $|h_i|^2 = -123\,dBm$, and $|h_j|^2 = -108\,dBm$. In Scenario B, where $|h_i|^2 > |h_j|^2$, the channel gains are set as $|h_i|^2 = -108\,dBm$, and $|h_j|^2 = -125\,dBm$.

In Figure 2.4, the effect of the latency requirements is analyzed for a user pair in Scenario A with $P_C = 0$. As stated in Section 2.5, SH-NOMA and H-NOMA perform the same in this scenario. Additionally, it is evident that SH-NOMA outperforms NOMA and OMA. NOMA solution has the worst performance for smaller values of

$\frac{D_i}{D_j}$ ratio, and converges to SH-NOMA as the latency ratio is increased to one. This behavior is expected because NOMA is applied during D_i, and the energy required for transmission is reduced as the transmission time increases. OMA and SH-NOMA solutions perform the same until the switching point in Corollary 2.4. After the switching point, OMA performs worse than SH-NOMA due to the NOMA gain.

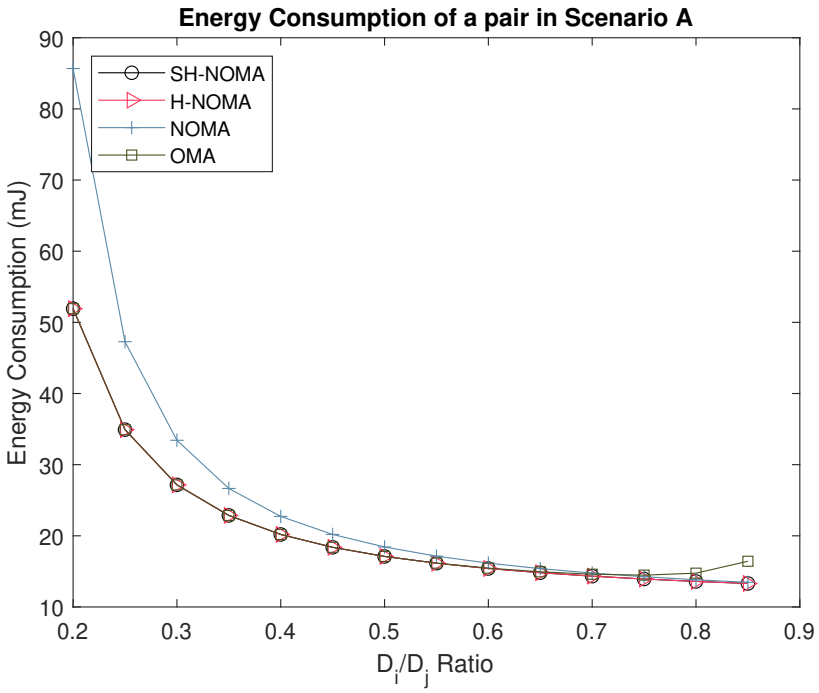

Figure 2.4. Energy consumption of a pair in scenario A with $P_C = 0$.

In Figure 2.5, the effect of the latency requirements is analyzed for a user pair in Scenario B with $P_C = 0$. As stated in Section 2.5, SH-NOMA performs better than H-NOMA in this scenario. Furthermore, it can be seen that SH-NOMA outperforms NOMA and OMA, similar to Scenario A. NOMA solution behaves the same as Scenario A since the channel gains of the users in the pair are swapped. OMA and SH-NOMA solutions perform the same until the switching point. After the switching point, OMA performs worse than SH-NOMA due to the NOMA gain.

In Figure 2.6, the effect of latency requirements is analyzed for a user pair in Scenario A with P_C taken into account. Due to the constant circuit power dissipation, the energy consumption is higher compared to Figure 2.4. SH-NOMA outperforms all other methods when applying NOMA is feasible. Otherwise, SH-NOMA falls back to

the OMA multiplexing. It can be seen that the performance of H-NOMA is severely degraded, and the switching to NOMA is not done in Scenario A. NOMA is also significantly affected by the constant circuit power and is more efficient than OMA when $\frac{D_i}{D_j} \in [0.20, 0.48]$.

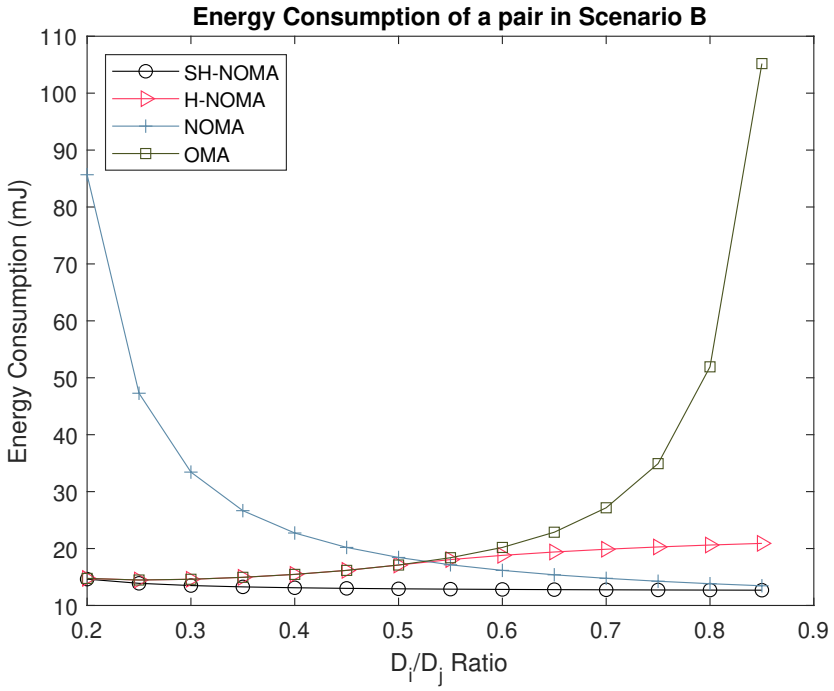

Figure 2.5. Energy consumption of a pair in scenario B with $P_C = 0$.

In Figure 2.7, the effect of latency requirements is analyzed for a user pair in Scenario B when P_C is taken into account. Similar to Scenario A, the energy consumption is higher compared to Figure 2.5 due to constant circuit power dissipation. SH-NOMA outperforms all other methods when applying NOMA is feasible. Otherwise, SH-NOMA falls back to the OMA multiplexing. It can be seen that the performance of H-NOMA is severely degraded. H-NOMA is activated only when $\frac{D_i}{D_j} > 0.8$ in Scenario B. NOMA is also significantly affected by the constant circuit power and is more efficient than OMA when $\frac{D_i}{D_j} \in [0.28, 0.48]$.

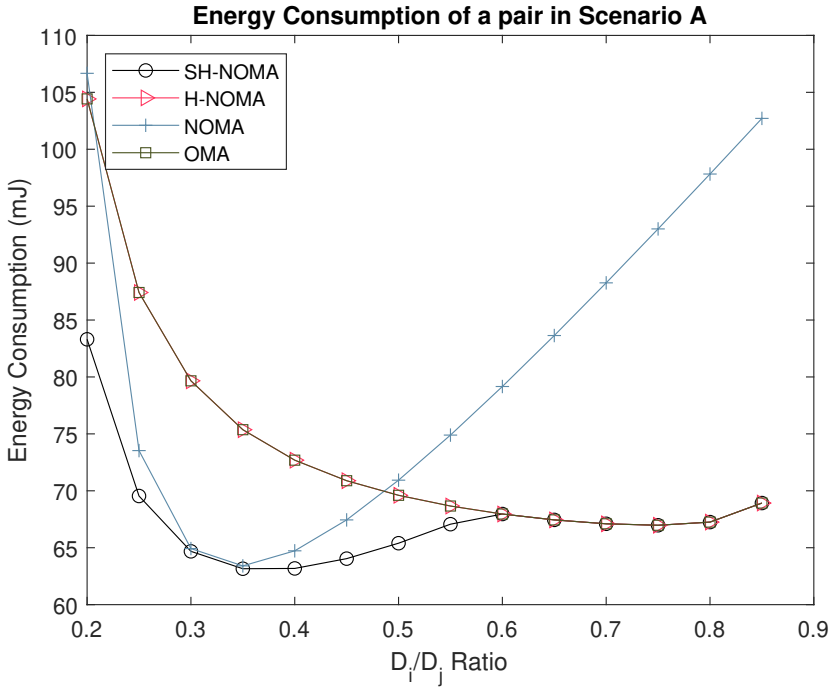

Figure 2.6. Energy consumption of a pair in scenario A with non-zero P_C.

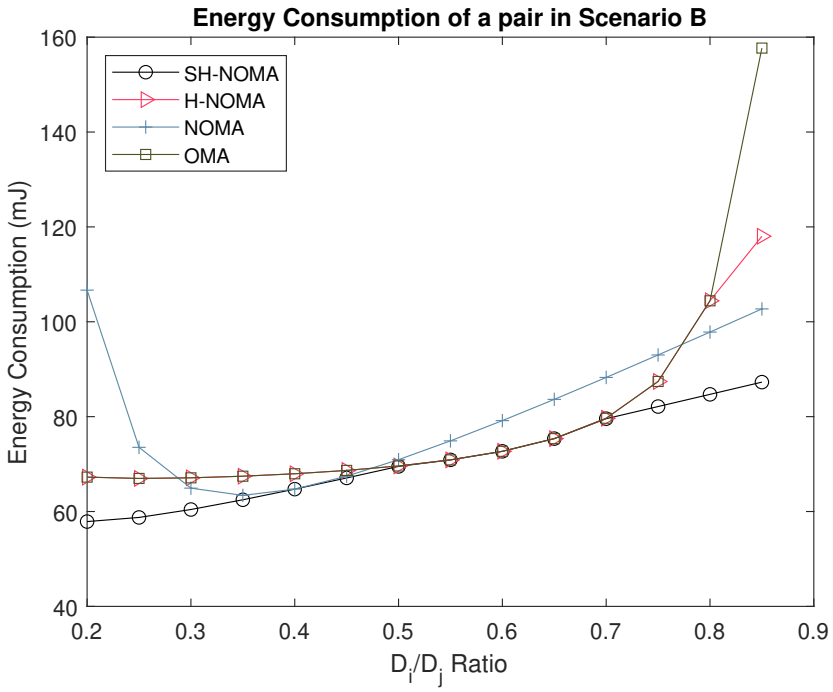

Figure 2.7. Energy consumption of a pair in scenario B with non-zero P_C.

2.6.2. Analysis of SH-NOMA with Optimal SCA

For this comparison, all users are assigned the same amount of data to be offloaded; because the H-NOMA method in the literature [36–38] cannot handle users with different data offloading requests. Therefore, N_u is set to N_μ for all the users. The total energy consumption comparison of SH-NOMA to other multiplexing methods with optimal SCA is given in Figure 2.8. SH-NOMA consumes 3.5% less energy than H-NOMA from [36–38], which agrees with the analytical results in Section 2.5. It should be noted that SH-NOMA and H-NOMA have the same receiver complexity. It can also be seen that SH-NOMA is more energy efficient than NOMA from [9], by 15% when users have heterogeneous latency requirements. Finally, the energy consumption of SH-NOMA is reduced from 4% and up to 15% compared to OMA. The average energy consumption per user with optimal SCA is given in Figure 2.9. As seen, energy consumption per user decreases as the number of available sub-channels increases. The improved energy efficiency is due to the higher number of combinations of users and sub-channels. Moreover, it can be seen that OMA becomes more energy efficient than NOMA when the number of users is larger than or equal to twenty.

2.6.3. Maximum Number of Iterations of TES

The maximum number of iterations for ES algorithms cannot be determined in closed form, as stated in Section 2.4. The maximum number of iterations is calculated by Monte Carlo simulations to analyze the behavior of the TES algorithm. The probability density function of the maximum number of iterations for the number of users is given in Table 2.2. As seen, the number of iterations for convergence is always lower than the number of users in the system. Therefore, if the maximum number of iterations is limited by the number of users in the system, as we have proposed in Section 2.4, the algorithm still converges to a stable solution.

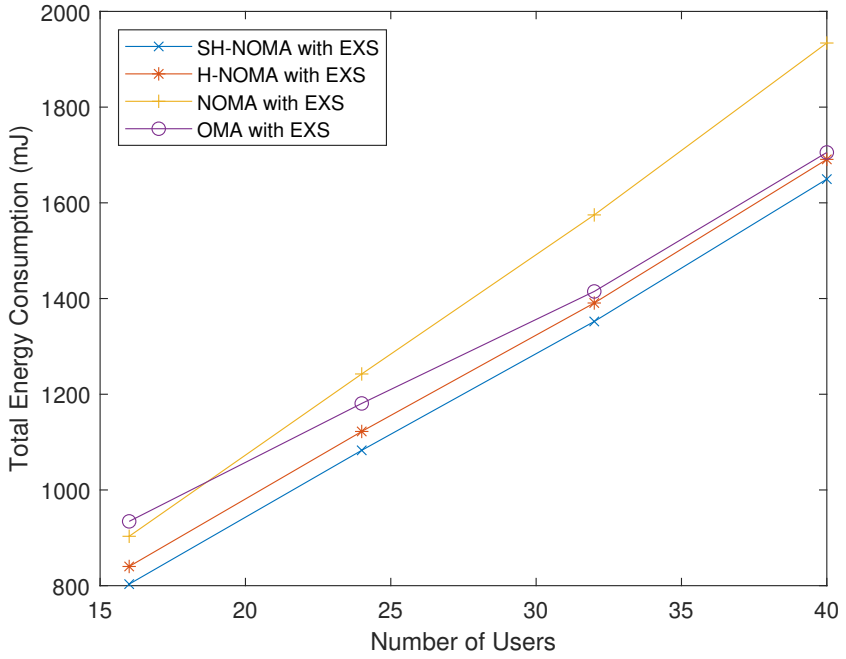

Figure 2.8. Total energy consumption for multiplexing methods.

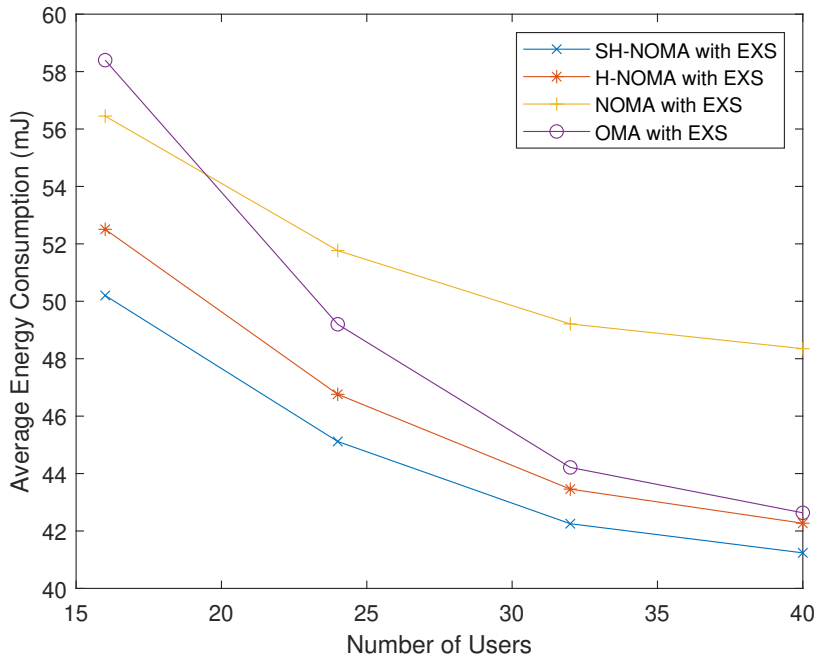

Figure 2.9. Average energy consumption for multiplexing methods.

Table 2.2. Probability distribution of maximum number of iterations.

	8 Users	**16 Users**	**24 Users**	**32 Users**
$p(I_{max} = 2)$	0.65133	0.21629	0.05983	0.01667
$p(I_{max} = 3)$	0.33225	0.65000	0.64933	0.53412
$p(I_{max} = 4)$	0.01613	0.12375	0.25708	0.37375
$p(I_{max} = 5)$	0.00029	0.00950	0.03129	0.06758
$p(I_{max} = 6)$	0.00000	0.00046	0.00208	0.00713
$p(I_{max} = 7)$	0.00000	0.00000	0.00038	0.00067
$p(I_{max} = 8)$	0.00000	0.00000	0.00000	0.00008
$p(I_{max} = 9)$	0.00000	0.00000	0.00000	0.00000

2.6.4. Performance Analysis of TES

In this part, the amount of data for each user is calculated from a uniform distribution with a mean value of N_μ and a standard deviation of $\frac{250000}{\sqrt{12}}$. As stated earlier, TES and 2ES algorithms have $O(N^3)$ complexity, and the optimal EXS algorithm has $O(N^N)$ complexity. The energy consumption comparison of different SCA algorithms with the optimal SH-NOMA method is given in Figure 2.10. From the figure, it is evident that TES significantly outperforms the 2ES algorithm, which is used in the literature widely [9, 35, 38]. The improvement in the energy consumption of TES compared to 2ES is 30%, which agrees with the analytical results given in Section 2.5. Additionally, the results show that the TES algorithm performs very close to the optimal EXS algorithm. The energy consumption difference between TES and EXS in the figure is less than 4 %. The average energy consumption per user with different SCA methods is given in Figure 2.9. Akin to the case for the multiplexing methods, energy consumption per user decreases as the number of available sub-channels is increased.

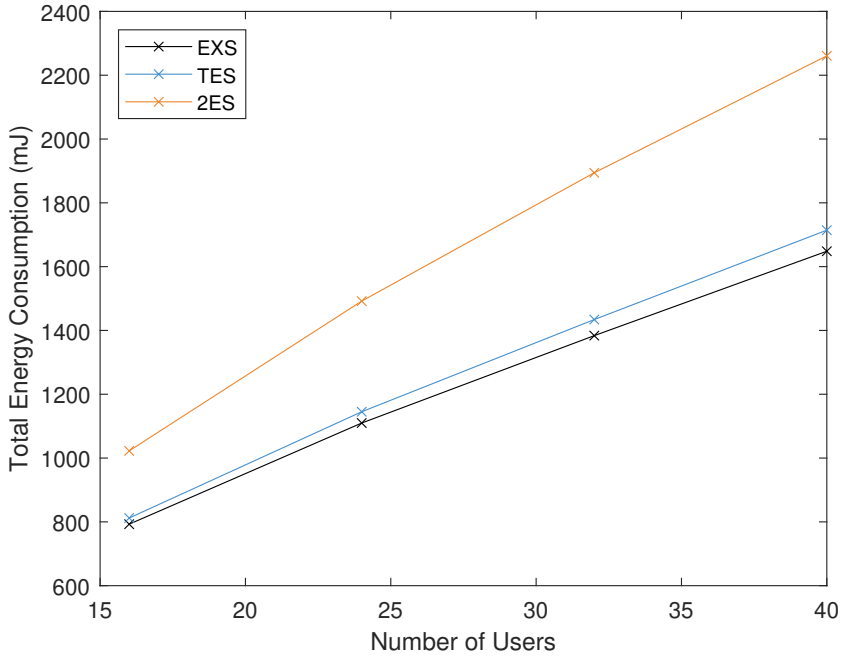

Figure 2.10. Total energy consumption of different SCA algorithms.

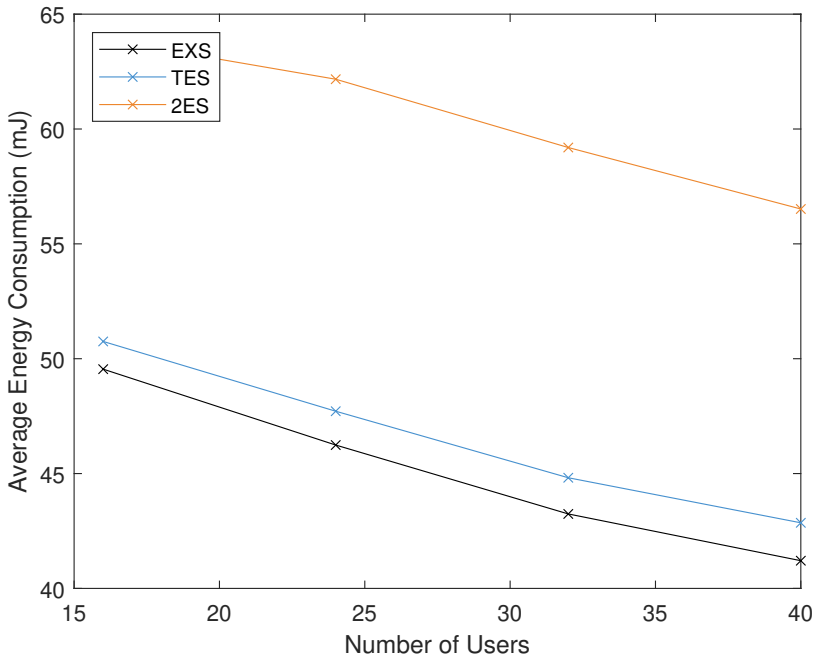

Figure 2.11. Average energy consumption of different SCA algorithms.

2.7. Concluding Remarks

In this chapter, we studied the Hybrid NOMA MEC Offloading resource allocation problem focusing on energy efficiency. We formulated the corresponding optimization problem and separated it into two sub-problems for power and time allocation and sub-channel allocation. For the first problem, we proposed a novel multiplexing scheme, SH-NOMA, that can be used with users with different QoS requirements, such as latency constraints and offloading data requirements. We have analytically determined the optimal power and time allocation formulas for the SH-NOMA scheme. Then, we compared SH-NOMA to other methods in the literature and shown analytically and by simulations that SH-NOMA outperforms available methods in the literature. For the second problem, which is NP-complete, we proposed the TES algorithm. We showed that this algorithm outperforms the existing 2ES algorithm in the literature with a similar level of complexity. Moreover, we showed that the TES algorithm performs very close to the optimal EXS algorithm with very high complexity. The proposed joint resource allocation method can be applied to the Hybrid NOMA MEC Offloading problems in the literature.

3. RESOURCE ALLOCATION FOR DOWNLINK HYBRID NOMA

In this chapter, we analyze the resource allocation problem for downlink H-NOMA. We first describe the considered system model and define the problem. Subsequently, we introduce the H-NOMA method for a single user pair. Afterward, the H-NOMA method is combined with OFDMA to serve more than two users by utilizing multiple sub-channels. Then, the performance of the proposed power control and sub-channel allocation algorithms is compared with similar methods from the literature by simulations.

3.1. System Model

In this work, we aim to minimize the energy consumption for the downlink transmission in an OFDMA-based network with the joint utilization of OMA and NOMA, which we refer to as H-NOMA. The OFDMA network has K sub-channels that can be allocated to the users. We assume two users per sub-channel to reduce the complexity of the SIC receiver and ensure robust performance in practical scenarios [76]. Furthermore, we assume perfect downlink CSI at the base station. The downlink CSI can either be received as feedback from the users, or it can be determined from the uplink CSI due to channel reciprocity for Time Division Duplex (TDD) systems [84].

An example network model with K groups and two NOMA users per group, each sharing the same sub-channel, is given in Figure 3.1. The user with the better channel conditions is denoted as user x, and the other user is denoted as user y. The data transfer requirements of the users are denoted as N_x and N_y, where we assume without loss of generality $N_x = R_N * N_y$ with $R_N > 0$. The latency requirements of the users are given as D_x and D_y. Throughout the article, we denote the shorter latency constraint as D_s and the longer latency constraint as D_l. The rest of the parameters are the common noise power P_N and the bandwidth of a sub-channel B.

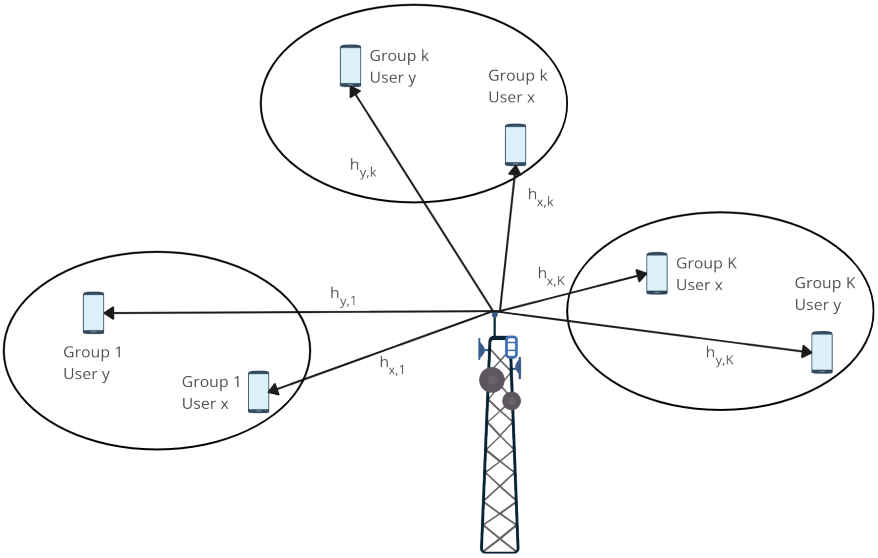

Figure 3.1. An example network diagram for downlink H-NOMA.

H-NOMA is compared to OMA and NOMA for different cases in Figure 3.2. The OMA time allocation is done according to the latency constraints of the users. The stricter latency-constrained user transmits during D_s and the other user during $D_l - D_s$. Both NOMA users are only active during D_s. User y treats the other user's signal as noise (TaN); user x utilizes a SIC receiver to cancel the interference of the signal transmitted to user y. Finally, for the proposed H-NOMA scheme, both users are active during $T_1 = D_s$. Then, the looser latency-constrained user transmits alone during $T_2 \leq D_l - D_s$.

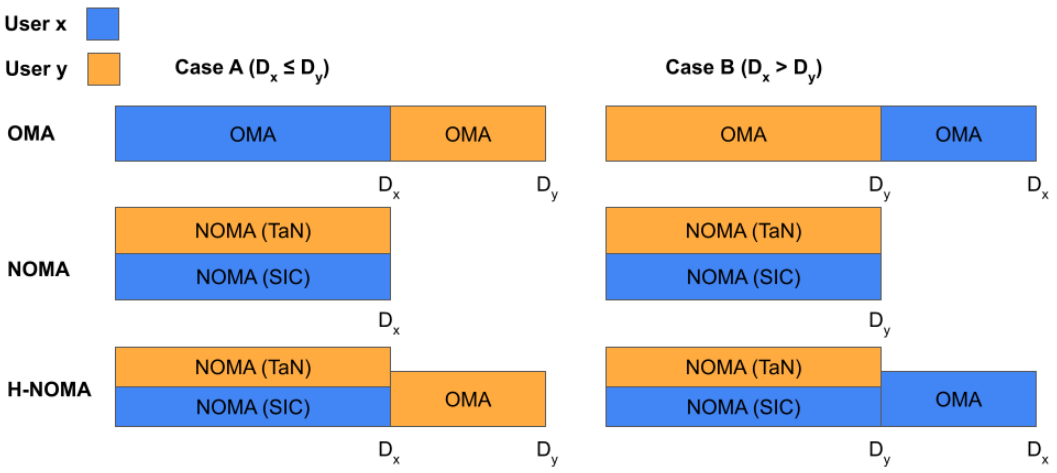

Figure 3.2. Comparison of H-NOMA to OMA and NOMA.

Table 3.1. Constant circuit power consumption for different multiplexing methods.

Method	OMA	NOMA	H-NOMA
Consumption	$P_C^u(T_1 + T_2)$	$P_C^u(2 * T_1)$	$P_C^u(2 * T_1 + T_2)$

The total power consumption for the downlink data transfer consists of the downlink transmission power and the uplink reception power. The downlink transmission power is the sum of the rate-dependent transmission power and the constant circuit power in the base station; the uplink reception power is the constant circuit power in the mobile device [77]. In this article, the total power consumption P is modeled as

$$P = \frac{P^b}{\alpha} + P_C^b + \frac{P_C^u}{\omega}, \tag{3.1}$$

where P^b is the rate-dependent transmission power of the base station, α is the efficiency of the power amplifier that satisfies $1 > \alpha > 0$, ω is the charge/discharge energy efficiency of the battery that powers the mobile device [85], P_C^b is the constant circuit power for the base station, and P_C^u is the constant circuit power for the user. The constant circuit power for the base station is assumed to be zero since the base station's transmit chain is always on. The constant circuit power consumption for different multiplexing methods is given in Table 3.1. Only a single user has its receiver on during each time period for the OMA method. Two users receive during the first period for the NOMA method. Finally, both users receive during the first period, and a single user receives during the second period for the H-NOMA method. Therefore, we can conclude that H-NOMA has higher constant circuit power consumption than other methods.

3.2. Power and Time Allocation for Downlink Hybrid NOMA

This section focuses on the power and time allocation for two downlink NOMA users that utilize the same sub-channel. The total energy consumption can be given as

$$(2\,T_1 + T_2)\frac{P_C^u}{\omega} + \sum_{i=1}^{2} T_i \left(\frac{P_{x,i} + P_{y,i}}{\alpha} \right), \tag{3.2}$$

where the constant circuit power consumption is considered for both users during T_1 and a single user during T_2. As stated in Section 3.1, T_1 is equal to D_s for H-NOMA, and the $2\,T_1\,P_C^u$ term is a constant.

The optimization problem for H-NOMA can be formulated as

$$\min_{P_{x,i},P_{y,i},T_2} \quad T_2\frac{\alpha P_C^u}{\omega} + \sum_{i=1}^{2} T_i\,(P_{x,i}+P_{y,i}) \tag{3.3a}$$

$$\text{s.t.} \quad \frac{N_y}{B} - \sum_{i=1}^{2} T_i \log_2(1+\frac{P_{y,i}|h_y|^2}{P_N+P_{x,i}|h_y|^2}) \leq 0, \tag{3.3b}$$

$$\frac{R_N N_y}{B} - \sum_{i=1}^{2} T_i \log_2(1+\frac{P_{x,i}|h_x|^2}{P_N}) \leq 0, \tag{3.3c}$$

$$-P_{x,i} \leq 0, \quad -P_{y,i} \leq 0, \tag{3.3d}$$

$$-T_2 \leq 0, \quad T_2 \leq D_l - D_s, \tag{3.3e}$$

where $P_{x,i}$ and $P_{y,i}$ are the transmission power allocation of users x and y in transmission period i, $P_{y,i}$. The constant term $2\,T_1\,P_C^u$ in the objective function is neglected, and the whole objective function is scaled with the power amplifier efficiency coefficient α.

We study two separate cases depending the on the latency constraints. The transmission periods are $T_1 = D_x$, and $T_2 \leq D_y - D_x$ for Case A ($D_x \leq D_y$), and $T_1 = D_y$, and $T_2 \leq D_x - D_y$ for Case B ($D_x > D_y$).

3.2.1. Case A ($D_x \leq D_y$)

The optimization problem for Downlink H-NOMA Case A is given by

$$\min_{P_{x,1},P_{y,i},T_2} \quad D_x P_{x,1} + D_x P_{y,1} + T_2 P_{y,2} + T_2\frac{\alpha P_C^u}{\omega} \tag{3.4a}$$

$$\text{s.t.} \quad \frac{N_y}{B} - D_x \log_2(1+\frac{P_{y,1}|h_y|^2}{P_N+P_{x,1}|h_y|^2}) - T_2 \log_2(1+\frac{P_{y,2}|h_y|^2}{P_N}) \leq 0, \tag{3.4b}$$

$$\frac{R_N N_y}{B} - D_x \log_2(1+\frac{P_{x,1}|h_x|^2}{P_N}) \leq 0, \tag{3.4c}$$

$$-P_{x,1} \leq 0, \quad -P_{y,1} \leq 0, \quad -P_{y,2} \leq 0, \tag{3.4d}$$

$$-T_2 \leq 0, \quad T_2 \leq D_y - D_x, \tag{3.4e}$$

which is a non-convex problem due to the multiplicative term $T_2 P_{y,2}$ in the objective function. This problem can be reduced by determining $P_{x,1}$ from constraint (3.4c) as

$$P_{x,1} = a_x P_N, \quad a_x = \frac{2^{\frac{R_N N_y}{B D_x}} - 1}{|h_x|^2}, \tag{3.5}$$

and substituting into the problem. The simplified optimization problem can be expressed as

$$\min_{P_{x,1}, P_{y,i}, T_2} \quad f_1(P_{y,1}, P_{y,2}, T_2) = D_x P_{y,1} + T_2 P_{y,2} + T_2 \frac{\alpha P_C^u}{\omega} \tag{3.6a}$$

$$\text{s.t.} \quad \frac{N_y}{B} - D_x \log_2(1 + \frac{P_{y,1}|h_y|^2}{P_N a_y}) - T_2 \log_2(1 + \frac{P_{y,2}|h_y|^2}{P_N}) \leq 0, \tag{3.6b}$$

$$-P_{y,1} \leq 0, \quad -P_{y,2} \leq 0, \tag{3.6c}$$

$$-T_2 \leq 0, \quad T_2 \leq D_y - D_x, \tag{3.6d}$$

where $a_y = a_x |h_y|^2 + 1$. The problem is still non-convex due to the multiplicative term $T_2 P_{y,2}$ in the objective function. This problem can be solved as a convex sequential problem as explained in [79]. First, a sub-problem that depends only on $P_{y,1}$ and $P_{y,2}$ is defined, and the optimal power allocation in terms of constants and T_2 is derived. Then, another sub-problem that depends only on T_2 is defined using the optimal power allocation, and the optimal time allocation can be found by solving this problem.

Theorem 3.1. *Optimal power and time allocation for H-NOMA in Case A is given as*

$$
\begin{aligned}
P_{x,1} &= \frac{P_N}{|h_x|^2}(2^{\frac{R_N N_y}{BD_x}} - 1),\\
P_{y,1} &= \frac{P_N}{|h_y|^2}(2^{\frac{N_y}{B(D_x+T_2)}} a_y^{\frac{D_x}{D_x+T_2}} - a_y),\\
P_{y,2} &= \frac{P_N}{|h_y|^2}(2^{\frac{N_y}{B(D_x+T_2)}} a_y^{\frac{D_x}{D_x+T_2}} - 1),\\
T_2 &= \begin{cases} D_y - D_x, & \text{if } c_a \geq 0 \\ \frac{a_z}{1+W(\nu_a)} - D_x, & \text{else if } \frac{a_z}{1+W(\nu_a)} > D_x \\ 0, & \text{otherwise} \end{cases}\\
c_a &= e^{\frac{a_z}{D_y}} \frac{a_z}{D_y} - e^{\frac{a_z}{D_y}} + 1 - \frac{\alpha P_C^u |h_y|^2}{\omega P_N},\\
a_z &= \frac{\ln(2) N_y}{B} + \ln(a_y) D_x,\\
\nu_a &= \frac{\alpha P_C^u |h_y|^2 - \omega P_N}{\omega P_N e},
\end{aligned}
\tag{3.7}
$$

where $W(.)$ is the Lambert function.

Proof. The power allocation sub-problem can be given as

$$
\min_{P_{x,1}, P_{y,i}} \quad f_{11}(P_{y,1}, P_{y,2}) = D_x P_{y,1} + T_2 P_{y,2} + T_2 \frac{\alpha P_C^u}{\omega} \tag{3.8a}
$$

$$
\text{s.t.} \quad \frac{N_y}{B} - D_x \log_2(1 + \frac{P_{y,1}|h_y|^2}{P_N(1 + a_x|h_y|^2)}) - T_2 \log_2(1 + \frac{P_{y,2}|h_y|^2}{P_N}) \leq 0, \tag{3.8b}
$$

$$
- P_{y,1} \leq 0, \quad -P_{y,2} \leq 0. \tag{3.8c}
$$

The power allocation sub-problem in (3.8) is convex, if the constraint (3.8b) is convex since the objective function and constraint (3.8c) are linear. The Hessian of (3.8b) is

$$
H(g_{11}) = \begin{bmatrix} \frac{D_x}{\left(\frac{P_N}{|h_y|^2} + a_x P_N + P_{y,1}\right)^2 \ln(2)} & 0 \\ 0 & \frac{T_2}{\left(\frac{P_N}{|h_y|^2} + P_{y,2}\right)^2 \ln(2)} \end{bmatrix}, \tag{3.9}
$$

which has non-negative eigenvalues for every feasible value of the optimization parameters and the constants, and it is positive semi-definite. Therefore, the power allocation

sub-problem is convex. The Lagrangian of the simplified problem is given by

$$L = D_x P_{y,1} + T_2 P_{y,2} + T_2 \frac{\alpha P_C^u}{\omega} + \boldsymbol{\mu}^T \boldsymbol{g_1}, \tag{3.10a}$$

$$\boldsymbol{g_1} = [g_{11}\ g_{12}\ g_{13}]^T, \tag{3.10b}$$

$$g_{11} = \frac{N_y}{B} - D_x \log_2(1 + \frac{P_{y,1}|h_y|^2}{P_N(1 + a_x|h_y|^2)}) - T_2 \log_2(1 + \frac{P_{y,2}|h_y|^2}{P_N}), \tag{3.10c}$$

$$g_{12} = -P_{y,1}, \quad g_{13} = -P_{y,2}, \tag{3.10d}$$

where $\boldsymbol{\mu_1} = [\mu_{11}\ \mu_{12}\ \mu_{13}]^T$ is the vector of KKT multipliers. The KKT conditions of this sub-problem can be expressed as

$$\frac{\partial L}{\partial P_{y,1}} = D_x - D_x \mu_{11} \frac{|h_y|^2}{\ln(2)\big(P_N(1 + a_x|h_y|^2) + P_{y,1}|h_y|^2\big)} - \mu_{12} = 0, \tag{3.11a}$$

$$\frac{\partial L}{\partial P_{y,2}} = T_2 - T_2 \mu_{11} \frac{|h_y|^2}{\ln(2)\big(P_N + P_{y,2}|h_y|^2\big)} - \mu_{13} = 0, \tag{3.11b}$$

$$\boldsymbol{g_1^T \mu_1} = 0. \tag{3.11c}$$

where constraint g_{11} is satisfied as equality to avoid extra energy consumption. Constraint g_{12} is met as inequality since, for H-NOMA, the transmit power in the first transmission period shall be positive. Constraint g_{13} is satisfied as inequality to increase energy efficiency by transmitting during the second transmission period, which is interference-free. Thus, μ_{11} shall be non-negative, and μ_{12} and μ_{13} are equal to zero. Utilizing (3.11a) and (3.11b), two expressions for μ_{11} can be derived as

$$\mu_{11} = \frac{\ln(2)\big(P_N(1 + a_x|h_y|^2) + P_{y,1}|h_y|^2\big)}{|h_y|^2}, \quad \mu_{11} = \frac{\ln(2)\big(P_N + P_{y,2}|h_y|^2\big)}{|h_y|^2}, \tag{3.12}$$

where μ_{11} is greater than zero, as KKT conditions require. By employing the expressions of μ_{11} in (3.12), $P_{y,2}$ can be expressed in terms of P_N and $P_{y,1}$ as follows

$$P_{y,2} = P_N * a_x + P_{y,1}. \tag{3.13}$$

Substituting (3.13) for $P_{y,2}$ in (3.8b), power allocation for user y is determined as

$$\begin{aligned} P_{y,1} &= P_N \frac{2^{\frac{N_y}{B(D_x+T_2)}} a_y^{\frac{D_x}{D_x+T_2}} - a_y}{|h_y|^2}, \\ P_{y,2} &= P_N \frac{2^{\frac{N_y}{B(D_x+T_2)}} a_y^{\frac{D_x}{D_x+T_2}} - 1}{|h_y|^2}. \end{aligned} \tag{3.14}$$

The time allocation sub-problem can be given by

$$\min_{T_2} \qquad f_{12}(T_2) = D_x P_N \frac{e^{\frac{N_y \ln(2)}{B(D_x+T_2)}} e^{\frac{D_x \ln(a_y)}{D_x+T_2}}}{|h_y|^2}$$

$$+ T_2 P_N \frac{e^{\frac{N_y \ln(2)}{B(D_x+T_2)}} e^{\frac{D_x \ln(a_y)}{D_x+T_2}} - 1}{|h_y|^2} + T_2 \frac{\alpha P_C^u}{\omega} \tag{3.15a}$$

$$\text{s.t.} \qquad T_2 \leq D_y - D_x, \tag{3.15b}$$

$$-T_2 \leq 0, \tag{3.15c}$$

where the constant term $\frac{D_x a_y}{|h_y|^2}$ is neglected. Since the constraint functions are linear, the optimization problem in (3.15) is convex if the second derivative of f_{12} is non-negative. The second derivative of f_{12} can be shown as

$$\frac{d^2 f_{12}}{dT_2^2} = e^{\frac{N_y \ln(2)}{B(T_2+D_x)}} e^{\frac{D_x \ln(a_y)}{T_2+D_x}} \frac{\left(BD_x \ln(a_y) + \ln(2) N_y\right)^2}{B^2 (T_2+D_x)^3 |h_y|^2}, \tag{3.16}$$

which is always positive for the valid values of the parameters. Thus, the time allocation sub-problem is convex. The Lagrangian for the time allocation sub-problem is

$$L(T_2) = f_{12}(T_2) + \mu_{11}^t (T_2 - D_y + D_x) - \mu_{12}^t T_2, \tag{3.17}$$

where μ_{12}^t is set to zero since T_2 cannot be negative. The derivative of the Lagrangian with $\mu_{12}^t = 0$ can be expressed as

$$\begin{aligned} \frac{dL}{dT_2} &= e^{\frac{a_z}{T_2+D_x}} - e^{\frac{a_z}{T_2+D_x}} \frac{a_z}{T_2+D_x} - 1 + \frac{\alpha P_C^u |h_y|^2}{\omega P_N} + \mu_{11}^t, \\ a_z &= \frac{\ln(2) N_y}{B} + \ln(a_y) D_x. \end{aligned} \tag{3.18}$$

There are two possible solutions to this problem depending on constraint (3.15b). If the constraint is satisfied as equality, then μ_{11}^t shall be greater than zero, which is

$$c_a = e^{\frac{a_z}{D_y}} \frac{a_z}{D_y} - e^{\frac{a_z}{D_y}} + 1 - \frac{\alpha P_C^u |h_y|^2}{\omega P_N} \geq 0. \tag{3.19}$$

If the constraint is satisfied as inequality, then μ_{11}^t is equal to zero, and T_2 can determined as follows

$$\begin{aligned} & e^{\frac{a_z}{T_2+D_x}} \frac{a_z}{T_2+D_x} - e^{\frac{a_z}{T_2+D_x}} = \frac{\alpha P_C^u |h_y|^2}{\omega P_N} - 1, \\ & e^{\frac{a_z}{T_2+D_x}-1} \left(\frac{a_z}{T_2+D_x} - 1 \right) = \frac{\alpha P_C^u |h_y|^2 - \omega P_N}{\omega P_N e}, \\ & \frac{a_z}{T_2+D_x} - 1 = W\left(\frac{\alpha P_C^u |h_y|^2 - \omega P_N}{\omega P_N e} \right), \\ & T_2 = \frac{a_z}{1 + W\left(\frac{\alpha P_C^u |h_y|^2 - \omega P_N}{\omega P_N e} \right)} - D_x, \\ & T_2 = \frac{a_z}{1 + W(\nu_a)} - D_x, \end{aligned} \tag{3.20}$$

where $W(.)$ is the Lambert function, and $\nu_a = \frac{\alpha P_C^u |h_y|^2 - \omega P_N}{\omega P_N e}$. □

Remark 3.2. *Theorem 3.1 gives the optimal power and time allocation of the downlink H-NOMA scenario with non-ideal circuit consumption when $D_x \leq D_y$. In the literature, the power and time allocation of the uplink is given in [36,40], and the power allocation of the downlink for only FBC scenarios is given in [21,22]. We introduce the H-NOMA solution in the infinite blocklength code regime.*

The H-NOMA solution is determined by the assumption that $P_{y,1}$ is larger than zero. When $P_{y,1} = 0$, the H-NOMA method reduces to the OMA method. The power allocation for OMA can be derived directly from Shannon rate equations as follows

$$\begin{aligned} P_{x,1} &= \frac{P_N}{|h_x|^2}(2^{\frac{R_N N_y}{BD_x}} - 1), \\ P_{y,1} &= 0, \\ P_{y,2} &= \frac{P_N}{|h_y|^2}(2^{\frac{N_y}{BT_2}} - 1). \end{aligned} \tag{3.21}$$

The optimization problem that minimizes the energy consumption of OMA with constant circuit power consumption is given by

$$\min_{T_2} \quad f_{oa}(T_2) = T_2\frac{P_N}{|h_y|^2}(2^{\frac{N_y}{BT_2}} - 1) + T_2\frac{\alpha P_C^u}{\omega} \tag{3.22a}$$

$$\text{s.t.} \quad -T_2 \leq 0, \tag{3.22b}$$

$$T_2 \leq D_y - D_x. \tag{3.22c}$$

Theorem 3.3. *The optimal time allocation for OMA in Case A can be expressed as*

$$\begin{aligned} T_2 &= \begin{cases} D_y - D_x, & \text{if } c_{oa} \geq 0 \\ T_2 = \frac{o_x}{1+W(\nu_{oa})}, & \text{otherwise} \end{cases} \\ c_{oa} &= e^{\frac{o_x}{D_y - D_x}}\frac{o_x}{D_y - D_x} - e^{\frac{o_x}{D_y - D_x}} + 1 - \frac{\alpha P_C^u |h_y|^2}{\omega P_N}, \\ o_x &= \frac{\ln(2) N_y}{B}, \\ \nu_{oa} &= \frac{\alpha P_C^u |h_y|^2 - \omega P_N}{\omega P_N e}. \end{aligned} \tag{3.23}$$

Proof. The optimization problem in (3.22) is convex on the condition that the objective function is convex and the constraint functions are linear. The second derivative of the

objective function can be given by

$$\frac{d^2 f_o}{dT_2^2} = \frac{P_N 2^{\frac{N_y}{BT_2}} \left(\ln(2) N_y\right)^2}{B^2 (T_2)^3 |h_y|^2}, \tag{3.24}$$

which is non-negative for all the possible values of the parameters, and the optimization problem is convex. The Lagrangian for the OMA time allocation problem is

$$L(T_2) = f_o(T_2) + \mu_{o1}(T_2 - D_x + D_y) - \mu_{o2} T_2, \tag{3.25}$$

where μ_{o2} is set to zero since T_2 cannot be negative. The derivative of the Lagrangian with $\mu_{o2} = 0$ can be expressed as

$$\begin{aligned} \frac{dL}{dT_2} &= e^{\frac{o_x}{T_2}} - e^{\frac{o_x}{T_2}} \frac{o_x}{T_2} - 1 + \frac{\alpha P_C^u |h_y|^2}{\omega P_N} + \mu_{o1}, \\ o_x &= \frac{\ln(2) N_y}{B}. \end{aligned} \tag{3.26}$$

There are two possible solutions to this problem depending on constraint (3.22c). If the constraint is satisfied as equality, then μ_{o1} shall be greater than zero. This condition is

$$c_1 = e^{\frac{o_x}{D_y - D_x}} \frac{o_x}{D_y - D_x} - e^{\frac{o_x}{D_y - D_x}} + 1 - \frac{\alpha P_C^u |h_y|^2}{\omega P_N} \geq 0. \tag{3.27}$$

If the constraint is satisfied as inequality, then μ_{11}^t is equal to zero, and T_2 can be determined as follows

$$\begin{aligned} & e^{\frac{o_x}{T_2}} \frac{o_x}{T_2} - e^{\frac{o_x}{T_2}} = \frac{\alpha P_C^u |h_y|^2}{\omega P_N} - 1, \\ & e^{\frac{o_x}{T_2} - 1} \left(\frac{o_x}{T_2} - 1 \right) = \frac{\alpha P_C^u |h_y|^2 - \omega P_N}{\omega P_N e}, \\ & \frac{o_x}{T_2} - 1 = W\left(\frac{\alpha P_C^u |h_y|^2 - \omega P_N}{\omega P_N e} \right), \\ & T_2 = \frac{b_x}{1 + W\left(\frac{\alpha P_C^u |h_y|^2 - \omega P_N}{\omega P_N e} \right)} - D_y, \\ & T_2 = \frac{o_x}{1 + W\left(\nu_{oa}\right)}, \end{aligned} \tag{3.28}$$

where $\nu_{oa} = \frac{\alpha P_C^u |h_y|^2 - \omega P_N}{\omega P_N e}$. □

Corollary 3.4. *The activation conditions of H-NOMA, and the fall-back methods in Case A are given by*

$$\begin{cases} \textit{if } \left((P_{y,1} < 0) \,\&\, (E_H > E_O) \right), & \textit{OMA}, \\ \textit{else if } \left((c_a \geq 0) \,\&\, \left(\dfrac{a_z}{1 + W\left(\nu_a\right)} > D_x \right) \right), & \textit{H-NOMA}, \\ \textit{otherwise}, & \textit{NOMA}. \end{cases} \tag{3.29}$$

Proof. The if condition can be proved as follows; the solution given in Theorem 3.1 is applicable if $P_{y,1} \geq 0$, and H-NOMA is not activated unless it is more efficient than OMA. The $else\ if$ condition follows from the conditions that results $T_2 = 0$ in Theorem 3.1 since for $T_2 = 0$ H-NOMA is equivalent to NOMA. □

3.2.2. Case B ($D_x > D_y$)

The optimization problem for Downlink H-NOMA Case B is given by

$$\min_{P_{x,i},P_{y,2},T_2} \quad D_y P_{y,1} + D_y P_{x,1} + T_2 P_{x,2} + T_2 \frac{\alpha P_C^u}{\omega} \tag{3.30a}$$

$$\text{s.t.} \quad \frac{R_N N_y}{B} - D_y \log_2(1 + \frac{P_{x,1}|h_x|^2}{P_N}) - T_2 \log_2(1 + \frac{P_{x,2}|h_x|^2}{P_N}) \leq 0, \tag{3.30b}$$

$$\frac{N_y}{B} - D_y \log_2(1 + \frac{P_{y,1}|h_y|^2}{P_N + P_{x,1}|h_y|^2}) \leq 0, \tag{3.30c}$$

$$-P_{y,1} \leq 0, \quad -P_{x,1} \leq 0, \quad -P_{x,2} \leq 0, \tag{3.30d}$$

$$-T_2 \leq 0, \quad T_2 \leq D_x - D_y, \tag{3.30e}$$

which is a non-convex problem due to the multiplicative term $T_2 P_{x,2}$ in the objective function. This problem can be solved as a convex sequential problem similarly to Case A. First, a sub-problem that depends only on $P_{x,1}$, $P_{x,2}$, and $P_{y,1}$ is defined, and the optimal power allocation in terms of constants and T_2 is derived. Then, another sub-problem that depends only on T_2 is defined using the optimal power allocation, and the optimal time allocation can be found by solving this problem.

Theorem 3.5. *Optimal power and time allocation for H-NOMA in Case B is given by*

$$
\begin{aligned}
P_{x,1} &= \frac{P_N}{|h_x|^2}\left(2^{\frac{N_y(R_N D_y - T_2)}{BD_y(D_y+T_2)}} - 1\right),\\
P_{x,2} &= \frac{P_N}{|h_x|^2}\left(2^{\frac{N_y(R_N+1)}{B(D_y+T_2)}} - 1\right),\\
P_{y,1} &= \frac{P_N}{|h_x|^2}\left(2^{\frac{N_y}{BD_y}} - 1\right)\left(2^{\frac{N_y(R_N D_y - T_2)}{BD_y(D_y+T_2)}} - 1\right) + \frac{P_N}{|h_y|^2}\left(2^{\frac{N_y}{BD_y}} - 1\right),\\
T_2 &= \begin{cases} D_x - D_y, & \text{if } c_b \geq 0\\ \frac{b_x}{1+W(\nu_b)} - D_y, & \text{else if } \frac{b_x}{1+W(\nu_b)} > D_y\\ 0, & \text{otherwise}\end{cases}\\
c_b &= e^{\frac{b_x}{D_x}}\frac{b_x}{D_x} - e^{\frac{b_x}{D_x}} + 1 - \frac{\alpha P_C^u |h_x|^2}{\omega P_N},\\
b_x &= \frac{\ln(2)(R_N+1)N_y}{B},\\
\nu_b &= \frac{\alpha P_C^u |h_x|^2 - \omega P_N}{\omega P_N e}.
\end{aligned}
\tag{3.31}
$$

Proof. The power allocation sub-problem can be given as

$$
\begin{aligned}
\min_{P_{x,i},P_{y,1}} \quad & f_{21}(P_{x,1},P_{x,2},P_{y,1}) = D_y P_{y,1} + D_y P_{x,1} + T_2 P_{x,2} + T_2\frac{\alpha P_C^u}{\omega} && \text{(3.32a)}\\
\text{s.t.} \quad & \frac{R_N N_y}{B} - D_y \log_2(1+\frac{P_{x,1}|h_x|^2}{P_N})\\
& - T_2\log_2(1+\frac{P_{x,2}|h_x|^2}{P_N}) \leq 0, && \text{(3.32b)}\\
& \frac{N_y}{B} - D_y\log_2(1+\frac{P_{y,1}|h_y|^2}{P_N + P_{x,1}|h_y|^2}) \leq 0, && \text{(3.32c)}\\
& -P_{y,1} \leq 0, \quad -P_{x,1} \leq 0, \quad -P_{x,2} \leq 0, && \text{(3.32d)}
\end{aligned}
$$

Akin to Case A, the power allocation sub-problem in (3.32) is convex, if the constraint (3.32b) is convex since the objective function and constraint (3.32c) are linear. The Hessian of constraint (3.32b) is given by

$$
H(g_{11}) = \begin{bmatrix} \frac{D_y}{\left(\frac{P_N}{|h_x|^2}+P_{x,1}\right)^2\ln(2)} & 0\\ 0 & \frac{T_2}{\left(\frac{P_N}{|h_x|^2}+P_{x,2}\right)^2\ln(2)}\end{bmatrix}, \tag{3.33}
$$

which has non-negative eigenvalues for every feasible value of the optimization parameters and the constants, and it is positive semi-definite. Therefore, the power allocation

sub-problem is convex. The Lagrangian of the sub-problem is given by

$$L = D_y P_{y,1} + D_y P_{x,1} + T_2 P_{x,2} + T_2 \frac{\alpha P_C^u}{\omega} + \boldsymbol{\mu_2}^T \boldsymbol{g_2}, \tag{3.34a}$$

$$\boldsymbol{g_2} = [g_{21}\ g_{22}\ g_{23}\ g_{24}]^T, \tag{3.34b}$$

$$g_{21} = \frac{R_N N_y}{B} - D_y \log_2(1 + \frac{P_{x,1}|h_x|^2}{P_N}) - T_2 \log_2(1 + \frac{P_{x,2}|h_x|^2}{P_N}), \tag{3.34c}$$

$$g_{22} = \frac{N_y}{B} - D_y \log_2(1 + \frac{P_{y,1}|h_y|^2}{P_N + P_{x,1}|h_y|^2}), \tag{3.34d}$$

$$g_{23} = -P_{x,1}, \quad g_{24} = -P_{x,2}, \quad g_{25} = -P_{y,1}, \tag{3.34e}$$

where $\boldsymbol{\mu_2} = [\mu_{21}\, \mu_{22}\, \mu_{23}\, \mu_{24}\, \mu_{25}]^T$ is the vector of KKT multipliers. The KKT conditions of this sub-problem can be expressed as

$$\frac{\partial L}{\partial P_{x,1}} = D_y - \frac{D_y \mu_{21} |h_x|^2}{\ln 2\,(|h_x|^2 P_{x,1} + P_N)} + \frac{D_y \mu_{22} B P_{y,1} (|h_y|^2)^2}{\ln 2\,(|h_y|^2 P_{x,1} + P_N)\,(|h_y|^2 P_{y,1} + |h_y|^2 P_{x,1} + P_N)} - \mu_{23} = 0, \tag{3.35a}$$

$$\frac{\partial L}{\partial P_{x,2}} = T_2 \left(1 - \frac{\mu_{21} |h_x|^2}{\ln 2\,(|h_x|^2 P_{x,2} + P_N)}\right) - \mu_{24} = 0, \tag{3.35b}$$

$$\frac{\partial L}{\partial P_{y,1}} = D_y \left(1 - \frac{\mu_{22} |h_y|^2}{\ln 2\,(|h_y|^2 P_{y,1} + |h_y|^2 P_{x,1} + P_N)}\right) - \mu_{25} = 0, \tag{3.35c}$$

$$\boldsymbol{g_2^T \mu_2} = 0. \tag{3.35d}$$

where constraints g_{21} and g_{22} are satisfied as equality to avoid extra energy consumption. Constraint g_{23} is satisfied as inequality since, for H-NOMA, the transmit power in the first transmission period shall be positive. Constraint g_{24} is satisfied as inequality to increase energy efficiency by transmitting during the second transmission period, which is interference-free. Constraint g_{25} is satisfied as inequality to satisfy the data transfer requirement of user y. Thus, μ_{21} and μ_{22} are non-negative, and μ_{23}, μ_{24}, and μ_{25} are equal to zero. Utilizing (3.35b) and (3.35c), μ_{21} and μ_{22} can be derived as

$$\mu_{21} = \frac{\ln(2)\big(P_N + P_{x,2}|h_x|^2\big)}{|h_x|^2}, \tag{3.36a}$$

$$\mu_{22} = \frac{\ln(2)\big(P_N + P_{x,1}|h_y|^2 + P_{y,1}|h_y|^2\big)}{|h_y|^2}, \tag{3.36b}$$

where μ_{21} and μ_{22} are greater than zero, as required by KKT conditions.

The relation between the allocated power values can be derived as

$$P_{y,1} = (2^{\frac{N_y}{BD_y}} - 1)\frac{P_N}{|h_y|^2} + (2^{\frac{N_y}{BD_y}} - 1)P_{x,1}, \tag{3.37}$$

from (3.34d). Substituting in (3.36a) for μ_{21}, (3.36b) for μ_{22} and (3.36a) for $P_{y,1}$ in (3.35a), $P_{x,2}$ can be expressed in terms of $P_{x,1}$ and constants as

$$P_{x,2} = (2^{\frac{N_y}{BD_y}} - 1)\frac{P_N}{|h_x|^2} + 2^{\frac{N_y}{BD_y}}P_{x,1}. \tag{3.38}$$

Finally, by substituting $P_{x,2}$ into (3.32b), power allocation is determined as

$$\begin{aligned}
P_{x,1} &= \frac{P_N}{|h_x|^2}\left(2^{\frac{N_y(R_N D_y - T_2)}{BD_y(D_y+T_2)}} - 1\right), \\
P_{x,2} &= \frac{P_N}{|h_x|^2}\left(2^{\frac{N_y(R_N+1)}{B(D_y+T_2)}} - 1\right), \\
P_{y,1} &= \frac{P_N}{|h_x|^2}\left(2^{\frac{N_y}{BD_y}} - 1\right)\left(2^{\frac{N_y(R_N D_y - T_2)}{BD_y(D_y+T_2)}} - 1\right) + \frac{P_N}{|h_y|^2}\left(2^{\frac{N_y}{BD_y}} - 1\right).
\end{aligned} \tag{3.39}$$

The time allocation sub-problem can be given by

$$\begin{aligned}
\min_{T_2} \quad & f_{22}(T_2) = D_y\frac{P_N}{|h_x|^2}\left(e^{\frac{N_y \ln(2)(R_N+1)}{B(D_y+T_2)}}\right) \\
& \quad + T_2\frac{P_N}{|h_x|^2}\left(e^{\frac{N_y \ln(2)(R_N+1)}{B(D_y+T_2)}} - 1\right) + T_2\frac{\alpha P_C^u}{\omega} && \text{(3.40a)} \\
\text{s.t.} \quad & T_2 \leq D_x - D_y, && \text{(3.40b)} \\
& -T_2 \leq 0, && \text{(3.40c)}
\end{aligned}$$

which is convex if the second derivative of f_{22} is non-negative since the constraint functions are linear. The second derivative of f_{22} can be shown as

$$\frac{d^2 f_{22}}{dT_2^2} = e^{\frac{N_y(R_N+1)\ln(2)}{B(T_2+D_y)}}\frac{P_N\left((R_N+1)\ln(2)N_y\right)^2}{B^2(T_2+D_y)^3|h_x|^2}, \tag{3.41}$$

which is always positive for the valid values of the parameters. Thus, the time allocation sub-problem is convex. The Lagrangian for the time allocation sub-problem is given by

$$L(T_2) = f_{22}(T_2) + \mu_{21}^t(T_2 - D_x + D_y) - \mu_{22}^t T_2, \tag{3.42}$$

where μ_{22}^t is set to zero since T_2 cannot be negative. The derivative of the Lagrangian

with $\mu_{22}^t = 0$ can be expressed as

$$\begin{aligned} \frac{dL}{dT_2} &= e^{\frac{b_x}{T_2+D_y}} - e^{\frac{b_x}{T_2+D_y}} \frac{b_x}{T_2+D_y} - 1 + \frac{\alpha P_C^u |h_x|^2}{\omega P_N} + \mu_{21}^t, \\ b_x &= \frac{\ln(2)(R_N+1)N_y}{B}. \end{aligned} \tag{3.43}$$

Similar to Case A, there are two possible solutions to this problem depending on constraint (3.40b). If the constraint is satisfied as equality, then μ_{21}^t shall be greater than zero. This condition is true when

$$c_b = e^{\frac{b_x}{D_x}} \frac{b_x}{D_x} - e^{\frac{b_x}{D_x}} + 1 - \frac{\alpha P_C^u |h_x|^2}{\omega P_N} \geq 0. \tag{3.44}$$

If the constraint is satisfied as inequality, then μ_{21}^t is equal to zero, and T_2 can be determined as follows

$$\begin{aligned} & e^{\frac{b_x}{T_2+D_y}} \frac{b_x}{T_2+D_y} - e^{\frac{b_x}{T_2+D_y}} = \frac{\alpha P_C^u |h_x|^2}{\omega P_N} - 1, \\ & e^{\frac{b_x}{T_2+D_y}-1} \left(\frac{b_x}{T_2+D_y} - 1 \right) = \frac{\alpha P_C^u |h_x|^2 - \omega P_N}{\omega P_N e}, \\ & \frac{b_x}{T_2+D_y} - 1 = W\left(\frac{\alpha P_C^u |h_x|^2 - \omega P_N}{\omega P_N e} \right), \\ & T_2 = \frac{b_x}{1 + W\left(\frac{\alpha P_C^u |h_x|^2 - \omega P_N}{\omega P_N e} \right)} - D_y, \\ & T_2 = \frac{b_x}{1 + W(\nu_b)} - D_y, \end{aligned} \tag{3.45}$$

where $\nu_b = \frac{\alpha P_C^u |h_x|^2 - \omega P_N}{\omega P_N e}$. □

Remark 3.6. *Theorem 3.5 gives the optimal power and time allocation of the downlink H-NOMA scenario with non-ideal circuit consumption when $D_x > D_y$. In the literature, the power and time allocation of the uplink is given in [36,40], and the power allocation of the downlink for only FBC scenarios is given in [21,22]. We introduce the H-NOMA solution in the infinite blocklength code regime.*

The H-NOMA solution is determined by the assumption that $P_{x,1}$ is larger than zero. When $P_{x,1} = 0$, the H-NOMA method reduces to the OMA method. The power

allocation for OMA can be derived directly from Shannon rate equations as follows

$$\begin{aligned} P_{x,1} &= 0, \\ P_{x,2} &= \frac{P_N}{|h_x|^2}(2^{\frac{R_N N_y}{BT_2}} - 1), \\ P_{y,1} &= \frac{P_N}{|h_y|^2}(2^{\frac{N_y}{BD_y}} - 1). \end{aligned} \tag{3.46}$$

The optimization problem that minimizes the energy consumption of OMA with constant circuit power consumption is given by

$$\min_{T_2} \quad f_{ob}(T_2) = T_2 \frac{P_N}{|h_x|^2}(2^{\frac{N_y}{BT_2}} - 1) + T_2 \frac{\alpha P_C^u}{\omega} \tag{3.47a}$$

$$\text{s.t.} \quad -T_2 \leq 0, \tag{3.47b}$$

$$T_2 \leq D_x - D_y, \tag{3.47c}$$

Theorem 3.7. *The optimal time allocation for OMA in Case B can be expressed as*

$$\begin{aligned} T_2 &= \begin{cases} D_x - D_y, & \text{if } c_{ob} \geq 0 \\ T_2 = \frac{o_x}{1+W(\nu_{ob})}, & \text{otherwise} \end{cases} \\ c_{ob} &= e^{\frac{o_x}{D_x - D_y}} \frac{o_x}{D_x - D_y} - e^{\frac{o_x}{D_x - D_y}} + 1 - \frac{\alpha P_C^u |h_x|^2}{\omega P_N}, \\ \nu_{ob} &= \frac{\alpha P_C^u |h_x|^2 - \omega P_N}{\omega P_N e}. \end{aligned} \tag{3.48}$$

Proof. The proof follows Theorem 3.3. □

Corollary 3.8. *The activation conditions of H-NOMA, and the fall-back methods in Case B are given by*

$$\begin{aligned} &\textit{if } \left((P_{x,1} < 0) \,\&\, (E_H > E_O)\right), && \textit{OMA}, \\ &\textit{else if } \left((c_b \geq 0) \,\&\, \left(\frac{b_x}{1 + W(\nu_b)} > D_x\right)\right), && \textit{H-NOMA}, \\ &\textit{otherwise}, && \textit{NOMA}. \end{aligned} \tag{3.49}$$

Proof. The if condition can be proved as follows; the solution given in Theorem 3.5 is applicable if $P_{y,1} \geq 0$, and H-NOMA is not activated unless it is more efficient than OMA. The *else if* condition follows from the conditions that results $T_2 = 0$ in Theorem 3.5 since for $T_2 = 0$ H-NOMA is equivalent to NOMA. □

3.3. Sub-channel Allocation with OFDMA

The two-user H-NOMA idea can be extended to multiple users by assigning an H-NOMA pair to each sub-channel. The sub-channel allocation (SCA) problem for $2K$ users and K sub-channels is given by

$$\min_{\Psi} \quad \sum_{i=1}^{2K-1} \sum_{j=i+1}^{2K} \sum_{k=1}^{K} \psi_{i,j,k}[(P_{i,k}^1 + P_{j,k}^1)T_1 + (P_{i,k}^2 + P_{j,k}^2)T_2] \tag{3.50a}$$

$$\text{s.t.} \quad \psi_{i,j,k} \in \{0,1\} \quad \forall i,j,k, \quad \sum_i \sum_j \psi_{i,j,k} = 2, \quad \forall k, \tag{3.50b}$$

$$\sum_j \sum_k \psi_{i,j,k} = 1, \quad \forall i, \quad \sum_i \sum_k \psi_{i,j,k} = 1, \quad \forall j, \tag{3.50c}$$

where $P_{i,k}^1$, $P_{j,k}^1$, $P_{i,k}^2$, $P_{j,k}^2$, T_1, and T_2 are the optimal power and time allocation values of the users on sub-channel k. The constant circuit power consumption is not effective for the SCA problem and omitted in the objective function. The SCA problem is a 3DAP, shown to be NP-complete in [80]. The optimal solution to this problem can be found by the Exhaustive Search (EXS) algorithm, which is very complex. In this section, first, we present the existing exchange stable algorithms in the literature. The 2ES algorithm is first introduced in [81] and utilized for SCA problems in [9, 35, 38]. The TES algorithm is proposed in [82] and utilized for SCA problems in [40]. Then, we introduce two low-complexity algorithms to solve the 3DAP; the first is the Two-Round Hungarian (TH) algorithm, and the second is the B-TES algorithm.

3.3.1. Exchange Stable Algorithms in the Literature

The 2ES algorithm is a game theoretic algorithm that solves the matching problem based on the exchange stability notion in [81]. The 2ES algorithm is initialized with a random assignment where all agents are paired and assigned to resources. Then, each agent searches through the agents for a swapping opportunity. The swap is allowed if the reward is increased for all participating agents. The algorithm stops when the maximum number of iterations is reached, or no further swaps are permitted. The TES algorithm is another game theoretic algorithm for the matching problem, based on the compensational stability notion in [82]. The TES algorithm is similar to the

2ES algorithm except for the different swapping conditions. In the TES algorithm, a swap is permitted if the total reward in the system is increased. In summary, the 2ES algorithm favors the individual welfare of the swapping agents, whereas the TES algorithm favors the total welfare of the network. The reward calculation is based on a matrix that contains the reward information for every possible permutation of assignments. The dimensions of the matrix for a SCA problem with K sub-channels and $2K$ users is $2K \times 2K \times K$. For the SCA problem, the matrix is an energy consumption matrix that contains the energy consumption value per each matching. The energy consumption value is calculated using the allocation formulas derived in Section 3.2.

3.3.2. Two-Round Hungarian Algorithm

The Hungarian algorithm is optimal for the two-dimensional assignment problem (2DAP) [86]. In this work, we propose the Two-Round Hungarian algorithm to solve the 3DAP, where the problem is solved in a sub-optimal fashion by dividing it into two problems that can be treated as 2DAPs. In the first round, K sub-channels are allocated to the K of the existing $2K$ users by an efficient implementation of the Hungarian algorithm for rectangular assignment problems in [87]. As an input to the algorithm, the channel gain matrix that consists of $2K$ users and K sub-channels is constructed. In the second round, the K users not assigned in the first round are assigned to the sub-channels. The cost matrix of this round is the energy consumption matrix calculated by the optimal power and time allocation values determined in Section 3.2. The detailed steps of the TH algorithm are given in Figure 3.3.

3.3.3. Bootstrapped Total-Reward Exchange Stable Algorithm

In this work, we propose an extension to the TES algorithm in [40], which we refer to as the B-TES algorithm. The TES algorithm utilizes a random initial matching matrix, whereas, in B-TES, we add a bootstrapping step to initialize the algorithm with a more energy-efficient matching matrix. We employ the TH algorithm, which we have introduced earlier in this section, to determine the initial matching matrix. Then,

the TES algorithm is utilized to determine the final matching matrix. The maximum number of iterations is set to K for a K sub-channel scenario as in [40]. The steps of the B-TES algorithm are given in Figure 3.4.

1: Construct the $2K \times K$ channel gain matrix (H^{2D}).
2: Run the Hungarian algorithm to assign the first user to each sub-channel.
3: **for** ($idx_s < K$) **do**
4: **for** ($idx_u < K$) **do**
5: Calculate the energy consumption (EC) of the assignment (u,s).
6: **end for**
7: **end for**
8: Construct the $K \times K$ cost matrix (C^{2D}) with the calculated EC values.
9: Run the Hungarian algorithm to assign the second user to each sub-channel.
10: Construct the matching matrix (M_P) by combining the two runs.
11: **return** M_P

Figure 3.3. Two-Round Hungarian Algorithm.

3.3.4. Complexity Analysis

The complexity of the EXS algorithm is calculated as $O(N^N)$ in Chapter 2. Moreover, the complexity of the ES and TES algorithms are also derived as $O(N^3)$ in Chapter 2. The TH algorithm comprises constructing the cost matrices and running the Hungarian algorithm twice. The complexity of two-dimensional cost matrix construction is $O(N^2)$, and the complexity of the Hungarian algorithm $O(N^3)$. Therefore, the total number of computations for TH is in the order of $(2K)^3 + K^3 + (2K)^2 + K^2$, which is equivalent to $O(N^3)$ in Big-O notation. The B-TES algorithm comprises a single run of both the TH and the TES algorithms. Since both algorithms have the complexity of $O(N^3)$, the B-TES algorithm also has the complexity of $O(N^3)$.

Run the TH algorithm to acquire the initial matching matrix (M_P).
Set $idx = 0$ and $state = 1$.
while $(idx < K)\&(state == 1)$ **do**
  Increment idx and set $state = 0$.
  for $(idx_s < 2K)$ **do**
    for $(idx_c < 2K)$ **do**
      Calculate the original energy consumption E_T from M_P.
      Set $M_P^s = M_P$.
      Swap the user in sub-channel idx_s with idx_c and update M_P^s.
      Calculate the swapped energy consumption E_T^s from M_P^s.
      if $E_T^s < E_T$ **then**
        Approve the swap, set $state = 1$ and $M_P = M_P^s$.
      end if
    end for
  end for
end while
return M_P

Figure 3.4. B-TES algorithm.

3.4. Performance Evaluation

In this section, we assess the proposed algorithms against existing ones in the literature. First, we compare the H-NOMA with OMA and NOMA for a single pair via simulations. Then, we extend our comparison to the multi-user scenario where the EXS algorithm does the sub-channel allocation. Afterward, we switch to the SCA problem and compare the proposed B-TES algorithm with the existing methods in the literature.

The simulation parameters are given in Table 3.2, where R_l is the cell radius for a larger cell, R_s is the cell radius for a smaller cell, G is the transmit antenna gain, f_c is the carrier frequency, γ_L is the path loss exponent, σ_S is the shadowing standard

deviation, N_0 is the noise floor, B is the bandwidth of a single sub-channel, D_μ is the mean value of the latency constraints per user, D_σ is the standard deviation of the latency constraints per user, N_μ is the mean value of the data transmission requirements per user, N_σ is the standard deviation of the data transmission requirements per user, α is the power amplifier efficiency, ω is the battery charge/discharge energy efficiency, and P_C^u is the constant circuit power.

Table 3.2. Simulation parameters.

Symbol	**Parameter**	**Value**
R_l	Larger cell radius	$2000\,m$
R_s	Smaller cell radius	$1000\,m$
G	Transmit antenna gain	$18\,dB$
f_c	Carrier frequency	$800\,MHz$
γ_L	Path loss exponent	3
σ_S	Shadowing loss standard deviation	$6\,dB$
N_0	Receiver noise floor	$-116\,dBm$
B	Bandwidth of a single sub-channel	$360\,kHz$
D_μ	Mean value of the latency constraint	$2.25\,s$
D_σ	Standard deviation of the latency constraint	$\frac{1.5}{\sqrt{12}}\,s$
N_μ	Mean value of the data transfer requirement	$500000\,bits$
N_σ	Standard deviation of the data transfer requirement	$\frac{250000}{\sqrt{12}}\,bits$
α	Power amplifier efficiency of the base station	0.35
ω	Battery charge/discharge efficiency of the mobile device	0.92
P_C^u	Constant power consumption of the receiver	$50\,mW$

3.4.1. Assessment of the H-NOMA Method for the Single-user Scenario

This sub-section compares the H-NOMA method to OMA and NOMA methods for a single pair. Energy consumption of H-NOMA and other methods in a larger cell is given for Case A in Figure 3.5. It is evident that H-NOMA outperforms OMA when the D_s/D_l ratio is larger than 0.5, and NOMA converges to H-NOMA when $D_s = D_l$.

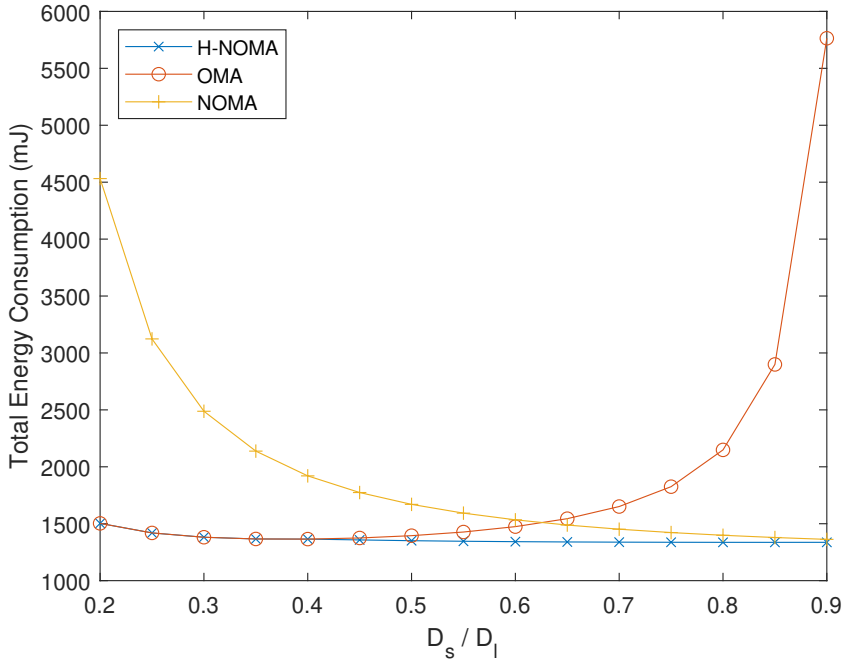

Figure 3.5. Energy consumption comparison of a pair for case A in a larger cell.

The energy consumption of H-NOMA and other methods in a larger cell is given for Case B in Figure 3.6. It is evident that H-NOMA outperforms OMA when the D_s/D_l ratio is larger than 0.5, and NOMA converges to H-NOMA when $D_s = D_l$.

Energy consumption of H-NOMA and other methods in a smaller cell is given for Case A in Figure 3.7. It is shown that H-NOMA outperforms OMA when the D_s/D_l ratio is larger than 0.55, and NOMA converges to H-NOMA when $D_s = D_l$. Moreover, compared to the larger cell scenario, the energy consumption difference between H-NOMA and other methods is smaller because H-NOMA consumes more energy due to constant circuit power consumption and less energy due to the transmit power. As the cell radius is decreased, the transmit power is reduced, and H-NOMA becomes less energy efficient.

Finally, the energy consumption of H-NOMA and other methods in a smaller cell (with a radius equal to R_s) is given for Case B in Figure 3.8. It is shown that H-NOMA outperforms OMA for a smaller part of D_s/D_l and converges to NOMA when $D_s = D_l$.

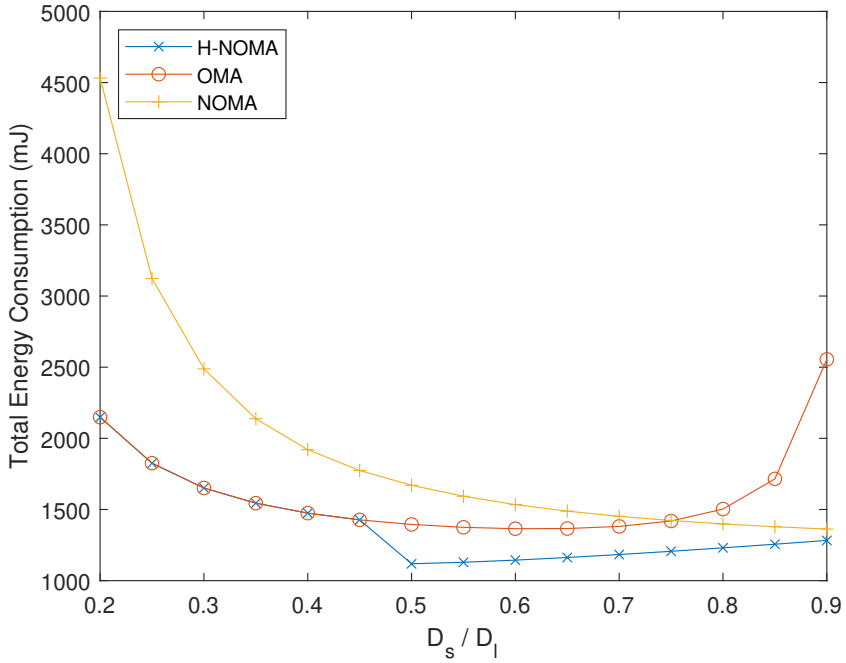

Figure 3.6. Energy consumption comparison of a pair for Case B in a larger cell.

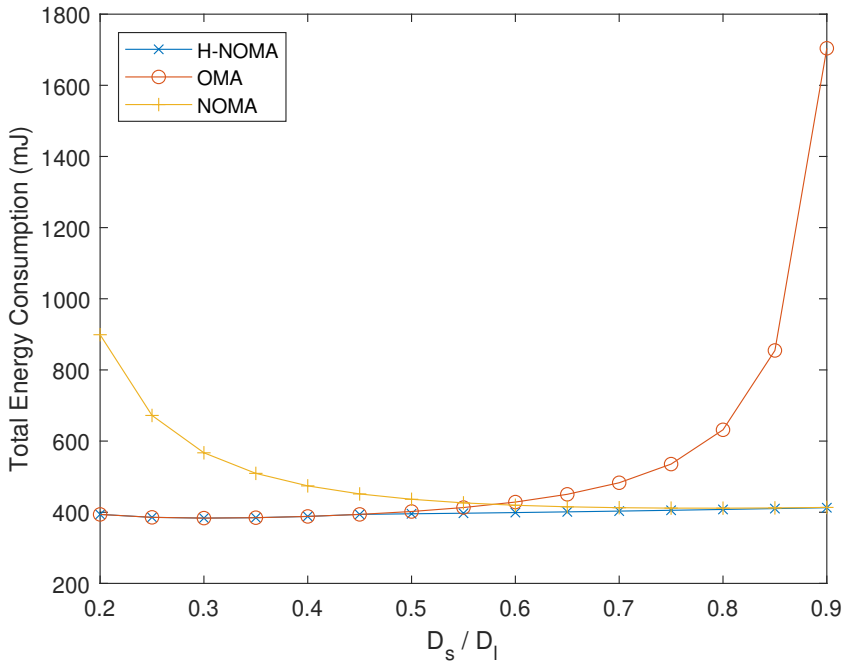

Figure 3.7. Energy consumption comparison of a pair for Case A in a smaller cell.

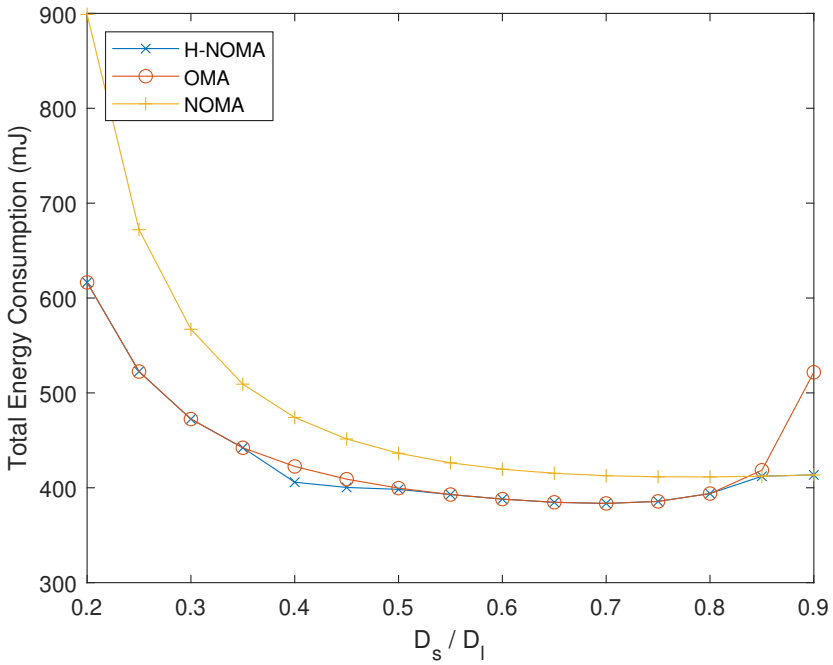

Figure 3.8. Energy consumption comparison of a pair for case B in a smaller cell.

3.4.2. Assessment of the H-NOMA Method for the Multi-user Scenario

In this sub-section, the H-NOMA method is compared to the OMA and NOMA methods for multiple users, where the optimal EXS algorithm performs the sub-channel allocation. The energy consumption comparison of H-NOMA to other multiplexing methods from the literature in a larger cell scenario is given in Figure 3.9. H-NOMA outperforms NOMA and OMA by up to 9% and 16%, respectively. Additionally, NOMA outperforms OMA by a 7% margin when the cell radius is large.

The energy consumption comparison of H-NOMA to other multiplexing methods from the literature in a smaller cell scenario is given in Figure 3.10. In this scenario, H-NOMA outperforms NOMA and OMA again by up to 11% and 13%, respectively. The energy consumption difference between H-NOMA and OMA is smaller because H-NOMA consumes more constant circuit power, as stated earlier. Moreover, the performance of OMA is significantly improved when the cell radius is decreased since it consumes the least amount of constant circuit power. OMA consumes less energy than NOMA if the number of users are larger than 25 for a smaller cell radius.

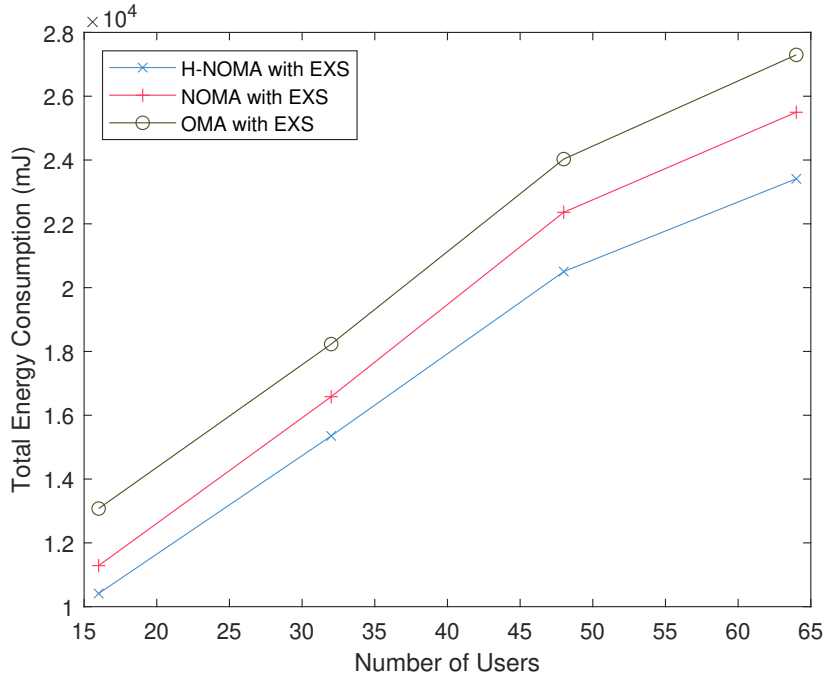

Figure 3.9. Energy consumption of multiplexing methods in a larger cell.

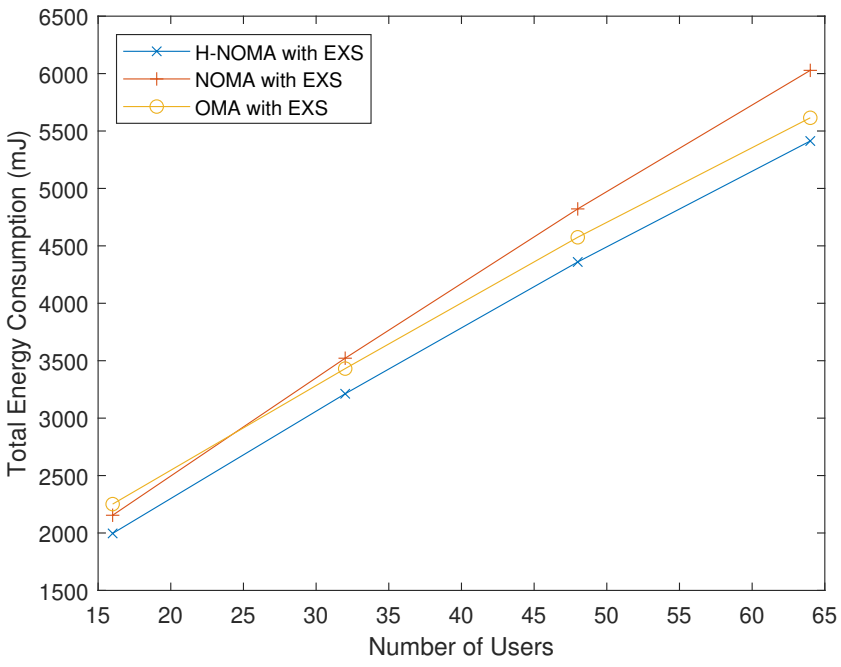

Figure 3.10. Energy consumption of multiplexing methods in a smaller cell.

3.4.3. Effects of Imperfect CSI on H-NOMA

The analyzed H-NOMA, NOMA, and OMA methods rely on CSI to determine the power and/or time allocations. The effects of imperfect CSI are analyzed in this sub-section by considering a bounded error for the CSI similar to the model in [88]. We utilize the worst-case robust approach as described in [88] and allocate powers to ensure that the required data rates are satisfied even with the worst case of the bounded error. The bounded CSI error is set to 10%.

The energy consumption comparison of H-NOMA to other multiplexing methods from the literature with perfect and imperfect CSI is given in Figure 3.11. At seen from the figure, all methods are affected from the CSI imperfection, with 9% for H-NOMA, 10% for NOMA, and 11% for OMA. Therefore, we can deduce that H-NOMA performs better compared to other methods in the literature with imperfect CSI.

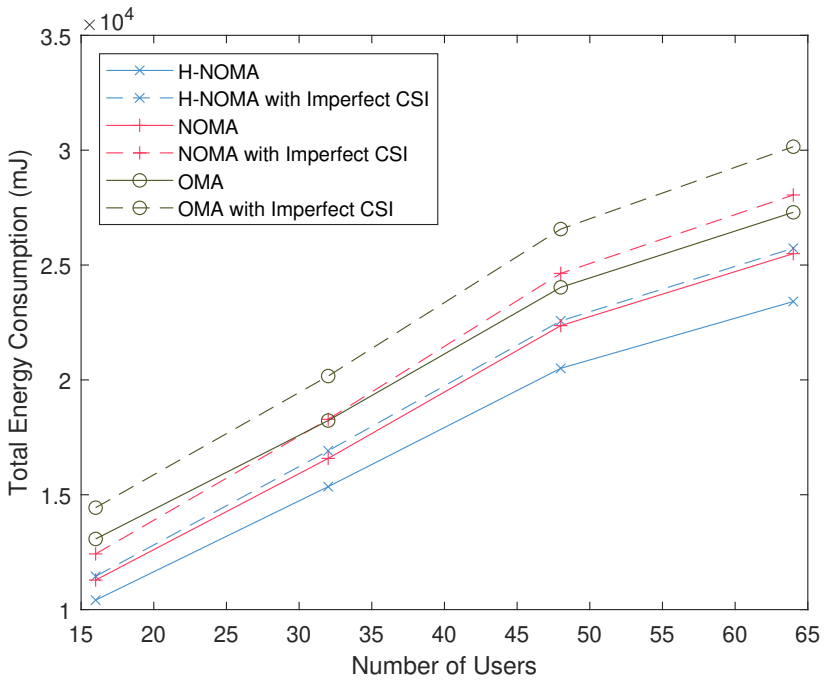

Figure 3.11. Energy consumption of multiplexing methods with imperfect CSI.

3.4.4. Assessment of the Sub-channel Allocation Algorithms

The energy consumption comparison of different SCA algorithms with the optimal H-NOMA method is given in Figure 3.12. As stated in Section 3.3, B-TES, TES, TH, and 2ES algorithms have $O(N^3)$ complexity, and the optimal EXS algorithm has $O(N^N)$ complexity. The figure shows that B-TES, TES, and TH significantly outperform the 2ES algorithm used in the literature [9, 35, 38].

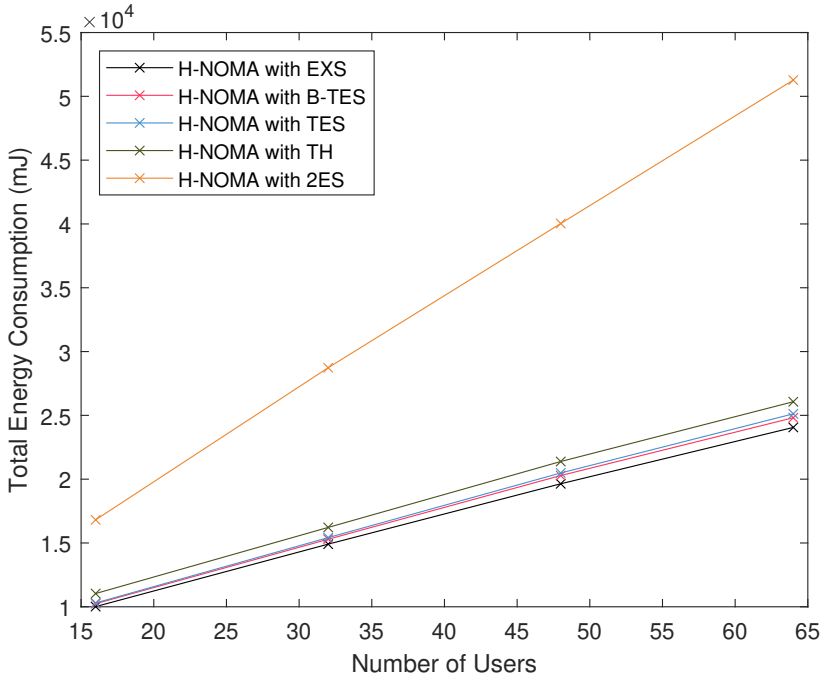

Figure 3.12. Energy consumption comparison of different SCA methods.

The energy consumption comparison of EXS, B-TES, and TES algorithms with the optimal H-NOMA method is given in Figure 3.13. The B-TES algorithm outperforms the TES algorithm [40] for all scenarios, and the difference increases up to 1% as the number of users is increased. Additionally, the results show that the B-TES algorithm performs very close to the optimal EXS algorithm. The energy consumption difference between B-TES and EXS is less than or equal to 3 % in this simulation.

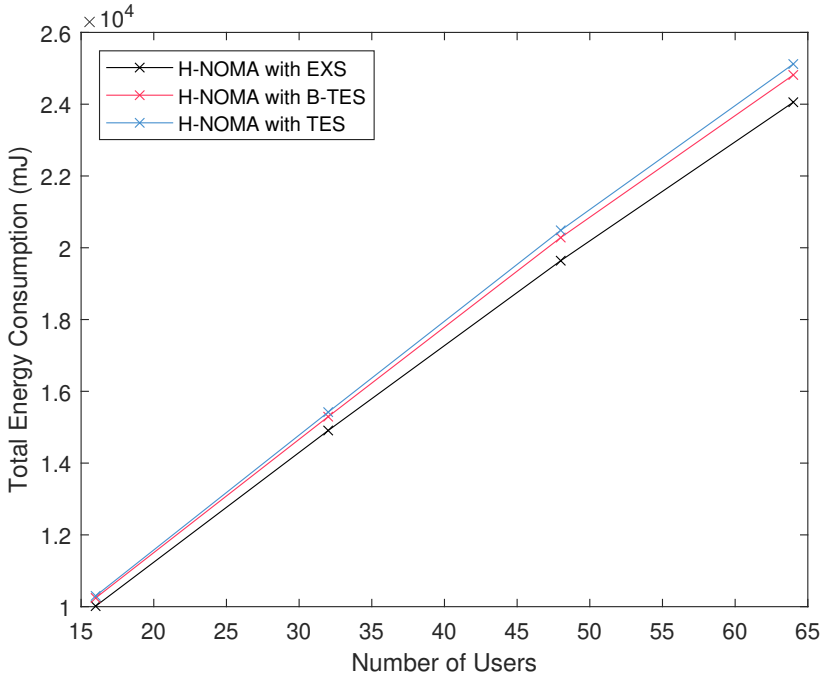

Figure 3.13. Energy consumption comparison of B-TES to TES and EXS.

3.4.5. Investigation of the Total Energy Conservation

In this section, the total energy conservation of a base station is studied by setting the average downlink throughput to 1 Gbps which is the expected load of a 5G base station [89]. The sub-channel allocation per pair is increased to 2.88 MHz, and the number of users is set to 64 to support the high throughput scenario.

We compare the proposed methods' energy consumption reduction to Turkey's annual household electricity consumption. The average annual electricity consumption of a residential building in Turkey is estimated as 2000 kWh [90]. Utilizing the number of base stations given in [91] and the projection model in [92], the number of base stations in Turkey can be estimated as 300000 at the beginning of 2023.

The energy conservation values by utilizing H-NOMA compared to other methods from the literature are given in Table 3.3. The yearly conserved energy by H-NOMA is 5 and 2.5 times the average annual electricity consumption of a single household compared to OMA and H-NOMA. Considering all base stations in Turkey, the total

energy saving by applying H-NOMA is roughly equal to the consumption of 1500000 and 750000 households compared to OMA and NOMA.

Table 3.3. Energy conservation of a base station by H-NOMA.

	Daily	**Yearly**
H-NOMA vs OMA	29.5 kWh	10782.1 kWh
H-NOMA vs NOMA	14.1 kWh	5171.9 kWh

The energy conservation values by utilizing B-TES compared to other methods from the literature are given in Table 3.4. The yearly energy saving by B-TES is 11 and 0.8 times the average annual electricity consumption of a single household compared to 2ES and TES, respectively. The total reduction in the consumed energy by utilizing B-TES is roughly equal to the consumption of 3300000 and 240000 households compared to 2ES and TES.

Table 3.4. Energy conservation of a base station by B-TES.

	Daily	**Yearly**
B-TES vs 2ES	63.4 kWh	23142.2 kWh
B-TES vs TES	4.6 kWh	1680.2 kWh

3.5. Concluding Remarks

In this chapter, we analyzed the resource allocation problem for H-NOMA in the downlink. First, we solved the optimization problem for a single H-NOMA pair in the downlink, focusing on energy efficiency while considering the circuit power consumption in the receiving users. We determined the optimal power and time allocation for H-NOMA of a single pair. Then, we extended the scenario to multiple users by utilizing OFDMA and SCA algorithms. We introduced the B-TES algorithm to solve the SCA problem with low complexity. Afterward, we showed that H-NOMA outperforms OMA and NOMA methods for both single-user and multi-user test cases. We demonstrated that the B-TES algorithm outperforms the existing 2ES and TES algorithms in the

literature. Furthermore, we showed that the B-TES algorithm performs very close (3%) to the highly complex EXS algorithm. The proposed algorithms can be utilized to reduce the energy consumption in downlink NOMA scenarios where users have heterogeneous latency and data transfer requirements.

4. DISTRIBUTED DOWNLINK RESOURCE ALLOCATION FOR HETNETS

In this chapter, we analyze the distributed resource allocation problem for downlink HetNets. We first describe the considered system model. Afterward, the MEIM algorithm is introduced to solve the sub-channel allocation problem. Then, the MP-XPC and the MP-XPCE algorithms for power allocation are presented and studied thoroughly. Later, the performance of the proposed algorithms is compared with the methods from the literature.

4.1. System Model

In this work, we analyze a network with one macrocell and $N_B - 1$ picocell base stations, where the base stations are inter-connected with backhaul links. Each base station serves N_U users by utilizing a single sub-channel per user in the downlink with N_S sub-channels. The users in the same cell are assigned to separate resource blocks in OFDMA; therefore, intra-cell interference is prevented. Still, inter-cell interference shall be considered for the utilized resource blocks. In Figure 4.1, an example multi-user network with one macrocell, five picocells, and two users per base station is given. In the diagram, the backhaul links are shown as solid lines, and the wireless links are shown as dashed lines.

The SINR of the received signal by user l on sub-channel k in cell i is given by

$$\begin{aligned} \gamma_i^k &= \frac{p_i^k}{n_i^k + \sum_{j=1}^{N_B} h_{ij}^{kl} p_j^k}, \\ h_{ij}^{kl} &= \begin{cases} 0, & \text{if } i = j, \\ \frac{g_{ij}^{kl}}{g_{ii}^{kl}}, & \text{otherwise,} \end{cases} \end{aligned} \tag{4.1}$$

where γ_i^k is the SINR of user l on sub-channel k in cell i, p_i^k is the transmit power of the base station in cell i on sub-channel k, and n_i^k is the normalized thermal noise power. g_{ij}^{kl} and h_{ij}^{kl} are the channel gain and the normalized interference channel gain between

the receive antenna of user l in cell i and the transmit antenna of the base station in cell j on sub-channel k.

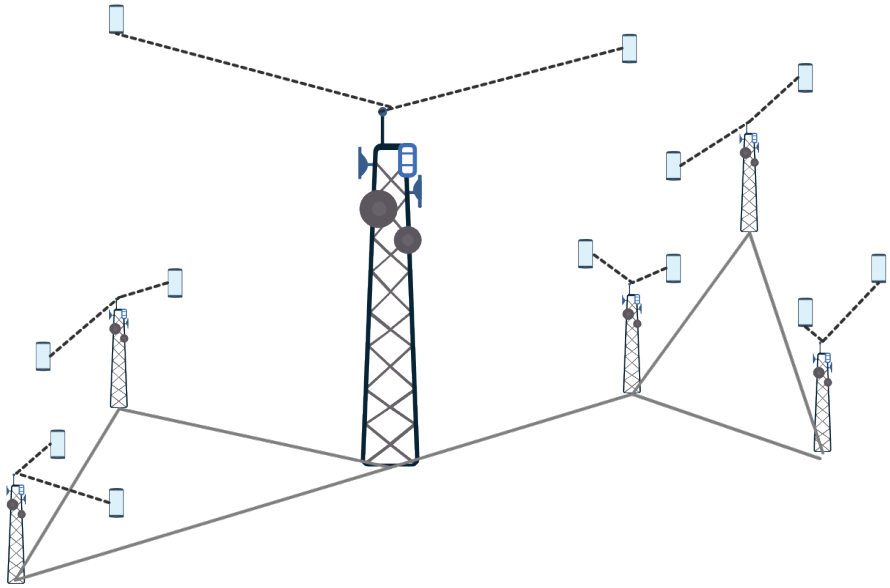

Figure 4.1. An example network with one macrocell and five picocells.

The Signal to Interference-Noise Exponential Ratio (SINX), which is utilized in the proposed power control algorithms, can be defined as

$$\begin{aligned} x_i^k &= p_i^k \left(z_i^k\right)^a, \\ z_i^k &= n_i^k + \sum_{j=1}^{N_B} h_{ij}^{kl} p_j^k, \end{aligned} \tag{4.2}$$

where x_i^k is the target SINX of user l on sub-channel k in cell i, z_i^k is the normalized interference-noise power of user l on sub-channel k in cell i, and a is the exponential parameter of the normalized interference.

In the proposed power control algorithms, the base stations share their SINX values to reach a consensus value. The connectivity between the base stations can be analyzed with the help of graph theory, where the graph's vertices are base stations, and the graph's edges are the backhaul links between the base stations. The degree of a vertex is the number of incident edges to the vertex. The set of vertices and edges

for the unweighted undirected graph in Figure 4.1 can be given as

$$\begin{aligned} V &= \{v_1, v_2, v_3, v_4, v_5, v_6\}, \\ E &= \{(v_1, v_2), (v_1, v_3), (v_2, v_3), (v_3, v_4), (v_4, v_5), (v_4, v_6), (v_5, v_6)\}. \end{aligned} \tag{4.3}$$

The Laplacian matrix of the undirected graph can be defined as [93]

$$L_{ij} = \begin{cases} deg(v_i), & \text{if } i = j, \\ -1, & \text{else if } (v_i, v_j) \in E \,||\, (v_j, v_i) \in E, \\ 0, & \text{otherwise,} \end{cases} \tag{4.4}$$

where $deg(v_i)$ is the degree of vertex i. The Laplacian matrix of the graph in (4.3) can be given by

$$\mathbf{L} = \begin{bmatrix} 2 & -1 & -1 & 0 & 0 & 0 \\ -1 & 2 & -1 & 0 & 0 & 0 \\ -1 & -1 & 3 & -1 & 0 & 0 \\ 0 & 0 & -1 & -1 & 3 & -1 \\ 0 & 0 & 0 & -1 & 2 & -1 \\ 0 & 0 & 0 & -1 & -1 & 2 \end{bmatrix}. \tag{4.5}$$

which is always positive semi-definite for an undirected graph. The Laplacian matrix has a simple zero eigenvalue if the graph is connected, and a consensus can only be achieved if the Laplacian matrix has a simple zero eigenvalue [94].

Base stations in 4G and 5G systems transmit cell-specific reference signals (CS-RS) with a constant power that depends on the cell size. Each user can estimate the signal power, the interference power, and the noise power by utilizing the CS-RS [95]. We assume that each user periodically sends the measured power levels to its serving base station. We define effective interference as the ratio of the interference power to the signal power for the CS-RS. The effective interference of user l in cell i on sub-channel k can be expressed as

$$\nu_i^k = \frac{\sum_{j \neq i} g_{ij}^{kl} p_j}{g_{ii}^{kl} p_i}, \tag{4.6}$$

where p_i and p_j are the transmit power of the CS-RS for the analyzed base station

and the interfering base stations, respectively. Each base station can determine the effective interference per user by dividing the interference power by the signal power based on the received power levels.

4.2. Proposed Sub-Channel Allocation Algorithm

This section studies the downlink sub-channel allocation problem in two-tier HetNets that utilize OFDMA. We propose the MEIM algorithm for the sub-channel allocation problem, which reduces the maximum effective interference in the network in a distributed fashion without any dependence on the transmit power allocation for the users. The effective interference in cell i on sub-channel k can be expressed in terms of channel gains and sub-channel allocation as

$$\nu_i^k = \sum_{l=1}^{N_U} \frac{\phi_i^{kl}}{g_{ii}^{kl} p_i} \sum_{j \neq i} g_{ij}^{kl} p_j, \tag{4.7}$$

where ϕ_i^{kl} are the entries of the two-dimensional sub-channel assignment matrix $\mathbf{\Phi_i}$.

In the downlink direction, the channel gain values between a user and a neighbor base station do not depend on the sub-channel allocation in the neighbor cell. Therefore, the effective interference value of a cell is independent of neighbor cells, and minimizing the maximum effective interference in each cell and the whole network are equivalent. Therefore, we can define an independent assignment problem for each base station and solve the problem in a distributed fashion. The optimization problem to minimize the maximum effective interference on the sub-channels in cell i can be defined as

$$\min_{\mathbf{\Phi_i}} \max_{k} \quad \sum_{l=1}^{N_U} \frac{\phi_i^{kl}}{g_{ii}^{kl} p_i} \sum_{j \neq i} g_{ij}^{kl} p_j, \tag{4.8a}$$

$$\text{s.t.} \quad \phi_i^{kl} \in \{0, 1\} \quad \forall k, l, \tag{4.8b}$$

$$\sum_{l} \phi_i^{kl} = 1, \quad \forall k, \tag{4.8c}$$

$$\sum_{k} \phi_i^{kl} = 1, \quad \forall l, \tag{4.8d}$$

where constraint (4.8b) states that the sub-channel allocation matrix is binary. Con-

straints (4.8c) and (4.8d) express that each sub-channel of a base station is assigned to a single user, and each user is allocated a single sub-channel of a base station. The maximization operation selects the sub-channel with the maximum effective interference, and the minimization operation minimizes the effective interference value of the sub-channel with maximum effective interference. This problem can be classified as a linear bottleneck assignment problem (LBAP) [96]. In the LBAP, the objective is to minimize the maximum cost induced by a single agent. Different algorithms are available in the literature to solve the LBAP optimally [96]. In this article, we utilize the Gabow-Tarjan (GT) algorithm, which solves the problem optimally and has the complexity of $O(N^2\sqrt{N \log N})$ [97].

The effective interference value per sub-channel is required at the base stations to form the LBAP. As stated in Section 4.1, the effective interference that each user experiences can be derived by estimating the signal power and the interference power from the CS-RS. This work assumes that users convey the estimated power values to their serving base stations. The execution steps for the MEIM algorithm are given in Figure 4.2. Periodically, all the base stations run the MEIM algorithm in parallel to minimize the maximum interference when there are changes in the network.

The MEIM algorithm starts with all the base stations transmitting CS-RS in parallel (Step 1). All the base stations in the HetNet transmit CS-RS for the users to determine the downlink channel gain between the serving base station and themselves (Step 2). The users determine the relevant signal and interference power from the CS-RS and send it to their serving base stations (Steps 3-6). Each base station calculates the effective interference values for all the users it serves by utilizing (4.7) (Steps 7-9). Then, each base station constructs the LBAP as in (4.8) and finds the optimal solution of the LBAP (Steps 10-11).

1: **for** all base stations (in parallel) **do**
2: The base station transmits CS-RS.
3: **for** all users (in parallel) **do**
4: The user estimates the signal power and the interference power.
5: The user reports the estimated values to its serving base station.
6: **end for**
7: **for** all users served by the base station **do**
8: The base station calculates the effective interference for all sub-channels using (4.7).
9: **end for**
10: The base station constructs the LBAP as in (4.8).
11: The base station finds the optimal solution to the LBAP (Φ_i) and allocates sub-channels to users accordingly.
12: **end for**

Figure 4.2. MEIM algorithm.

The complexity of the MEIM algorithm per base station can be calculated by determining the number of operations to construct and solve the LBAP. The complexity of creating the LBAP is $O(N^2)$ since there are $N_U * N_S$ effective interference values to be calculated, and the complexity of solving the LBAP is $O(N^2\sqrt{N \log N})$. Thus, the total complexity of the MEIM algorithm is bounded by $O(N^2\sqrt{N \log N})$.

Theorem 4.1. *The MEIM algorithm assigns users to sub-channels to minimize the maximum effective interference in the network.*

Proof. Utilizing the MEIM algorithm, each base station constructs an LBAP in (4.8) and solves the LBAP optimally [96]. Therefore, the resulting sub-channel allocation of the MEIM algorithm is the optimal solution per base station. As we have indicated in this section, the effective interference in a cell does not depend on the sub-channel allocation in other cells. Therefore, the MEIM algorithm minimizes the maximum effective interference in the network by solving the LBAP for each cell independently. □

Remark 4.2. *Theorem 4.1 shows that the MEIM minimizes the maximum effective interference by using the available CS-RS in a single step. This is a significant improvement to the sub-channel algorithms in the literature [59,69], which require multiple iterations combined with power assignment.*

4.3. Proposed Power Control Algorithm

In this section, we focus on the power allocation problem in the HetNets. We assume that the sub-channel allocation is done beforehand, and the power allocation algorithm is run per sub-channel independently. There is no interference between sub-channels since OFDMA prevents intra-cell interference. We propose two algorithms to increase the total throughput in the network by assigning higher power to the users with favorable channel conditions.

4.3.1. The MP-XPC Algorithm

In the MP-XPC algorithm, all the base stations share their SINX values and converge to a common SINX target, where the definition of SINX is given in (4.2). The interval of the a value is selected as $\in [-1, 0)$ throughout this work. The value of a determines the trade-off between fairness and throughput, shown in Section 4.4. The MP-XPC algorithm does not consider $a \in [0, \infty)$ and $a \in (-\infty, -1)$ regions due to the severe decline in fairness, and the degradation in throughput, respectively. The MP-XPC algorithm does not require pre-defined targets because the SINX targets are determined in a distributed fashion by message passing. After each iteration, the base stations exchange their SINX values with neighbor base stations via the backhaul links. Then, the target SINX for the user on sub-channel k in cell i is calculated from the average of the received neighbor SINX values as

$$x_i^{kT}(t) = \frac{1}{|N_i|} \sum_{j \in N_i} x_j^k(t), \tag{4.9}$$

where N_i is the number of neighbor base stations of cell i, $x_i^{kT}(t)$ is the target SINX of the user in cell i, and $x_j^k(t)$ is the SINX value of the user in cell j.

The power update formula for MP-XPC can be expressed as

$$\dot{p_i^k}(t) = -\beta\Big(1 - \frac{x_i^{kT}(t)}{x_i^k(t)}\Big)p_i^k(t), \tag{4.10}$$

where $x_i^T(t)$ is updated at each iteration by (4.9). It is apparent from the power update formula that the system converges once all the users reach their SINX targets. The MP-XPC algorithm is shown in Figure 4.3. The algorithm is always active to ensure that the system can dynamically respond to the changes in the network. However, the power values are no longer updated after convergence.

1: All base stations set their transmit power to a random initial value per sub-channel.
2: **for** all active sub-channels **do**
3: **for** all base stations in parallel **do**
4: The base station transmits to the users with the set transmit power.
5: **for** all users in a cell in parallel **do**
6: The user estimates the received signal power.
7: The user estimates the interference-noise power.
8: The user reports the estimated values to its serving base station.
9: **end for**
10: **for** all users served by the base station **do**
11: The base station calculates the SINX value by (4.2).
12: The base station exchanges the SINX value with the neighbor base stations.
13: The base station calculates the target SINX value by (4.9).
14: The base station updates the transmit power value by (4.10).
15: **end for**
16: **end for**
17: **end for**

Figure 4.3. MP-XPC algorithm.

The MP-XPC algorithm starts with all the base stations initializing their transmit power to users with a random value (Step 1). The algorithm is executed per sub-channel

(Steps 2-17). Each base station transmits to the users with the transmit power set initially or in the previous iteration (Step 4). Each user calculates the received signal power ($\hat{y}_i^k$) as a by-product of channel estimation and estimates the interference-noise power $\hat{w}_i^k$ by subtracting the received signal power from the total received power (Steps 6-7). Then each user sends the estimated values to the serving base station (Step 8). Afterward, the serving base station utilizes the information it receives from its connected user on the sub-channel to determine the SINX values. First, the channel gain value for each user g_{ii}^k is estimated as

$$\hat{g}_{ii}^k = \frac{\hat{y}_i^k}{p_i^k}, \tag{4.11}$$

utilizing the known transmit power value and the estimated received signal power. From these values, the normalized interference-noise power can be estimated as

$$\hat{z}_i^k = \frac{\hat{w}_i^k}{\hat{g}_{ii}^k}, \tag{4.12}$$

and the SINX value can be calculated as $p_i^k \left(\hat{z}_i^k\right)^a$ (Step 11). Finally, the base stations exchange the SINX value with each other, and update their target SINX and transmit power values (Steps 12-14).

4.3.2. The MP-XPCE Algorithm

In HetNets, multiple small cells work in the cell radius of a single macrocell base station. The MP-XPC algorithm can be extended by setting an SINR target to the macrocell user, which we refer to as MP-XPCE. For the system to be feasible, the upper bound of the SINR target is the scenario where the small cell transmit powers are set to zero, which is given by

$$\gamma_m^{kT} \leq \gamma_m^{kU} = \frac{p_m^k}{n_m^k}, \tag{4.13}$$

where γ_m^{kT} and γ_m^{kU} are the target SINR and the upper bound of the SINR of the macrocell user on sub-channel k. p_m^k is the transmit power of the macrocell on sub-channel k, and n_m^k is the noise power at the receiver of the user served on sub-channel k by the macrocell.

The SINX target of the macrocell user is calculated as follows

$$x_m^{kT}(t) = \gamma_m^{kT} * \left(z_m^k(t)\right)^{(a+1)}, \tag{4.14}$$

where $z_m^k(t)$ is the normalized interference-noise power and the relation follows from the definitions of SINR and SINX in (4.1) and (4.2), respectively. To ensure that the rest of the network is not affected by the constant macrocell SINX target $x_m^{kT}(t)$, the macrocell base station sends a modified SINX value to its neighbors. To determine the modified SINX value, first, the ratio of the average SINX value of neighbors of the macrocell to the macrocell SINX target is calculated as follows

$$\alpha_m^k(t) = \frac{\frac{1}{|N_m|}\sum_{j\in N_m} x_j^k(t)}{x_m^{kT}(t)}, \tag{4.15}$$

where $\alpha_m^k(t)$ is the ratio of the macrocell SINX target to the average SINX value of the neighbor cells of the macrocell, N_m is the number of neighbor base stations of the macrocell, and $x_j^k(t)$ is the SINX value of the user in cell j. Then, at each iteration the modified SINX value of the macrocell is evaluated as

$$x_m^{kM}(t) = x_m^k(t)\alpha_m^k(t). \tag{4.16}$$

Due to the modifications to the macrocell SINX target value in (4.14) and the macrocell SINX value in (4.16), the power update formula for MP-XPCE differs for the macrocell and picocells that are neighbors of the macrocell. The macrocell power update formula is given by

$$\dot{p_m^k}(t) = -\beta\Big(1 - \frac{x_m^{kT}(t)}{x_m^k(t)}\Big)p_m^k(t), \tag{4.17}$$

where $x_m^{kT}(t)$ is the required SINX value to reach the SINR target of the macrocell. For the picocells that are neighbors of the macrocell, the power update formula is

$$\dot{p_p^k}(t) = -\beta\Big(1 - \frac{x_p^{kT}(t)}{x_p^k(t)}\Big)p_p^k(t), \tag{4.18}$$

where $x_p^{kT}(t)$ is updated with the neighbor values as follows

$$x_p^{kT}(t) = \frac{1}{|N_i|}\left(x_m^{kM}(t) + \sum_{j\in N_i, j\neq m} x_j^k(t)\right). \tag{4.19}$$

For other picocells the original power update equation in (4.10) is valid.

4.3.3. Convergence Analysis of MP-XPC

In this sub-section, the convergence analysis of the MP-XPC algorithm is presented. First we define the normalized Interference-Noise exponent $e_i(t)$, which is

$$e_i(t) = (z_i(t))^a \,. \tag{4.20}$$

where the sub-channel index k is dropped for simplicity. Then, the power update equation of the MP-XPC algorithm can be expressed in vector form as

$$\dot{\mathbf{p}}(t) = -\mathbf{B_d}{\mathbf{E_d}}^{-1}(t)\mathbf{L}\mathbf{E_d}(t)\mathbf{p}(t), \tag{4.21}$$

where $\mathbf{B_d} = diag\Big[\frac{\beta}{N_i}\Big]_{i=1}^{N}$, $\mathbf{E_d}(t) = diag\Big[e_i(t)\Big]_{i=1}^{N}$, and $\mathbf{L}$ is the symmetric Laplacian matrix of the base station connectivity graph. The power update algorithm can be converted to a simpler form by utilizing (4.2) and (4.20)

$$\dot{\mathbf{p}}(t) = -\mathbf{B_d}{\mathbf{E_d}}^{-1}(t)\mathbf{L}\mathbf{x}(t), \tag{4.22}$$

which converges if and only if $\mathbf{L}\mathbf{x}(t) = 0$, since $\mathbf{B_d}$ and ${\mathbf{E_d}}^{-1}(t)$ are positive semi-definite diagonal matrices.

Lemma 4.3. *If a scalar function $V(\mathbf{p}(t))$ satisfies the following conditions*

- *$V(\mathbf{p}(t))$ is lower-bounded,*
- *$\dot{V}(\mathbf{p}(t))$ is negative semi-definite,*
- *$\dot{V}(\mathbf{p}(t))$ is is uniformly continuous in time,*

then $\lim_{t\to\infty}\dot{V}(\mathbf{p}(t)) = 0$ by Barbalat's Lemma [98].

Theorem 4.4. *The MP-XPC algorithm converges to a stable solution where all users have equal SINX values.*

Proof. The Lyapunov-like function $V(\mathbf{p}(t))$ that corresponds to the total power consumption can be expressed as

$$V(\mathbf{p}(t)) = \mathbf{1}^T\mathbf{p}(t), \tag{4.23}$$

which satisfies $V(\mathbf{p}(t)) \geq 0$, since the power allocation cannot be negative.

The derivative of the Lyapunov-like function can be given by

$$\begin{aligned} \dot{V}(\mathbf{p}(t)) &= -\mathbf{1}^T \mathbf{B_d} \mathbf{L_s}(t) \mathbf{p}(t), \\ \mathbf{L_s}(t) &= \mathbf{E_d}^{-1}(t) \mathbf{L} \mathbf{E_d}(t), \end{aligned} \tag{4.24}$$

which is negative semi-definite, since $\mathbf{B_d}$ is a positive definite diagonal matrix, $\mathbf{L_s}(t)$ is the similar matrix to the positive semi-definite Laplacian matrix $\mathbf{L}$. The third condition of the Barbalat's Lemma is satisfied when the second derivative of the Lyapunov-like function is bounded [98]. The second derivative is

$$\ddot{V}(\mathbf{p}(t)) = \mathbf{1}^T \mathbf{B_d} \mathbf{L_s}(t) \mathbf{B_d} \mathbf{L_s}(t) \mathbf{p}(t) - \mathbf{1}^T \mathbf{B_d} \dot{\mathbf{L_s}}(t) \mathbf{p}(t), \tag{4.25}$$

where the first part of the equation is bounded, since $\mathbf{B_d}$, $\mathbf{E_d}(t)$, $\mathbf{E_d}^{-1}(t)$ and $\mathbf{L}$ are bounded. The second part of the equation is bounded if $\dot{\mathbf{L_s}}(t)$ is also bounded. The derivative of $\mathbf{L_s}(t)$ is given by

$$\dot{\mathbf{L_s}}(t) = \dot{\mathbf{E_d}}^{-1}(t) \mathbf{L} \mathbf{E_d}(t) + \mathbf{E_d}^{-1}(t) \mathbf{L} \dot{\mathbf{E_d}}(t), \tag{4.26}$$

which is bounded if $\dot{\mathbf{E_d}}^{-1}(t)$ and $\dot{\mathbf{E_d}}(t)$ are bounded. Further analysis can be done element by element for these diagonal matrices. The derivatives of $e_i(t)$ and $\frac{1}{e_i(t)}$ and can expressed as

$$\begin{aligned} \dot{e}_i(t) &= a \left(\sum_{j=1}^{N_B} h_{ij} p_j(t) + n_i \right)^{(a-1)} \sum_{j=1}^{N_B} h_{ij} \dot{p}_j(t), \\ \left(\frac{\dot{1}}{e_i(t)} \right) &= \frac{\dot{e}_i(t)}{e_i^2(t)}, \end{aligned} \tag{4.27}$$

where both derivatives are bounded, since $p_j(t)$, $\dot{p}_j(t)$ and a are bounded, and $e_i^2(t) > 0$. Therefore, utilizing Lemma 4.3, we can deduce that $\lim_{t\to\infty} \dot{V}(\mathbf{p}(t)) = 0$. Since $\mathbf{B_d}$ and $\mathbf{E_d}(t)$ are diagonal matrices with positive entries, we can state that $\lim_{t\to\infty} \mathbf{L}\mathbf{x}(t) = 0$ by utilizing (4.24). Since the Laplacian matrix has a simple eigenvalue at zero with the all-ones vector as the eigenvector, we can deduce that all users have equal SINX values when the algorithm converges. □

Remark 4.5. *Theorem 4.4 states that the MP-XPC algorithm converges to a solution where the users have equal SINX values. On the other hand, the SINR values of the users differ, which depend on the channel conditions, and the experienced interference power.*

Corollary 4.6. *The SINR values of the users after convergence are*

$$\gamma_i(t) = \frac{x^*}{\left(n_i + \sum_{j=1}^{N_B} h_{ij} p_j(t)\right)^{(a+1)}}, \tag{4.28}$$

where x^* is the final SINX value after convergence.

Proof. The derivation follows from the definition of SINR in (4.1), and the definition of SINX in (4.2). □

Remark 4.7. *Corollary 4.6 gives the SINR values of different users after convergence. It can be seen from* (4.28) *that the users with higher effective interference values experience lower SINR, whereas the users with lower effective interference experience higher SINR when $a > -1$.*

4.3.4. Convergence Analysis of MP-XPCE

In this sub-section, the convergence analysis of the MP-XPCE algorithm is given. The power update equation of the MP-XPCE algorithm in vector form is given by

$$\dot{\mathbf{p}}(t) = -\mathbf{B_d}{\mathbf{E_d}}^{-1}(t)\mathbf{L}\mathbf{A_d}(t)\mathbf{x}(t), \tag{4.29}$$

where $\mathbf{A_d}(t) = diag\Big[\alpha_i\Big]_{i=1}^{N}$, and the values of the diagonal elements are

$$\alpha_i = \begin{cases} \alpha_m^k(t), & \text{if } i = m, \\ 1, & \text{otherwise}, \end{cases} \tag{4.30}$$

in other words, the matrix $\mathbf{A_d}(t)$ is a diagonal matrix with all the entries set to one, except for the macrocell related entry. The algorithm converges if and only if $\mathbf{L}\mathbf{A_d}(t)\mathbf{x}(t) = 0$, since $\mathbf{B_d}$ and ${\mathbf{E_d}}^{-1}(t)$ are positive semi-definite diagonal matrices.

Theorem 4.8. *The MP-XPCE algorithm converges to a stable solution where all picocell users have equal SINX values, and the macrocell user reaches the SINR target.*

Proof. The Lyapunov-like function $V(\mathbf{p}(t))$ that corresponds to the total power consumption can be defined depending on the power allocation as

$$V(\mathbf{p}(t)) = \mathbf{1}^T\mathbf{p}(t), \tag{4.31}$$

which satisfies the first condition of the Barbalat's Lemma, $V(\mathbf{p}(t)) \geq 0$, since the power allocation cannot be negative. The derivative of the Lyapunov-like function is

$$\dot{V}(\mathbf{p}(t)) = -\mathbf{1}^T \mathbf{B_d} \mathbf{E_d}^{-1}(t) \mathbf{L} \mathbf{E_d}(t) \mathbf{A_d}(t) \mathbf{p}(t), \tag{4.32}$$

which is negative semi-definite and satisfies the second condition of Barbalat's Lemma, since $\mathbf{B_d}$ is a positive definite diagonal matrix, $\mathbf{A_d}(t)$ is a positive definite diagonal matrix, $\mathbf{E_d}^{-1}(t)\mathbf{L}\mathbf{E_d}(t)$ is the similar matrix $\mathbf{L_s}(t)$ to the positive semi-definite Laplacian matrix $\mathbf{L}$, which is bounded. The second derivative of $V(\mathbf{p}(t))$ can be determined by

$$\ddot{V}(\mathbf{p}(t)) = \mathbf{b}^T \left(\mathbf{L_s}(t) \mathbf{A_d}(t) \dot{\mathbf{p}}(t) - \mathbf{L_s}(t) \dot{\mathbf{A}}_\mathbf{d}(t) \mathbf{p}(t) - \dot{\mathbf{L}}_\mathbf{s}(t) \mathbf{A_d}(t) \mathbf{p}(t) \right), \tag{4.33}$$

where $\mathbf{b}^T$ is the vector of $\frac{\beta}{N_i}$ values and is bounded. The first term in parenthesis is

$$\mathbf{L_s}(t) \mathbf{A_d}(t) \mathbf{B_d} \mathbf{L_s}(t) \mathbf{A_d}(t) \mathbf{p}(t), \tag{4.34}$$

which is bounded, since $\mathbf{L_s}(t)$ and $\mathbf{A_d}(t)$ are bounded. The second term in parenthesis is bounded if $\dot{\mathbf{A}}_\mathbf{d}(t)$ is bounded. From the definition of $\mathbf{A_d}(t)$ in (4.30) it can be deduced that all the elements of $\dot{\mathbf{A}}_\mathbf{d}(t)$ is equal to zero, except for the diagonal term that corresponds to the macrocell. The derivative of the macrocell related term is

$$\dot{\alpha_m}(t) = \frac{\left(\sum_{j \in N_m} \dot{e_j}(t) p_j(t) \right)}{e_m(t)^{\frac{a+1}{a}}} + \sum_{j \in N_m} e_j(t) p_j(t) \frac{\dot{e_m}(t)}{e_m(t)^{\frac{2a+1}{a}}}, \tag{4.35}$$

which is bounded, since $e_i(t)$, $\dot{e_i}(t)$, $p_i(t)$, and $\dot{p_i}(t)$ are bounded for all values i. The third term in the parenthesis is bounded if $\dot{\mathbf{L}}_\mathbf{s}(t)$ is also bounded as shown previously in the convergence analysis of MP-XPC. Akin to the proof of Theorem 4.4, by utilizing Lemma 4.3, we can deduce that $\lim_{t \to \infty} \dot{V}(\mathbf{p}(t)) = 0$. We can show that $\lim_{t \to \infty} \mathbf{L} \mathbf{A_d}(t) \mathbf{x}(t) = 0$ from (4.32) because $\mathbf{B_d}$ and $\mathbf{E_d}(t)$ are diagonal matrices with positive entries. Since the Laplacian matrix has a simple eigenvalue at zero with the all-ones vector as the eigenvector, we can deduce that all elements of the $\mathbf{A_d}(t)\mathbf{x}(t)$ vector are equal to the SINX value of the picocells after convergence (x_p^*). From (4.17), the SINX value of the macrocell can be calculated as $x_m^{kT}(t)$, which corresponds to the SINR value of γ_m^{kT}. □

Remark 4.9. *Theorem 4.8 states that the MP-XPC algorithm converges to a solution where all the picocell users have equal SINX values, and the macrocell user reaches a SINX value that corresponds to the target macrocell SINR value. The SINR values of the users differ depending on the channel conditions and the experienced interference power.*

Corollary 4.10. *SINR values of the users after convergence can be expressed as follows*

$$\gamma_i(t) = \begin{cases} \gamma_m^T, & \text{if } i = m, \\ \dfrac{x_p^*}{\left(n_i + \sum_{j=1}^{N_B} h_{ij} p_j(t)\right)^{(a+1)}}, & \text{otherwise,} \end{cases} \tag{4.36}$$

where x_p^* is the converged SINX value of the picocell users.

Proof. The derivation follows from (4.1) and (4.2). □

Remark 4.11. *Corollary 4.10 gives the SINR values of different users after convergence. It can be seen from* (4.36) *that the picocell users with higher effective interference values experience lower SINR, whereas the picocell users with lower effective interference experience higher SINR when $a > -1$.*

4.4. Performance Evaluation

In this section, first, we analyze the performance of the proposed power allocation algorithms in a single sub-channel scenario. Then, we combine the proposed sub-channel and power allocation algorithms and assess the performance against the joint sub-channel and power allocation methods from the literature. Finally, we show the convergence behavior of the studied methods.

This section analyzes scenarios where a cluster of picocells is deployed within the macrocell. A multi-user scenario with twenty-one picocells and one macrocell, where each base station serves two users, is given in Figure 4.4. The base stations and users are denoted by squares and triangles, respectively. The macrocell and the macrocell users are in green, and the picocells and the picocell users are in red.

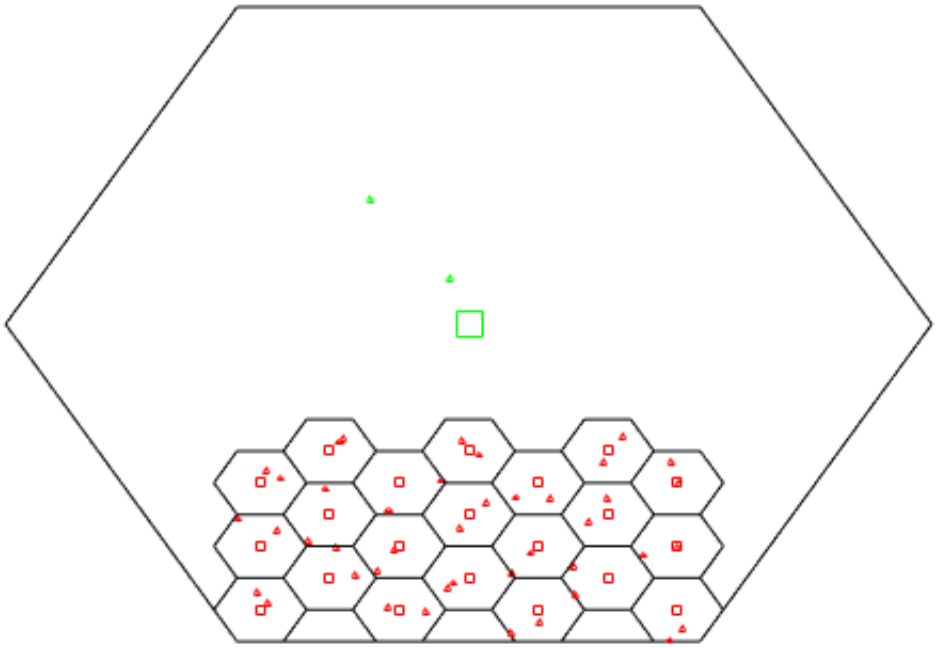

Figure 4.4. Example multi-user scenario with 21 picocells and 1 macrocell.

The simulation parameters are given in Table 4.1, where P_M^{TM} is the maximum transmit power of the macrocell base station, P_P^{TM} is the maximum transmit power of the picocell base station, P_M^{TRS} is the CS-RS transmit power of the macrocell base station, P_P^{TRS} is the CS-RS transmit power of the picocell base station, R_M is the macrocell radius, and R_P is the picocell radius. N_0 is the noise floor, f_c is the carrier frequency, G is the base station antenna gain, γ_L is the path loss exponent, and σ_S is the standard deviation of shadowing.

4.4.1. Exponential Parameter Selection for MP-XPC

In this sub-section, we evaluate different values of a for the MP-XPC algorithm when each cell serves a single user. The average throughput (R_m) and the JFI with respect to the throughput of users served by fifteen picocells for different a values of the MP-XPC algorithm are given in Figure 4.5. When $a = -1$, all users converge to the same SINR value and equal throughput, corresponding to a JFI of 1. The fairness decreases as the a value increases since larger a values correspond to higher power assignments to the users with better channel conditions, boosting the SINR variance.

Table 4.1. Simulation parameters.

Symbol	**Parameter**	**Value**
R_M	Macrocell radius	$2000\,m$
R_P	Picocell radius	$200\,m$
P_M^{TM}	Macrocell maximum transmit power	$46\,dBm$
P_P^{TM}	Picocell maximum transmit power	$26\,dBm$
P_M^{TRS}	Macrocell CS-RS transmit power	$43\,dBm$
P_P^{TRS}	Picocell CS-RS transmit power	$23\,dBm$
N_0	Receiver noise floor	$-116\,dBm$
f_c	Carrier frequency	$800\,MHz$
G	Transmit antenna gain	$18\,dB$
γ_L	Path loss exponent	3
σ_S	Shadowing loss standard deviation	$6\,dB$

The scenario with twenty-one picocells is shown in Figure 4.6, which performs similarly to the scenario with sixteen cells. For both scenarios, $a = -0.5$ is a good candidate for the exponential configuration parameter because it results in acceptable fairness ($JFI > 80\%$) and significantly higher throughput than total fairness at $a = -1$.

4.4.2. Single Sub-channel Scenario

The MP-XPC algorithm with $a = -0.5$ is compared to the CBPA algorithm for fifteen and twenty-one picocells and one macrocell in Table 4.2, respectively. As can be seen from the table, the average throughput of the MP-XPC algorithm is significantly higher than the average of the CBPA algorithm from [55]. This difference is expected since the MP-XPC algorithm allocates higher power values to the users with better channel conditions. On the other hand, the MP-XPC algorithm is not as fair as the CBPA algorithm. The table shows the reduction in fairness as around 15%.

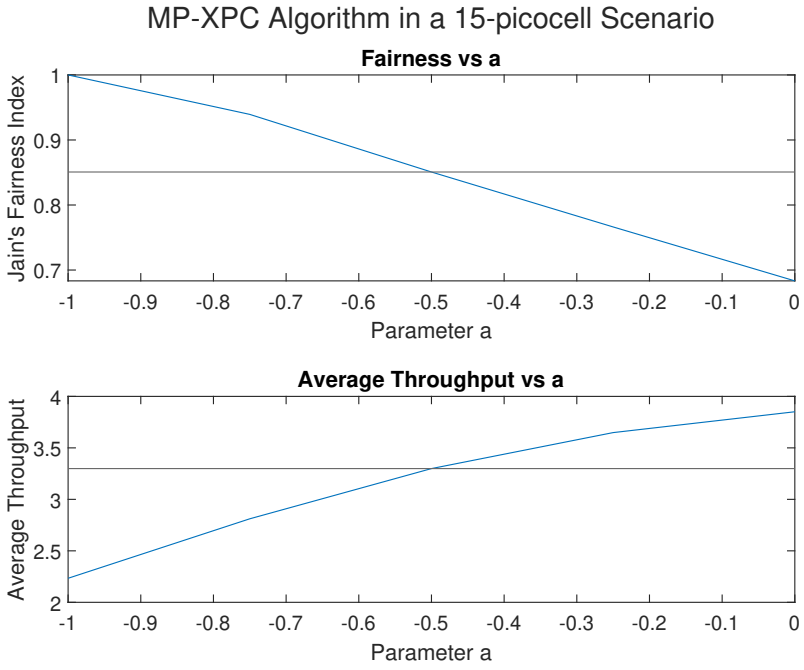

Figure 4.5. MP-XPC algorithm with different a values in a 15-picocell scenario.

Table 4.2. Assessment of MP-XPC without macrocell SINR target.

	15 picocells		21 picocells	
	JFI	R_m	JFI	R_m
MP-XPC	0.84	2.99	0.86	3.10
CBPA	1	1.79	1	1.91

The MP-XPCE algorithm with $a = -0.5$ is compared to the CBPA-M [56] and LQP [54] algorithms for fifteen and twenty-one picocells and one macrocell in Table 4.3, respectively. Since the macrocell has a target SINR in this scenario, the fairness is calculated only for the picocells. As can be seen from the table, the average throughput of the MP-XPC algorithm is significantly higher than the CBPA-M and LQP algorithms from the literature. This difference is expected since the MP-XPCE algorithm allocates higher power values to the users with better channel conditions. Similar to the MP-XPC algorithm, the MP-XPCE algorithm is not as fair as its counterparts, shown in the table. Moreover, the macrocell SINR target (γ_M) is satisfied with MP-XPCE and LQP but not with CBPA-M.

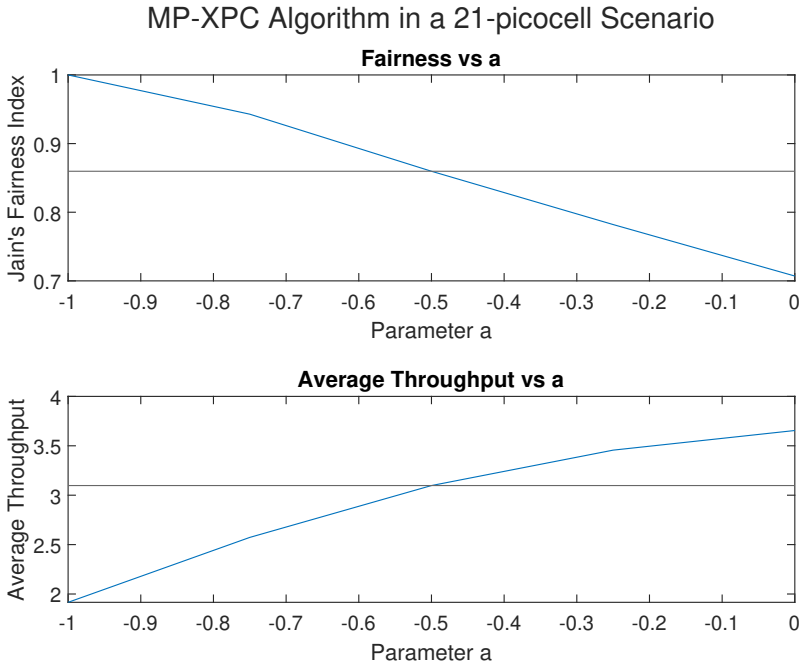

Figure 4.6. MP-XPC algorithm with different a values in a 21-picocell scenario.

Table 4.3. Assessment of MP-XPCE with 15 dB macrocell SINR target.

	15 picocells			21 picocells		
	JFI	R_m	γ_M	JFI	R_m	γ_M
MP-XPCE	0.75	2.24	15 dB	0.73	2.04	15 dB
CBPA-M	1	1.35	1.32 dB	1	1.13	0.31 dB
LQP	1	1.25	15 dB	1	0.98	15 dB

4.4.3. Multi Sub-channel Scenario

In this sub-section, we combine the MEIM algorithm with the MP-XPC and MP-XPCE algorithms and refer to these methods as JRA and JRAE, respectively. We assess the performance of the JRA and the JRAE methods against the existing resource allocation methods in the literature. The behavior of these algorithms are tabulated depending on their fairness and throughput. Afterward, the convergence behavior of these algorithms are presented.

The JRA method is compared to the CBPA algorithm [55], and the JFPUA method [59] for twenty-five cells with three users and five users per cell in Table 4.4. Since the CBPA algorithm only focuses on power allocation, we utilize the MEIM algorithm to handle the sub-channel allocation. In the table, AJFI corresponds to the average fairness values of the users that use the same sub-channel, TJFI corresponds to the fairness of all users, and R_m corresponds to the average throughput of the network. It is evident from the tables that when JRA is utilized, the total throughput is increased significantly with a minor loss in fairness compared to the existing algorithms in the literature.

Table 4.4. JRA assessment without macrocell SINR target in a 21 cell scenario.

	3 users per cell			5 users per cell		
	AJFI	TJFI	R_m	AJFI	TJFI	R_m
JRA	0.88	0.87	3.42	0.90	0.89	3.82
CBPA	1	0.96	2.29	1	0.97	2.77
JFPUA	1	1	1.84	1	1	2.17

In Figure 4.7 and Figure 4.8, the convergence behavior of the power allocation of the JRA method is compared to JFPUA and CBPA in a network with nine cells and two users per cell. All eighteen users converge to the same SINR value ($\gamma = 4.17\,dB$) for the JFPUA method, which is expected by design [59]. The users on the same sub-channel converge to the same SINR value for the CBPA method, ($\gamma_1 = 7.61\,dB$) and ($\gamma_2 = 4.17\,dB$). On the other hand, for the JRA method, all users converge to different SINR values depending on their channel conditions. The mean values of the final SINR reached by the JRA method are $13.97\,dB$ and $7.46\,dB$ on sub-channels one and two, respectively. These results also show that JRA significantly outperforms JFPUA and CBPA regarding average SINR.

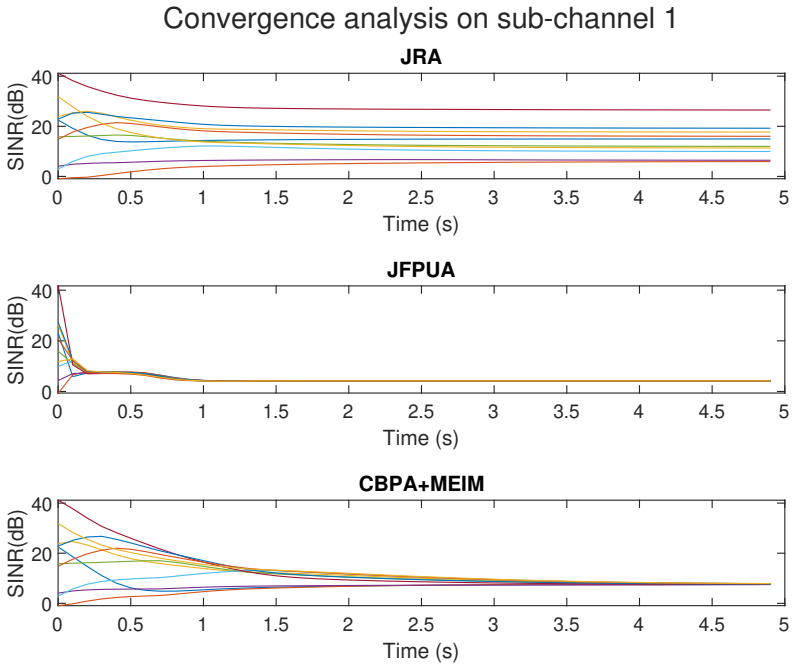

Figure 4.7. Convergence in a 9-cell with 2 users per cell scenario.

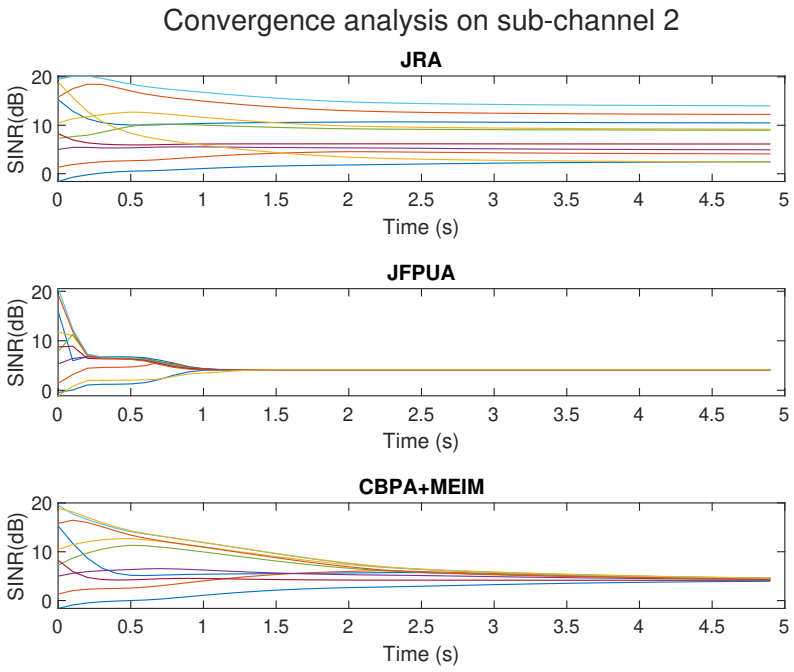

Figure 4.8. Convergence in a 9-cell with 2 users per cell scenario.

The JRAE method is compared to the LQP algorithm [54], and the CBPA-M algorithm [56] for twenty-five cells with three users and five users per cell in Table 4.5. Since the LQP and the CBPA-M algorithms only focus on power allocation, we utilize the MEIM algorithm to handle the sub-channel allocation. In the table, AJFI corresponds to the average fairness values of the users that use the same sub-channel, R_m corresponds to the average throughput of the network, and γ_M corresponds to the average macrocell SINR value. It is evident from the tables that when JRAE is utilized, the total throughput is increased significantly with a minor loss in fairness compared to the existing algorithms in the literature.

Table 4.5. JRAE assessment with 15 dB macrocell SINR target in a 21 cell scenario.

	3 users per cell			5 users per cell		
	AJFI	R_m	γ_M	AJFI	R_m	γ_M
JRAE	0.87	3.19	15 dB	0.90	3.61	15 dB
LQP	1	2.17	15 dB	1	2.66	15 dB
CBPA-M	1	2.35	5 dB	1	2.77	7.61 dB

In Figure 4.9 and Figure 4.10, the convergence behavior of the power allocation of the JRA method is compared to LQP and CBPA-M in a network with nine cells and two users per cell. The users on the same sub-channel converge to the same SINR value for the CBPA-M method, ($\gamma_1 = 8.54\,dB$) and ($\gamma_2 = 4.62\,dB$), and the macrocell SINR target is not satisfied. On the other hand, for the JRAE and LQP methods, the macrocell SINR target is reached. The picocell users on the same sub-channel converge to the same SINR value for the LQP method, ($\gamma_1 = 7.71\,dB$) and ($\gamma_2 = 4.51\,dB$). For the JRAE method, all picocell users converge to different SINR values depending on their channel conditions. The mean values of the final SINR reached by the picocell users for the JRAE method are $9.19\,dB$ and $7.00\,dB$ on sub-channels one and two, respectively. These results also show that JRAE significantly outperforms LQP and CBPA-M regarding average SINR.

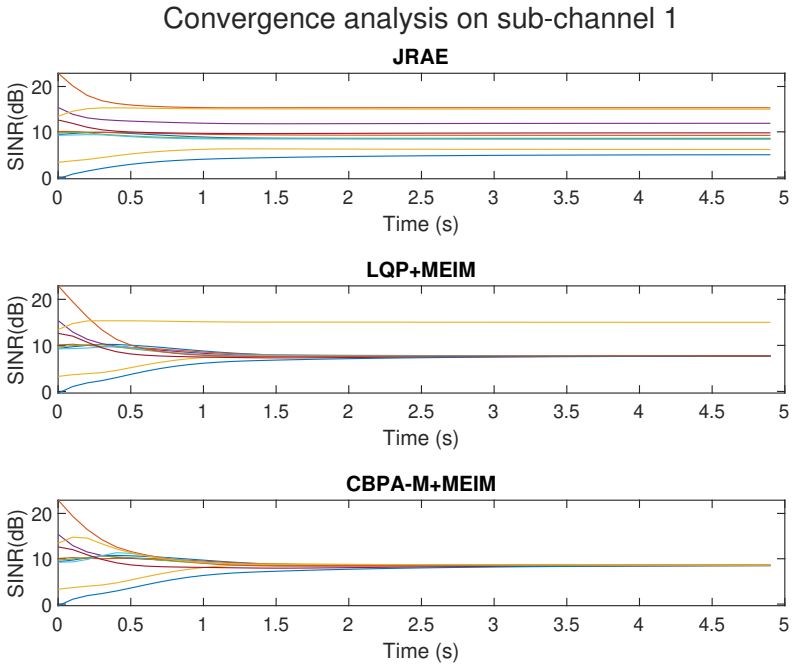

Figure 4.9. Convergence in a 9-cell with 2 users per cell scenario.

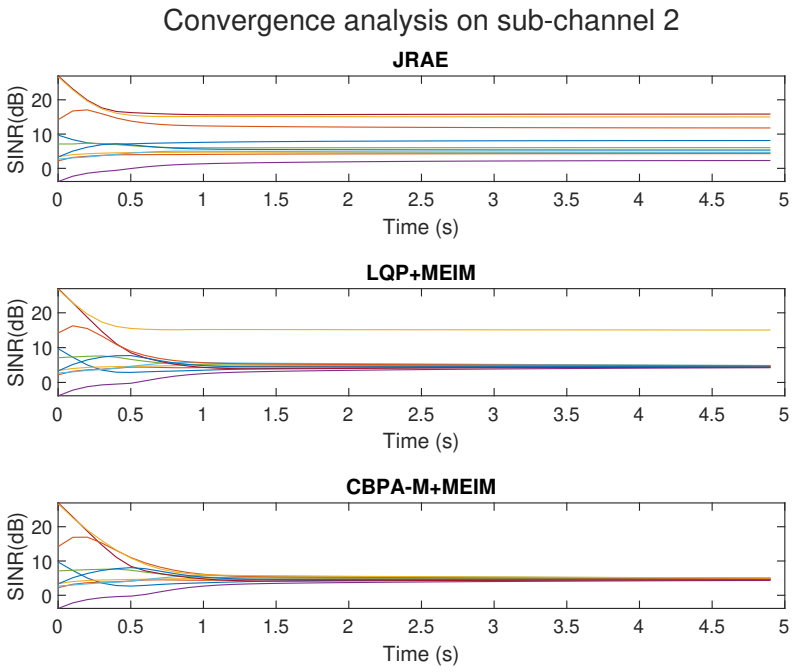

Figure 4.10. Convergence in a 9-cell with 2 users per cell scenario.

4.5. Concluding Remarks

In this chapter, we studied the distributed resource allocation problem for HetNets. We first proposed a distributed sub-channel allocation algorithm independent of the network's power allocation, which aims to minimize the maximum effective interference in the system. Then, we introduced the MP-XPC algorithm that allocates powers to the users that utilize the same sub-channel in a distributed fashion. The MP-XPC algorithm does not require pre-defined feasible SINR targets for the users and always converges to a viable solution. We extended the MP-XPC algorithm for scenarios where the macrocell has an SINR target, and referred to it as the MP-XPCE algorithm.

Furthermore, we showed that the MP-XPC and the MP-XPCE algorithms improve the throughput significantly compared to the available target-free power allocation algorithms in the literature. Finally, we introduced the JRA and JRAE methods, which utilize the MEIM algorithm for sub-channel allocation and the MP-XPC and the MP-XPCE algorithms for power allocation, respectively. We presented that these methods increase the throughput with a slight reduction in fairness compared to the existing target-free frequency and power allocation algorithms in the literature. The proposed methods can be utilized to improve the total throughput of the system in a distributed fashion.

5. CONCLUSION

This research is focused on the resource allocation problem for next-generation networks. We have worked on resource allocation algorithms for three different scenarios.

First, we have investigated the uplink H-NOMA MEC offloading resource allocation problem. We have given an optimal solution to the power and time allocation problem with non-ideal circuit power consumption. We have proposed a low complexity TES algorithm for the sub-channel allocation problem that outperforms the widely used 2ES algorithm. We have had two major contributions to this topic in this research. The first one is the optimal SH-NOMA method that outperforms the existing NOMA and H-NOMA methods in the literature for heterogeneous latency and data transfer requirements, different channel conditions, and non-ideal circuit power. The second contribution is the TES algorithm, which outperforms the 2ES algorithm regarding energy efficiency with no additional complexity.

Then, we have applied the same methodology to the downlink H-NOMA multiplexing scenario. We have given the optimal power and time allocation to the downlink communication which is different than the uplink due to the interference relations. We have further improved our sub-channel allocation algorithm, and proposed the B-TES algorithm. We have had two major findings in his topic. The first is the H-NOMA method for downlink, which is the first downlink H-NOMA application for users with heterogeneous latency and data transfer requirements in the infinite blocklength regime. The second contribution is the B-TES algorithm, which outperforms the 2ES algorithm, and the TES algorithm that we proposed in the uplink H-NOMA research.

Afterward, we have switched to the distributed downlink resource allocation for HetNets. We have proposed a sub-channel allocation method that depends on the

measured interference power on a sub-channel instead of the full CSI. Then, we have introduced the MP-XPC algorithm which is a target-free distributed algorithm that works without the full CSI. Afterward, we have extended the MP-XPC algorithm for the special scenario where the macrocell user has an SINR target. We have drawn three important conclusions out of this research topic. The first one is the MEIM algorithm, which is a low complexity sub-channel allocation algorithm that does not require full CSI. The second result is the MP-XPC and the MP-XPCE algorithms, which improve the throughput performance of the existing target-free algorithms significantly. The final improvement is the JRA method, which performs joint power and sub-channel allocation in a distributed fashion.

The performance of the proposed H-NOMA algorithms can be enhanced with D2D relaying. Both half-duplex and full-duplex relaying mechanisms can be analyzed to improve energy efficiency and throughput. An extension of the distributed resource allocation problem for HetNets can also be studied by allowing full-duplex transmission for small cell base stations. We have left these items as future work.

To sum up, the proposed resource allocation methods can be utilized to increase the efficiency of the next generation networks by utilizing NOMA, Hybrid NOMA, MEC Offloading, and Heterogeneous Networks.

REFERENCES

1. Jiang, D. and G. Liu, "An Overview of 5G Requirements", *5G Mobile Communications*, pp. 3–26, 2016.

2. Jonsson, P., "Mobility Report", 2022, `ericsson.com/en/reports-and-papers`, accessed on June 21, 2022.

3. Taleb, T., K. Samdanis, B. Mada, H. Flinck, S. Dutta and D. Sabella, "On Multi-access Edge Computing: A Survey of the Emerging 5G Network Edge Cloud Architecture and Orchestration", *IEEE Communications Surveys & Tutorials*, Vol. 19, No. 3, pp. 1657–1681, 2017.

4. Liu, Y., Z. Qin, M. Elkashlan, Z. Ding, A. Nallanathan and L. Hanzo, "Non-orthogonal Multiple Access for 5G and Beyond", *Proceedings of the IEEE*, Vol. 105, No. 12, pp. 2347–2381, 2017.

5. An, J., K. Yang, J. Wu, N. Ye, S. Guo and Z. Liao, "Achieving Sustainable Ultra-dense Heterogeneous Networks for 5G", *IEEE Communications Magazine*, Vol. 55, No. 12, pp. 84–90, 2017.

6. Ding, Z., X. Lei, G. K. Karagiannidis, R. Schober, J. Yuan and V. K. Bhargava, "A Survey on Non-orthogonal Multiple Access for 5G Networks: Research Challenges and Future Trends", *IEEE Journal on Selected Areas in Communications*, Vol. 35, No. 10, pp. 2181–2195, 2017.

7. Dai, L., B. Wang, Z. Ding, Z. Wang, S. Chen and L. Hanzo, "A Survey of Non-orthogonal Multiple Access for 5G", *IEEE Communications Surveys & Tutorials*, Vol. 20, No. 3, pp. 2294–2323, 2018.

8. Budhiraja, I., N. Kumar, S. Tyagi, S. Tanwar, Z. Han, M. J. Piran and D. Y. Suh, "A Systematic Review on NOMA Variants for 5G and Beyond", *IEEE Access*,

Vol. 9, pp. 85573–85644, 2021.

9. Di, B., L. Song and Y. Li, "Sub-channel Assignment, Power Allocation, and User Scheduling for Non-orthogonal Multiple Access Networks", *IEEE Transactions on Wireless Communications*, Vol. 15, No. 11, pp. 7686–7698, 2016.

10. Chang, Z., L. Lei, H. Zhang, T. Ristaniemi, S. Chatzinotas, B. Ottersten and Z. Han, "Energy-efficient and Secure Resource Allocation for Multiple-antenna NOMA with Wireless Power Transfer", *IEEE Transactions on Green Communications and Networking*, Vol. 2, No. 4, pp. 1059–1071, 2018.

11. Lai, X., Q. Zhang and J. Qin, "Downlink NOMA Networks with Hybrid Long-packet and Short-packet Communications in Flat Rayleigh Fading Channels", *IEEE Systems Journal*, Vol. 14, No. 3, pp. 3410–3413, 2019.

12. Xu, Y., D. Cai, F. Fang, Z. Ding, C. Shen and G. Zhu, "Outage Constrained Power Efficient Design for Downlink NOMA Systems with Partial HARQ", *IEEE Transactions on Communications*, Vol. 68, No. 8, pp. 5188–5201, 2020.

13. Awad, M. K., M. W. Baidas and A. Ahmad, "Resource Allocation for Downlink Non-orthogonal Multiple Access in Joint Transmission Coordinated Multi-point Networks", *Computer Communications*, Vol. 173, pp. 134–149, 2021.

14. Ni, W., X. Liu, Y. Liu, H. Tian and Y. Chen, "Resource Allocation for Multi-cell IRS-aided NOMA Networks", *IEEE Transactions on Wireless Communications*, Vol. 20, No. 7, pp. 4253–4268, 2021.

15. Zeng, M., N.-P. Nguyen, O. A. Dobre, Z. Ding and H. V. Poor, "Spectral and Energy-efficient Resource Allocation for Multi-carrier Uplink NOMA Systems", *IEEE Transactions on Vehicular Technology*, Vol. 68, No. 9, pp. 9293–9296, 2019.

16. Budhiraja, I., N. Kumar and S. Tyagi, "ISHU: Interference Reduction Scheme for D2D Mobile Groups Using Uplink NOMA", *IEEE Transactions on Mobile*

Computing, 2021.

17. Fang, F., K. Wang, Z. Ding and V. C. Leung, "Energy-efficient Resource Allocation for NOMA-MEC Networks with Imperfect CSI", *IEEE Transactions on Communications*, Vol. 69, No. 5, pp. 3436–3449, 2021.

18. Vaezi, M., G. A. A. Baduge, Y. Liu, A. Arafa, F. Fang and Z. Ding, "Interplay Between NOMA and Other Emerging Technologies: A Survey", *IEEE Transactions on Cognitive Communications and Networking*, Vol. 5, No. 4, pp. 900–919, 2019.

19. Kiani, A. Y., S. A. Hassan, B. Su, H. Pervaiz and Q. Ni, "Minimizing the Transaction Time Difference for NOMA-based Mobile Edge Computing", *IEEE Communications Letters*, Vol. 24, No. 4, pp. 853–857, 2020.

20. Ding, Z., D. Xu, R. Schober and H. V. Poor, "Hybrid NOMA Offloading in Multiuser MEC Networks", *IEEE Transactions on Wireless Communications*, Vol. 21, No. 7, pp. 5377–5391, 2022.

21. Xu, Y., C. Shen, T.-H. Chang, S.-C. Lin, Y. Zhao and G. Zhu, "Transmission Energy Minimization for Heterogeneous Low-latency NOMA Downlink", *IEEE Transactions on Wireless Communications*, Vol. 19, No. 2, pp. 1054–1069, 2019.

22. Xu, Y., C. Shen, D. Cai and G. Zhu, "Latency Constrained Non-orthogonal Packets Scheduling with Finite Blocklength Codes", *IEEE Transactions on Vehicular Technology*, Vol. 69, No. 10, pp. 12312–12316, 2020.

23. Bhat, R. V., M. Motani and T. J. Lim, "Hybrid NOMA for an Energy Harvesting MAC with Non-ideal Batteries and Circuit Power", *IEEE Transactions on Wireless Communications*, Vol. 18, No. 8, pp. 3961–3973, 2019.

24. Wei, X., H. Al-Obiedollah, K. Cumanan, W. Wang, Z. Ding and O. A. Dobre, "Spectral-Energy Efficiency Trade-off Based Design for Hybrid TDMA-NOMA System", *IEEE Transactions on Vehicular Technology*, Vol. 71, No. 3, pp. 3377–3382,

2022.

25. Zhang, D., Q. Wu, M. Cui, G. Zhang and D. Niyato, "Throughput Maximization for IRS-assisted Wireless Powered Hybrid NOMA and TDMA", *IEEE Wireless Communications Letters*, Vol. 10, No. 9, pp. 1944–1948, 2021.

26. Ding, Z., R. Schober and H. V. Poor, "Unveiling the Importance of SIC in NOMA Systems—Part II: New Results and Future Directions", *IEEE Communications Letters*, Vol. 24, No. 11, pp. 2378–2382, 2020.

27. Mao, Y., C. You, J. Zhang, K. Huang and K. B. Letaief, "A Survey on Mobile Edge Computing: The Communication Perspective", *IEEE Communications Surveys & Tutorials*, Vol. 19, No. 4, pp. 2322–2358, 2017.

28. Zhang, J., X. Hu, Z. Ning, E. C.-H. Ngai, L. Zhou, J. Wei, J. Cheng and B. Hu, "Energy-latency Tradeoff for Energy-aware Offloading in Mobile Edge Computing Networks", *IEEE Internet of Things Journal*, Vol. 5, No. 4, pp. 2633–2645, 2017.

29. Masoudi, M. and C. Cavdar, "Device vs Edge Computing for Mobile Services: Delay-aware Decision Making to Minimize Power Consumption", *IEEE Transactions on Mobile Computing*, Vol. 20, No. 12, pp. 3324–3337, 2020.

30. Ye, Y., L. Shi, H. Sun, R. Q. Hu and G. Lu, "System-centric Computation Energy Efficiency for Distributed NOMA-based MEC Networks", *IEEE Transactions on Vehicular Technology*, Vol. 69, No. 8, pp. 8938–8948, 2020.

31. Ye, Y., R. Q. Hu, G. Lu and L. Shi, "Enhance Latency-constrained Computation in MEC Networks Using Uplink NOMA", *IEEE Transactions on Communications*, Vol. 68, No. 4, pp. 2409–2425, 2020.

32. Wu, Y., B. Shi, L. P. Qian, F. Hou, J. Cai and X. S. Shen, "Energy-efficient Multi-task Multi-access Computation Offloading via NOMA Transmission for IoTs", *IEEE Transactions on Industrial Informatics*, Vol. 16, No. 7, pp. 4811–4822, 2019.

33. Huang, Y., Y. Liu and F. Chen, "NOMA-aided Mobile Edge Computing via User Cooperation", *IEEE Transactions on Communications*, Vol. 68, No. 4, pp. 2221–2235, 2020.

34. Pan, Y., M. Chen, Z. Yang, N. Huang and M. Shikh-Bahaei, "Energy-efficient NOMA-based Mobile Edge Computing Offloading", *IEEE Communications Letters*, Vol. 23, No. 2, pp. 310–313, 2018.

35. Yu, H., Z. Zhou, Z. Jia, X. Zhao, L. Zhang and X. Wang, "Multi-Timescale Multi-Dimension Resource Allocation for NOMA-Edge Computing-based Power IoT with Massive Connectivity", *IEEE Transactions on Green Communications and Networking*, 2021.

36. Ding, Z., J. Xu, O. A. Dobre and H. V. Poor, "Joint Power and Time Allocation for NOMA-MEC Offloading", *IEEE Transactions on Vehicular Technology*, Vol. 68, No. 6, pp. 6207–6211, 2019.

37. Li, H., F. Fang and Z. Ding, "Joint Resource Allocation for Hybrid NOMA-assisted MEC in 6G Networks", *Digital Communications and Networks*, Vol. 6, No. 3, pp. 241–252, 2020.

38. Zhu, J., J. Wang, Y. Huang, F. Fang, K. Navaie and Z. Ding, "Resource Allocation for Hybrid NOMA MEC Offloading", *IEEE Transactions on Wireless Communications*, Vol. 19, No. 7, pp. 4964–4977, 2020.

39. Altin, I. and M. Akar, "Novel OMA and Hybrid NOMA Schemes for MEC offloading", *IEEE International Black Sea Conference on Communications and Networking (BlackSeaCom)*, pp. 1–5, Odessa, Ukraine, 2020.

40. Altin, I. and M. Akar, "A Joint Resource Allocation Method for Hybrid NOMA MEC Offloading", *Physical Communication*, p. 101809, 2022.

41. Sheng, M., Y. Dai, J. Liu, N. Cheng, X. Shen and Q. Yang, "Delay-aware Compu-

tation Offloading in NOMA MEC under Differentiated Uploading Delay", *IEEE Transactions on Wireless Communications*, Vol. 19, No. 4, pp. 2813–2826, 2020.

42. Fang, F., Y. Xu, Z. Ding, C. Shen, M. Peng and G. K. Karagiannidis, "Optimal Resource Allocation for Delay Minimization in NOMA-MEC Networks", *IEEE Transactions on Communications*, Vol. 68, No. 12, pp. 7867–7881, 2020.

43. Yang, Z., C. Pan, J. Hou and M. Shikh-Bahaei, "Efficient Resource Allocation for Mobile-edge Computing Networks with NOMA: Completion Time and Energy Minimization", *IEEE Transactions on Communications*, Vol. 67, No. 11, pp. 7771–7784, 2019.

44. Ding, Z., D. W. K. Ng, R. Schober and H. V. Poor, "Delay Minimization for NOMA-MEC Offloading", *IEEE Signal Processing Letters*, Vol. 25, No. 12, pp. 1875–1879, 2018.

45. Zeng, M., N.-P. Nguyen, O. A. Dobre and H. V. Poor, "Delay Minimization for NOMA-assisted MEC under Power and Energy Constraints", *IEEE Wireless Communications Letters*, Vol. 8, No. 6, pp. 1657–1661, 2019.

46. Su, B., Q. Ni, W. Yu and H. Pervaiz, "Optimizing Computation Efficiency for NOMA-Assisted Mobile Edge Computing with User Cooperation", *IEEE Transactions on Green Communications and Networking*, Vol. 5, No. 2, pp. 858–867, 2021.

47. Paymard, P., S. Rezvani and N. Mokari, "Joint Task Scheduling and Uplink/Downlink Radio Resource Allocation in PD-NOMA Based Mobile Edge Computing Networks", *Physical Communication*, Vol. 32, pp. 160–171, 2019.

48. Lopez-Perez, D., I. Guvenc, G. De la Roche, M. Kountouris, T. Q. Quek and J. Zhang, "Enhanced Intercell Interference Coordination Challenges in Heterogeneous Networks", *IEEE Wireless Communications*, Vol. 18, No. 3, pp. 22–30, 2011.

49. Foschini, G. J. and Z. Miljanic, "A Simple Distributed Autonomous Power Control Algorithm and Its Convergence", *IEEE Transactions on Vehicular Technology*, Vol. 42, No. 4, pp. 641–646, 1993.

50. Leung, K.-K. and C. W. Sung, "An Opportunistic Power Control Algorithm for Cellular Network", *IEEE/ACM Transactions on Networking*, Vol. 14, No. 3, pp. 470–478, 2006.

51. Rasti, M., A. R. Sharafat and J. Zander, "A Distributed Dynamic Target-SIR-tracking Power Control Algorithm for Wireless Cellular Networks", *IEEE Transactions on Vehicular Technology*, Vol. 59, No. 2, pp. 906–916, 2009.

52. Aslani, R. and M. Rasti, "Distributed Power Control Schemes for In-band Full-duplex Energy Harvesting Wireless Networks", *IEEE Transactions on Wireless Communications*, Vol. 16, No. 8, pp. 5233–5243, 2017.

53. Aslani, R. and M. Rasti, "A Distributed Power Control Algorithm for Energy Efficiency Maximization in Wireless Cellular Networks", *IEEE Wireless Communications Letters*, Vol. 9, No. 11, pp. 1975–1979, 2020.

54. Chandrasekhar, V., J. G. Andrews, T. Muharemovic, Z. Shen and A. Gatherer, "Power Control in Two-tier Femtocell Networks", *IEEE Transactions on Wireless Communications*, Vol. 8, No. 8, pp. 4316–4328, 2009.

55. Şenel, K. and M. Akar, "A Consensus-based Coverage Algorithm for Self-organizing Femtocell Networks", *IEEE Communications Letters*, Vol. 20, No. 1, pp. 141–144, 2015.

56. Senel, K. and M. Akar, "A Distributed Coverage Adjustment Algorithm for Femtocell Networks", *IEEE Transactions on Vehicular Technology*, Vol. 66, No. 2, pp. 1739–1747, 2016.

57. Jain, R. K., D.-M. W. Chiu, W. R. Hawe *et al.*, "A Quantitative Measure of Fair-

ness and Discrimination", *Eastern Research Laboratory, Digital Equipment Corporation, Hudson, MA*, 1984.

58. Senel, K. and M. Akar, "Fair Resource Allocation in Self-organizing Heterogeneous Networks with Imperfect Connections", *IEEE Transactions on Vehicular Technology*, Vol. 66, No. 12, pp. 11277–11285, 2017.

59. Sevim, O., H. Y. Öksüz and M. Akar, "Joint Frequency and Power Control for Self-Organizing OFDMA Femtocell Networks", *IEEE Transactions on Vehicular Technology*, Vol. 69, No. 5, pp. 5089–5101, 2020.

60. Wu, S., Y. Wei, S. Zhang and K. Ma, "Gossip Based Distributed Power Control Algorithm for 5G Ultra Dense Networks", *IEEE Wireless Communications and Networking Conference (WCNC)*, pp. 1–6, Barcelona, Spain, 2018.

61. Liu, Z., J. Wang, Y. Xia, R. Fan, H. Jiang and H. Yang, "Power Allocation Robust to Time-varying Wireless Channels in Femtocell Networks", *IEEE Transactions on Vehicular Technology*, Vol. 65, No. 4, pp. 2806–2815, 2015.

62. Zappone, A., L. Sanguinetti, G. Bacci, E. Jorswieck and M. Debbah, "Energy-efficient Power Control: A Look at 5G Wireless Technologies", *IEEE Transactions on Signal Processing*, Vol. 64, No. 7, pp. 1668–1683, 2015.

63. Zappone, A., L. Sanguinetti and M. Debbah, "Energy-delay Efficient Power Control in Wireless Networks", *IEEE Transactions on Communications*, Vol. 66, No. 1, pp. 418–431, 2017.

64. Liu, Z., S. Li, L. Hao, H. Yang, X. Guan and X. Li, "Power Control Based on the Stackelberg Game in Two-tier Femtocell Networks", *Physical Communication*, Vol. 23, pp. 1–11, 2017.

65. Liu, Y., L. Hao, Z. Liu, K. Sharif, Y. Wang and S. K. Das, "Mitigating Interference via Power Control for Two-tier Femtocell Networks: A Hierarchical Game

Approach", *IEEE Transactions on Vehicular Technology*, Vol. 68, No. 7, pp. 7194–7198, 2019.

66. Liu, Z., G. Hou, Y. Liu, X. Li and X. Guan, "Robust Power Control Strategy Based on Hierarchical Game with QoS Provisioning in Full-duplex Femtocell Networks", *Computer Networks*, Vol. 160, pp. 92–104, 2019.

67. Liu, Z., X. Li, Y. Yuan, Y. Yang and X. Guan, "Game Based Robust Power Allocation Strategy with QoS Guarantee in D2D Communication Network", *Computer Networks*, Vol. 193, p. 108130, 2021.

68. Pourkabirian, A., M. H. Anisi and F. Kooshki, "A Game-based Power Optimization for 5G Femtocell Networks", *Computer Communications*, Vol. 177, pp. 230–238, 2021.

69. Ha, V. N. and L. B. Le, "Fair Resource Allocation for OFDMA Femtocell Networks with Macrocell Protection", *IEEE Transactions on Vehicular Technology*, Vol. 63, No. 3, pp. 1388–1401, 2013.

70. Ngo, D. T., S. Khakurel and T. Le-Ngoc, "Joint Subchannel Assignment and Power Allocation for OFDMA Femtocell Networks", *IEEE Transactions on Wireless Communications*, Vol. 13, No. 1, pp. 342–355, 2013.

71. Zhang, H., C. Jiang, N. C. Beaulieu, X. Chu, X. Wen and M. Tao, "Resource Allocation in Spectrum-sharing OFDMA Femtocells with Heterogeneous Services", *IEEE Transactions on Communications*, Vol. 62, No. 7, pp. 2366–2377, 2014.

72. Zhou, L., C. Zhu, R. Ruby, X. Wang, X. Ji, S. Wang and J. Wei, "QoS-aware Energy-efficient Resource Allocation in OFDM-based Heterogenous Cellular Networks", *International Journal of Communication Systems*, Vol. 30, No. 2, p. e2931, 2017.

73. Taskou, S. K., M. Rasti, P. H. Nardelli and A. S. De Sena, "Distributed Joint

Power and Rate Control for NOMA/OFDMA in 5G and Beyond", *IEEE Global Communications Conference (GLOBECOM)*, pp. 01–06, Madrid, Spain, 2021.

74. Kara, F. and H. Kaya, "BER Performances of Downlink and Uplink NOMA in the Presence of SIC Errors over Fading Channels", *IET Communications*, Vol. 12, No. 15, pp. 1834–1844, 2018.

75. Sani, Y., A. Mauthe and C. Edwards, "Adaptive Bitrate Selection: A Survey", *IEEE Communications Surveys & Tutorials*, Vol. 19, No. 4, pp. 2985–3014, 2017.

76. Le, N. P., X. Huang, J. Choi, E. Dutkiewicz, S. L. Phung, A. Bouzerdoum *et al.*, "Performance Analysis of Uplink NOMA Systems with Hardware Impairments and Delay Constraints over Composite Fading Channels", *IEEE Transactions on Vehicular Technology*, Vol. 70, No. 7, pp. 6881–6897, 2021.

77. Cui, S., A. J. Goldsmith and A. Bahai, "Energy-constrained Modulation Optimization", *IEEE Transactions on Wireless Communications*, Vol. 4, No. 5, pp. 2349–2360, 2005.

78. Yang, Z., Z. Ding, P. Fan and N. Al-Dhahir, "A General Power Allocation Scheme to Guarantee Quality of Service in Downlink and Uplink NOMA Systems", *IEEE Transactions on Wireless Communications*, Vol. 15, No. 11, pp. 7244–7257, 2016.

79. Boyd, S. and L. Vandenberghe, *Convex Optimization*, Cambridge University Press, Cambridge, 2004.

80. Frieze, A. M., "Complexity of a 3-dimensional Assignment Problem", *European Journal of Operational Research*, Vol. 13, No. 2, pp. 161–164, 1983.

81. Bodine-Baron, E., C. Lee, A. Chong, B. Hassibi and A. Wierman, "Peer Effects and Stability in Matching Markets", *Algorithmic Game Theory: 4th International Symposium*, pp. 117–129, Amalfi, Italy, 2011.

82. Lazarova, E., P. Borm and A. Estévez-Fernández, "Transfers and Exchange-stability in Two-sided Matching Problems", *Theory and Decision*, Vol. 81, No. 1, pp. 53–71, 2016.

83. Alenitsyn, A. G., E. I. Butikov and A. S. Kondratyev, *Concise Handbook of Mathematics and Physics*, CRC Press, Florida, 1997.

84. Asplund, H., D. Astely, P. von Butovitsch, T. Chapman, M. Frenne, F. Ghasemzadeh, M. Hagström, B. Hogan, G. Jongren, J. Karlsson *et al.*, *Advanced Antenna Systems for 5G Network Deployments: Bridging the Gap Between Theory and Practice*, Academic Press, Massachusetts, 2020.

85. Perrone, D. and S. Di Stefano, "Survey of Lithium-ion Battery Performance for Potential Use in NASA Missions", *IECEC Proceedings of the Thirty-Second Intersociety Energy Conversion Engineering Conference*, Vol. 1, pp. 39–41, Hawaii, USA, 1997.

86. Kuhn, H. W., "The Hungarian Method for the Assignment Problem", *Naval research logistics quarterly*, Vol. 2, No. 1-2, pp. 83–97, 1955.

87. Bijsterbosch, J. and A. Volgenant, "Solving the Rectangular Assignment Problem and Applications", *Annals of Operations Research*, Vol. 181, No. 1, pp. 443–462, 2010.

88. Wang, K.-Y., A. M.-C. So, T.-H. Chang, W.-K. Ma and C.-Y. Chi, "Outage Constrained Robust Transmit Optimization for Multiuser MISO Downlinks: Tractable Approximations by Conic Optimization", *IEEE Transactions on Signal Processing*, Vol. 62, No. 21, pp. 5690–5705, 2014.

89. Holma, H., A. Toskala and T. Nakamura, *5G Technology: 3GPP New Radio*, John Wiley & Sons, New York, 2020.

90. Özçelep, Y., G. Bekdaş and S. Apak, "Investigation of Photovoltaic-hydrogen

Power System for a Real House in Turkey: Hydrogen Blending to Natural Gas Effects on System Design", *International Journal of Hydrogen Energy*, Vol. 46, No. 74, pp. 36678–36686, 2021.

91. Yetiş, C. and M. T. Kayili, "Determination of EMF Pollution in the Context of Urban Health: The Case of Safranbolu", *Computational Research Progress in Applied Science & Engineering: Transactions of Civil and Environmental Engineering*, Vol. 7, pp. 1–10, 2021.

92. Kaybal, F., G. Gebıç and A. Büyükbaş, "Mobile Spectrum Requirement Forecast for Turkey", *28th Signal Processing and Communications Applications Conference (SIU)*, pp. 1–4, Gaziantep, Turkey, 2020.

93. Chung, F. R. and F. C. Graham, *Spectral Graph Theory*, Vol. 92, American Mathematical Society, Rhode Island, 1997.

94. Ren, W., R. W. Beard and E. M. Atkins, "Information Consensus in Multi-vehicle Cooperative Control", *IEEE Control Systems Magazine*, Vol. 27, No. 2, pp. 71–82, 2007.

95. Penna, F., S. Stańczak, Z. Ren and P. Fertl, "MMSE Interference Estimation in LTE Networks", *IEEE International Conference on Communications (ICC)*, pp. 4548–4552, Sydney, Australia, 2014.

96. Burkard, R. E. and E. Cela, *Linear Assignment Problems and Extensions*, Springer, New York, 1999.

97. Gabow, H. N. and R. E. Tarjan, "Faster Scaling Algorithms for Network Problems", *SIAM Journal on Computing*, Vol. 18, No. 5, pp. 1013–1036, 1989.

98. Slotine, J.-J. E., W. Li *et al.*, *Applied Nonlinear Control*, Vol. 199 (1), Prentice Hall, New Jersey, 1991.

APPENDIX A: PERMISSIONS

The graphics and text created within the scope of this thesis work, whose copyrights were transferred to the publishing house, are used in the thesis in accordance with the "publishing policy applicable to the reuse of the text and graphics produced by the author" on the website of the publisher.